The role of mast cell-derived tumor necrosis factor in the resolution of hapten-induced skin inflammation

Thesis

for the degree of

doctor rerum naturalium

(Dr. rer. nat.)

approved by the Faculty of Natural Sciences

of Otto-von-Guericke-University Magdeburg

by M. Sc. Martin Andreas Voss

born on 24.07.1991 in Wolfen

Examiner:	Prof. Dr. rer. nat. Anne Dudeck
	Prof. Dr. rer. nat. Michael Huber
Submitted on:	24.05.2024
Defended on:	20.11.2024

Abstract

Allergic contact dermatitis (ACD) is a common inflammatory skin disease based on delayed type T cell-dependent hypersensitivity reactions. In recent years, Anne Dudeck and colleagues have demonstrated a key role of mast cells (MCs) in initiating both innate and adaptive immune responses during contact hypersensitivity (CHS)-induced skin inflammation, a mouse model for ACD [1]. For instance, MCs critically promote the maturation and migration of dendritic cells via the release of tumor necrosis factor (TNF) and consequently, the priming of $CD8^+$ T cells during CHS sensitization [2]. Intriguingly, they also found that in the absence of MC-derived TNF, although ear swelling as a measure for inflammation was initially reduced, skin thickness did not normalize at later time points. This suggests a novel role for MCs in the resolution of CHS.

Based on this, the aim of this thesis was to elucidate the mechanisms underlying MC-derived TNF effects on the resolution of CHS. In line with the reduced ear swelling, skin numbers of monocytes and $CD8^+$ T cells were strongly decreased in the absence of MC-derived TNF in the acute phase. Interestingly, key processes during the transition from inflammation to resolution including the downregulation of chemokine production, the cessation of leukocyte infiltration, and the induction of neutrophil apoptosis were not affected by the absence of MC-derived TNF, indicating that the persistent ear swelling was not linked to a chronification of inflammation. However, a strong reduction in skin protein levels of matrix metalloproteinases (MMP)-8 and proMMP-9, both produced by monocytes, was observed. Conversely, there was an increase in the amount of collagen I, suggesting that the persistent ear swelling in the absence of MC-derived TNF might be attributed to an altered tissue recovery. Importantly, the adoptive transfer of primed $CD8^+$ T cells rescued monocyte skin infiltration in the acute phase, indicating an indirect effect of MC-derived TNF on monocyte recruitment via the adequate priming of $CD8^+$ T cells during the sensitization phase. Moreover, the restoration of monocyte skin infiltration also prevented the ear swelling at later time points of CHS in the absence of MC-derived TNF, thereby suggesting a connection between the early recruitment of monocytes and the induction of an effective resolution program. Finally, I examined whether these findings are clinically relevant in the context of anti-TNF therapies, which are used for the therapy of autoimmune diseases. Indeed, the complete depletion of TNF before CHS sensitization resembled the inflammatory course observed in the absence of MC-derived TNF, suggesting a potential side effect of TNF inhibitors in the context of ACD.

In summary, the data obtained in this thesis reveal an intricate series of cellular events initiated by MC-derived TNF that is essential for adequate tissue recovery. Importantly, these findings are clinically relevant in the context of anti-TNF therapies, which efficiently inhibit acute inflammation, but may affect tissue remodeling in late phases or long term.

Zusammenfassung

Die allergische Kontaktdermatitis (AKD) ist eine häufig auftretende Hauterkrankung, die auf T-Zell-abhängigen Überempfindlichkeitsreaktionen vom verzögerten Typ basiert. In den letzten Jahren konnten Anne Dudeck und Kollegen eine Schlüsselrolle von Mastzellen (MZ) bei der Initiierung sowohl angeborener, als auch adaptiver Immunreaktionen im Rahmen der *contact hypersensitivity* (CHS)-induzierten Hautentzündung, einem Mausmodell der AKD, zeigen [1]. So fördern MZ durch die Freisetzung von Tumornekrosefaktor (TNF) die Reifung und Migration dendritischer Zellen und nachfolgend das Priming von $CD8^+$ T-Zellen während der Sensibilisierungsphase [2]. Weiterhin konnte beobachtet werden, dass in Abwesenheit des TNFs von MZ die Ohrschwellung als Maß für die Entzündung zwar anfänglich reduziert war, sich jedoch später nicht normalisierte. Diese Ergebnisse deuten auf eine neuartige Rolle von MZ bei der Auflösung der CHS hin.

Basierend darauf war das Ziel dieser Arbeit, die Mechanismen zu klären, durch die das TNF von MZ die Auflösung der CHS fördert. Übereinstimmend mit der verringerten Ohrschwellung konnte eine reduzierte Anzahl von Monozyten und $CD8^+$ T-Zellen in der Haut während der akuten Phase in Abwesenheit des TNFs von MZ gezeigt werden. Interessanterweise wurden frühe Prozesse während des Übergangs von der akuten Entzündung zur Auflösung, wie die Abnahme der Chemokinproduktion, die Beendigung der Leukozyteneinwanderung und die Induktion der Neutrophilen Apoptose, durch die Abwesenheit des TNFs von MZ nicht beeinflusst. Dies weist darauf hin, dass die anhaltende Ohrschwellung nicht mit einer Chronifizierung der Entzündung verbunden war. Jedoch wurde eine deutlich reduzierte Konzentration der Matrix-Metalloproteinasen (MMP)-8 und proMMP-9 festgestellt, die beide von Monozyten produziert werden. Im Gegensatz dazu nahm die Menge an Kollagen I zu. Dies deutet daraufhin, dass die anhaltende Ohrschwellung in Abwesenheit des TNFs von MZ möglicherweise auf eine veränderte Geweberegenerierung zurückzuführen ist. Die Monozyten-Infiltration in die Haut während der akuten Phase konnte durch einen adoptiven Transfer von geprimten $CD8^+$ T-Zellen wiederhergestellt werden. Somit beeinflusst das von MZ freigesetzte TNF indirekt die Monozyten-Rekrutierung, indem es das ädaquate Priming von $CD8^+$ T-Zellen während der Sensibilisierung vermittelt. Die Wiederherstellung der Hautinfiltration von Monozyten verhinderte auch die Ohrschwellung zu späteren Zeitpunkten der CHS in Abwesenheit des TNFs von MZ. Dies deutet auf einen Zusammenhang zwischen der frühen Rekrutierung von Monozyten und der Induktion eines effektiven Auflösungsprozesses hin. Schließlich wurde untersucht, ob diese Ergebnisse im Hinblick auf Anti-TNF-Therapien, die zur Behandlung von Autoimmunerkrankungen eingesetzt werden, klinisch relevant sind. Tatsächlich ähnelte der Entzündungsverlauf nach

vollständiger Depletion von TNF vor der Sensibilisierung dem, der in Abwesenheit des TNFs von MZ beobachtet wurde.

Zusammenfassend zeigen die vorliegenden Daten eine komplexe Abfolge von zellulären Ereignissen, die durch das von MZ freigesetzte TNF ausgelöst werden und für eine adäquate Gewebe-Regeneration unerlässlich sind. Diese Ergebnisse sind von klinischer Relevanz im Hinblick auf Anti-TNF-Therapien, welche die akute Entzündung zwar effektiv hemmen, jedoch später möglicherweise den Auflösungsprozess beeinflussen.

Table of Contents

Abstract ..... **II**

Zusammenfassung ..... **III**

Table of Contents ..... **V**

List of Figures ..... **VIII**

List of Tables ..... **IX**

List of Abbrevations ..... **X**

1 Introduction **1**

1.1 The immune system 1

1.1.1 Innate immune system 1

1.1.2 Adaptive immune system 1

1.2 Mast cells 2

1.2.1 MC development 2

1.2.2 MC heterogeneity 3

1.2.3 MC receptors 3

1.2.4 MC response and memory 4

1.2.5 MC functions in immunity and host defense 6

1.3 Allergic contact dermatitis 6

1.3.1 Structure of the skin 7

1.3.2 Haptens 7

1.3.3 Pathomechanisms in ACD 7

1.3.3.1 Sensitization phase 8

1.3.3.2 Elicitation phase 9

1.4 Resolution of inflammation 10

1.4.1 Initiation of the resolution phase 11

1.4.2 Cessation of immune cell infiltration 11

1.4.3 Neutrophil apoptosis and clearance by macrophages 11

1.4.4 Macrophage polarization and tissue recovery 12

2 Aim of the study **13**

3 Materials and Methods **14**

3.1 Chemicals and reagents 14

3.2 Consumables 16

3.3 Devices and software 17

3.4 Buffers and Media 18

3.5 Oligonucleotides 20

3.6 Antibodies 21
3.7 Commercial assays 23
3.8 Mice 23
3.9 Molecular-biological methods 24
3.9.1 DNA isolation from ear skin and tail biopsies 24
3.9.2 Genotyping of transgenic mice 25
3.9.3 Agarose gel electrophoresis 26
3.9.4 RNA extraction from ear skin biopsies 26
3.9.5 Preparation of cDNA 27
3.9.6 Gene expression analysis by quantitative PCR (qPCR) 27
3.10 Animal based-methods 28
3.10.1 Contact hypersensitivity 28
3.10.2 Adoptive Transfer of hapten-primed $CD8^+$ T cells 28
3.10.3 TNF depletion 28
3.11 Surgical methods and murine cell isolation 29
3.11.1 Blood collection and preparation 29
3.11.2 Preparation of single-cell suspensions from ear skin 29
3.11.3 Preparation of tissue homogenates from ear skin 29
3.11.4 Preparation of single-cell suspensions from spleen 30
3.11.5 Preparation of single suspensions from bone marrow 30
3.11.6 Preparation of single-cell suspensions from inguinal lymph node 30
3.11.7 Cell counting 30
3.12 Cell-biological methods 31
3.12.1 Generation of BMDCs 31
3.12.2 Lipopolysaccharide (LPS) stimulation of BMDCs 31
3.13 Immunological methods 31
3.13.1 Magnetic cell separation (MACS) 31
3.13.2 Flow cytometry 32
3.13.3 Quantification of cytokines, chemokines and MMPs using ELISA and multiplex approaches 32
3.14 Data analysis and statistics 33

4 Results 34

4.1 Impaired CHS response in the absence of MC-derived TNF 34
4.2 Characterization of the induction phase 35
4.2.1 Reduced infiltration of monocytes and T cells in absence of MC-derived TNF 35
4.2.2 Altered inflammatory micromilieu in the absence of MC-derived TNF 37
4.3 Analysis of the mechanism of MC-derived TNF effects on early monocyte recruitment to the skin 38

4.3.1 MC-derived TNF is dispensable for monocyte mobilization 38
4.3.2 MC-derived TNF indirectly promotes monocyte skin infiltration..... 40
4.3.3 MC-derived TNF indirectly promotes early monocyte recruitment and tissue recovery via an adequate priming of $CD8^+$ T cells 41
4.3.4 MC-derived TNF promotes tissue recovery, but not monocyte recruitment via TNFR1 signalling in cDCs 43
4.4 Characterization of the resolving phase..... 46
4.4.1 The continuing ear thickness is not associated with ongoing inflammation .. 46
4.4.2 Adequate induction of neutrophil apoptosis in absence of MC-derived TNF 48
4.4.3 MC-derived TNF promotes the polarization of M2-like macrophages..... 49
4.4.4 MC-derived TNF is essential for proper tissue recovery 49
4.5 The total depletion of TNF alters the resolution of CHS 52
5 Discussion 53
6 References 62
7 Declaration of Honor 77

List of Figures

Figure 1| MC biology. 5
Figure 2| The role of MCs in the pathophysiology of CHS. 8
Figure 3| Key events in the resolution of inflammation. 10
Figure 4| Impaired CHS response in absence of MC-derived TNF. 34
Figure 5| Reduced recruitment of monocytes and T cells in the absence of MC-derived TNF during the induction phase. 36
Figure 6| MC-derived TNF promotes the infiltration of dMonocytes. 37
Figure 7| Reduced levels of IL-6, TNF and IL-4 in $MC^{\Delta TNF}$ mice at 36 h post challenge. 38
Figure 8| MC-derived TNF is dispensable for iMonocyte mobilization during the induction phase of CHS. 39
Figure 9| TNFR1 signalling in monocytes is dispensable for their early recruitment during CHS. 40
Figure 10| MC-derived TNF promotes early monocyte recruitment and tissue recovery via its impact on efficient priming of $CD8^+$ T cells 42
Figure 11| TNFR1 surface expression is reduced in BMDCs derived from $DC^{\Delta TNFR1}$ mice. 43
Figure 12| Splenic and skin immune cell subsets are not changed in $DC^{\Delta TNFR1}$ mice under physiologic conditions. 44
Figure 13| Monocyte recruitment is not affected by the absence of TNFR1 signalling DCs. 46
Figure 14| The absence of MC-derived TNF does not lead to ongoing inflammatory processes. 47
Figure 15| MC-derived TNF is dispensable for the induction of neutrophil apoptosis. 48
Figure 16| Reduced numbers of M2-like macrophages in the absence of MC-derived TNF. 49
Figure 17| MC-derived TNF promotes collagen degradation in the resolution phase. 50
Figure 18| MC-derived TNF does not affect collagen production. 51
Figure 19| Impaired CHS response after TNF depletion in the sensitization phase. 52
Figure 20| MC-derived TNF indirectly promotes monocyte recruitment and subsequent tissue recovery by enduring an adequate priming of $CD8^+$ T cells. 60

List of Tables

Table 1| Chemicals and reagents 14
Table 2| Consumables 16
Table 3| Devices 17
Table 4| Software 18
Table 5| PCR-primers for genotyping of transgenic mice. 20
Table 6| Primers for qPCR. 21
Table 7| Antibodies for flow cytometry 21
Table 8| Antibodies for *in vivo* TNF neutralization. 23
Table 9| Critical commercial assays 23
Table 10| Mouse lines 24
Table 11 Reaction mix for genotyping. 25
Table 12 | Temperature profiles for the general Cre, GFP, IL-2, Mcpt5-Cre and tdRFP genotyping PCR. 25
Table 13| Temperature profiles for the CD11c-Cre genotyping PCR. 26
Table 14| Primers for qPCR. 27
Table 15| Temperature profiles for gene expression analysis 28

List of Abbrevations

7AAD	7-aminoactinomycin D
ACD	allergic contact dematitis
AMP	anti-microbial peptides
ANOVA	analysis of variance
APC	antigen-presenting cell
BAD	Bcl-2-associated death promoter
Bai-1	brain-specific angiogenesis inhibitor 1
Bcl-2	B-cell lymphoma 2
BM	bone marrow
BMDC	bone marrow-derived DC
BSA	bovine serum albumin
CCL	CC motif chemokine ligand
CCR	CC motif chemokine receptors
CD	cluster of differentiation
cDNA	complementary DNA
CHS	contact hypersensitivity
CTMC	connective tissue type mast cells
CX3CL1	CX3C motif chemokine ligand 1
CX3CR1	CX3C motif chemokine receptor 1
CXCL	CXC motif chemokine ligand
CXCR	CXC motif chemokine receptor
DAMP	danger-associated molecular pattern
DARC	duffy antigen receptor for chemokines
DC	dendritic cell
dMonocytes	dermal monocytes
DNA	deoxyribonucleic acid
DNFB	dinitrofluorobenzene

ECM	extracellular matrix
ELISA	enzyme-linked immunosorbent assays
FBS	fetal bovine serum
FcεRI	Fcε receptor I
GAG	glycosaminoglycan
GAS6	growth-arrest specific protein 6
GM-CSF	granulocyte-macrophage colony-stimulating factor
GM-CSFR	granulocyte-macrophage colony-stimulating factor receptor
HRP	horseradish peroxidase
IFN-γ	interferon-γ
IgE	Immunoglobulin E
IL	interleukin
IL-1RII	Interleukin-1R type II
iMonocytes	inflammatory monocytes
Iso	istopype
LC	langerhans cells
LPC	lysophosphatidylcholine
LPS	lipopolysaccharide
LTB_4	leukotriene B_4
LTC_4	leukotriene C_4
LXA_4	Lipoxin A_4
MACS	magnetic cell separation
MC	mast cell
MC_C	chymase-containg mast cell
MC_{CT}	tryptase- and chymase-containg mast cell
MCET	mast cell extracellular traps
MC_T	tryptase-containing mast cell
MERTK	MER tyrosine kinase

MFI	median fluorescence intensity
MHC	major-histocompatibility complex
MMC	mucosal mast cells
mMcpt	murine MC proteases
moDC	monocyte-derived DC
MRGPRX2	Mas-related G-protein coupled receptor X2
mTORC1	mammalian target of rapamycin complex 1
NK cell	natural killer cell
NLR	NOD-like receptor
ns	not significant
PAMP	pathogen-associated molecular pattern
PBS	phosphate-buffered saline
PCR	polymerase chain reaction
PGD_2	prostaglandin D_2
pMonocytes	patrolling monocytes
PRR	pattern recognition receptor
PtdSer	phosphatidylserine
qPCR	qnatitative PCR
RNA	ribonucleic acid
ROS	reactive oxygen species
RT	room temperature
S1P	sphingosine-1-phosphate
SCF	stem cell factor
SCFR	stem-cell factor receptor
SD	standard deviation
SP	substance P
SPF	specific pathogen-free
T_c	cytotoxic T cell

TGF- ß	transforming growth-factor ß
T_H	T helper cell
TIM-4	T-cell immunoglobulin mucin protein 4
TLR	toll-like receptor
TNF	tumor necrosis factor
TNFR1	TNF receptor 1
T_{reg}	regulatory T cells
UTP	uridine triphosphate
VCAM-1	vascular cell adhesion molcule 1
VEGF	vascular endothelial growth factor
VEGFR	vascular endothelial growth factor receptor
veh	vehicle
WT	wildtype

1 Introduction

1.1 The immune system

Every day, our body is exposed to a variety of microorganisms including bacteria, viruses, fungi and parasites, which may have harmful effects on our health. Our immune system efficiently protects us against most invading pathogens and can be divided into two main parts: the innate and the adaptive immune system [3].

1.1.1 Innate immune system

The innate immune system represents the first line of defense and is comprised of physical barriers, cellular components, and soluble mediators. Physical barriers such as the skin separate the body from the external environment. They are mainly composed of epithelial cells, which are closely connected by intercellular adhesion molecules (termed tight junctions), thereby preventing the easy entry of microorganisms [4]. Once a pathogen has overcome the barrier, tissue-resident innate immune cells such as macrophages, dendritic cells (DCs) and mast cells (MCs), which form a dense network beneath epithelial barriers, are rapidly activated and secrete anti-microbial peptides (AMP) such as defensins and cathelicidins that directly kill the invading pathogen [5,6]. Additionally, through the release of cytokines and chemokines, they mediate the recruitment of innate effector cells (e.g neutrophils, monocytes), which efficiently engulf microorganisms in a process termed phagocytosis and subsequently kill them via the production of reactive oxygen species (ROS) [7,8]. In order to rapidly respond to invading pathogens, innate immune cells possess a variety of pattern recognition receptors (PRR), including Toll-like receptors (TLRs) and nucleotide-binding oligomerization domain (NOD)-like receptors (NLRs), which can recognize on one hand highly conserved structures of bacteria, viruses and funghi (referred to as “pathogen-associated molecular patterns”, PAMPs) and on the other hand molecules associated with tissue damage and inflammation (referred to as “danger-associated molecular patterns”, DAMPs) [9].

1.1.2 Adaptive immune system

The adaptive immune system represents the second line of defense and mainly consists of T and B cells, as well as specific antibodies, termed immunoglobulins. An essential step in the induction of an adaptive immune response is the priming of naïve T cells by professional antigen-presenting cells (APCs), particularly DCs. In detail, DCs that have engulfed microorganisms migrate via the afferent lymphatics to the draining lymph nodes, where they present processed peptides of these microorganisms (known as “antigens”) in the context of major-histocompatibility complex (MHC) molecules to naïve

T cells [10,11]. Once a T cell recognizes its cognate antigen in combination with other activating signals (referred to as “costimulatory molecules”), it starts to proliferate, thereby generating T cell clones with the same antigenic specificity. These T cells differentiate subsequently into effector cells. The priming of $CD8^+$ T cells leads to the generation of cytotoxic T (T_c) cells, whereas $CD4^+$ T cells develop into distinct T helper (T_H) cell subsets depending on the cytokine micromilieu. These include T_H1, T_H2, and T_H17, which are induced for instance by Interleukin (IL)-12, IL-4 and transforming growth factor (TGF)-ß, respectively [12–14]. Finally, these effector cells leave the draining lymph node and migrate via the bloodstream to the site of inflammation. Upon restimulation by tissue-resident APCs, T_c cells directly kill pathogen-infected cells via the release of cytotoxic molecules such as perforin and granzyme B, whereas T_H cells are critically involved in the regulation of the inflammatory response via the modulation of innate immune cells such as macrophages. Additionally, T_H cells promote the production of specific antibodies by B cells [14].

1.2 Mast cells

MCs are highly evolutionary conserved and were first discovered by Paul Ehrlich in 1878. A characteristic feature of MCs is the high number of electron-dense secretory granules, which contain a variety of preformed mediators [15]. Due to MCs’ strategic location at interface organs such as the skin, gut and lung, they play a crucial role in the defense against invading pathogens, in particular during infections with parasites. However, MCs are also well known for their detrimental role in allergy and atopic disorders [1,8,16].

1.2.1 MC development

During embryonic development, MC progenitors are predominantly derived from erythro-myeloid progenitors in the extraembryonic yolk sac and after birth from hematopoietic stem cells in the bone marrow (BM). Upon lineage commitment, MC progenitors migrate via the bloodstream to various tissues, such as the skin, gut, lung and brain, where they fully mature [17]. In the skin, fibroblasts play an important role in the regulation of MC differentiation and proliferation. Leist *et al.* recently demonstrated, that immature MCs interact with fibroblasts via vascular cell adhesion molecule 1 (VCAM-1) and $\alpha_4\,\beta_7$ integrin, which induces MC differentiation mainly via membrane-bound stem cell factor (SCF). As a result, progenitor-homing genes including *Itgb7, Cxcr2* or *Cx3cr1* are downregulated, thereby allowing the positioning of MCs at the blood vessels [18]. These „perivascular MCs“ have an important role during the initiation of allergic responses in the skin, which will be discussed later (see section 1.3.3). Additionally, MCs are found in the interstitial space of the skin, where they reside in close proximity to other resident immune cells including macrophages and DCs [1,19].

1.2.2 MC heterogeneity

In mice, MCs are typically divided based on the localization and protease content into two main subsets: connective tissue type MCs (CTMCs) and mucosal MCs (MMCs). CTMCs are predominantly located in the skin and peritoneal cavity and express the murine MC proteases (mMcpt)-4, -5, and -6. In contrast, MMCs reside within the epithelium of the gastrointestinal and respiratory tract and produce mMcpt-1 and -2 [20]. Additionally, the characteristics of the secretory granules differ between both subsets. In general, MC secretory granules are comprised of a serglycin core structure, to which polysaccharide chains of the glycosaminoglycan (GAG) type are covalently bound. Due to the negative charge of the GAGs, positively charged mediators (e.g. histamine) are strongly captured within the secretory granules. While CTMC secretory granules possess GAGs of the heparin type, MMC secretory granules contain chondroitin sulfate [21]. Furthermore, CTMC secretory granules are homogenous in size and rich in histamine, whereas MMC secretory granules vary in size and contain a lower amount of histamine [21,22]. In humans, fewer isoforms of MC-specific proteases exist. Therefore, the classification is different compared to mice. Human MCs are divided into tryptase-containing (MC_T), chymase-containg (MC_C) or tryptase- and chymase-containg (MC_{CT}) [20,21].

The broad classification of murine MCs was recently challenged by a study from Dwyer *et al.*, which demonstrated a significant interorgan heterogeneity of CTMCs. By analyzing the differentially expressed genes between CTMCs from five different locations, they found that peritoneal MCs exhibited a distinct transcriptional signature compared to skin and tongue MCs. The authors stated, that this tissue-specific heterogeneity may be induced by the specific microenvironment [23]. These results were confirmed by a study from Akula *et al.*, which compared the transcriptome of peritoneal MCs to 10 different mouse tissues including ear skin, lung, brain, tongue, heart, liver, pancreas, duodenum proximal part of the colon, spleen and uterus [24]. Thus, the tissue microenvironment has a tremendous effect on the MC phenotype, thereby driving MC heterogeneity.

1.2.3 MC receptors

As sentinels of the innate immune system, MCs have to recognize a variety of different stimuli. To this end, they are equipped with a wide range of receptors (Figure **1A**). The most studied one is the high-affinity receptor for immunoglobulin E (IgE), also known as Fcε receptor I (FcεRI). IgE antibodies are produced by plasma cells upon interaction with T_H2 cells and are implicated in the defense against parasites, including helminths. However, they can also be directed against harmless environmental molecules - referred to as allergens-, thereby causing type I allergic reactions including allergic rhinitis,

asthma and atopic dermatitis [25,26]. Besides the FcεRI, the recently discovered Mas-related G-protein coupled receptor X2 (MRGPRX2, in rodents: MRGPRB2) is critically involved in the activation of MCs during allergy. It can be stimulated by endogenous ligands such as the neuropeptide substance P (SP), which subsequently causes non-histaminergic itch. Furthermore, several cationic peptidergic drugs (e.g. icatibant) were demonstrated to directly interact with the MRGPRX2, thereby causing IgE-independent allergic reactions, also referred to as „pseudoallergies“ [27]. In order to identify invading pathogens, MCs express several PRRs, such as TLRs and NLRs [16,26]. Finally, MCs possess a plethora of cytokine (e.g. IL-3R, IL-4R, IL-15R, IL-18R, IL-33R (also known as “ST2”)), chemokine (e.g. C-C chemokine receptors (CCR)1, 3-5 and C-X-C chemokine receptors (CXCR)1-4) and growth-factor receptors (e.g. SCF receptor (SCFR, also known as “cKIT”), granulocyte-macrophage colony-stimulating factor (GM-CSF) receptor (GM-CSFR), vascular endothelial growth factor (VEGF) receptor (VEGFR)), which enable the complex intercellular communication with other immune and non-immune cells during homeostasis, infection and inflammation [28,29].

1.2.4 MC response and memory

In general, the MC response can be divided into three distinct steps (Figure **1B**). At first, the high amount of intracellular granules is exocytosed, within seconds after activation, in a process called “degranulation” [21]. The dynamics and features of MC degranulation depend on the activating stimuli. While SP, the complement activation products C3a and C5a, as well as endothelin 1, induce the rapid release of small and spherical granules, IgE causes a sustained MC activation, finally leading to the formation and secretion of heterogeneously shaped granules [30]. Additionally, MCs are capable of exocytosing only small parts of the content of secretory granules, a process referred to as „piecemeal degranulation“ [31]. The secretory granules store a plethora of mediators such as histamine and proteases (e.g. tryptases, chymases), but also preformed and fully active cytokines including tumor necrosis factor (TNF) [21]. As a next step, the activation induces the rapid synthesis and release of proinflammatory lipid mediators such as prostaglandin D_2 (PGD_2), leukotriene B_4 (LTB_4) and LTC_4. Finally, there is a *de novo* synthesis of cytokines including, TNF, IL-3, IL-4, IL-5, IL-6, IL-10, IL-13 and macrophage-colony stimulating factor (M-CSF), chemokines including C-C chemokine ligand (CCL)2, 3, 5, and C-X-C chemokine ligand (CXCL)1, 2, 8, as well as growth factors such as SCF and VEGF [16,26,28]. Depending on the activating stimuli, these steps can occur consecutively or separately. For example, IgE induces both, MC degranulation and the *de novo* synthesis of lipid mediators and cytokines [32,33], whereas adenosine triphosphate (ATP) mainly promotes MC degranulation and only moderate cytokine production [34].

After degranulation, MCs are capable of replenishing their granule pool, predominantly via the synthesis of new secretory granules. This process is termed „regranulation“ and was already discovered over 50 years ago [35]. Recently, Iskarpatyoti *et al.* could also demonstrate MC regranulation *in vivo*. Furthermore, they found that this process requires a metabolic shift in MCs, which is mediated by the glucose-6-phosphate transporter Slc37a2 and the metabolic sensor mammalian target of rapamycin complex 1 (mTORC1) [36]. Intriguingly, MCs may adjust their granule content during regranulation. Friend *et al*. could demonstrate that newly synthesized secretory granules of MCs in the gut had an altered ultrastructure and protease composition, following an infection with the parasite *Trichinellla spiralis*. These changes may improve the MC response to subsequent exposures and are therefore referred to as „memory-like features“ [37]. However, they may also play a crucial role during allergy and autoimmunity [38].

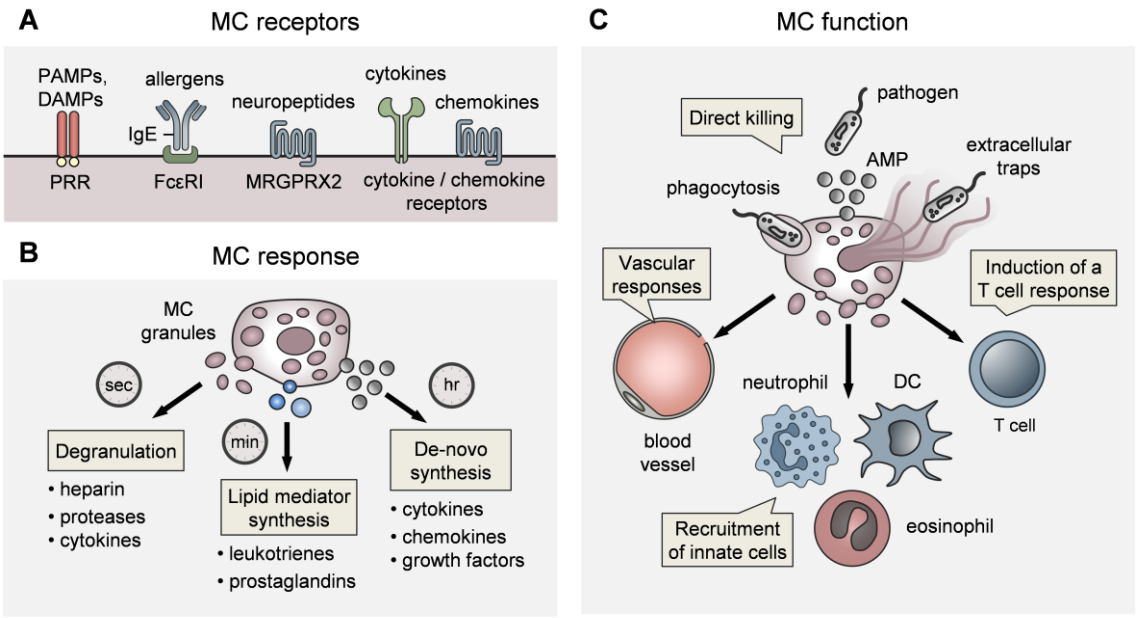

Figure 1| MC biology. A| In order to respond to different stimuli, MCs possess a variety of surface receptors including pattern-recognition receptors (PRR), the high affinity Immunoglobulin E (IgE) receptor (FcεRI), the Mas-related G-protein coupled receptor X2 (MRGPRX2), as well as cytokine and chemokine receptors. Pathogen-associated molecular patterns (PAMPs), danger-associated molecular patterns (DAMPs). **B|** The MC response is a three-step cascade. First, the high amount of secretory granules, which contain a variety of preformed mediators, is released within seconds in a process termed “degranulation”. Secondly, the activation induces a rapid lipid metabolism. Finally, there is a *de novo* synthesis of cytokines, chemokines and growth factors within hours. **C|** MCs play a crucial role in host defense. First, MCs directly kill invading pathogens through mechanisms including phagocytosis, the release of antimicrobial peptides (AMP) and the formation of extracellular traps. Secondly, MCs initiate immediate vascular responses and the recruitment of innate effector cells, such as neutrophils and eosinophils. Finally, MCs critically promote the induction of an adaptive immune response indirectly through the modulation of dendritic cell (DC) functionality and directly via the stimulation of T cells.

1.2.5 MC functions in immunity and host defense

Due to their strategic location at environmental interfaces, such as the skin and their immediate response, MCs critically contribute to inflammation and host defense (Figure **1C**). Upon sensing of PAMPs or DAMPs, MCs immediately induce vascular responses, including vasodilatation and a local increase in vessel permeability, which are a prerequisite for efficient immune cell infiltration and tissue migration. Subsequently, MCs mediate, via the release of cytokines and chemokines (e.g. TNF and CXCL2), the early recruitment and activation of innate effector cells, in particular neutrophils and eosinophils, which promote bacterial and parasite clearance, respectively [8,16,22]. MCs also directly participate in pathogen killing via three main mechanisms. At first, MCs secrete AMP (e.g. lipocalin-2, cathelicidin), which limit microbial growth or induce their death through the disruption of the cell membrane [6]. Secondly, MCs can engulf bacteria (e.g. enterobacteria) via phagocytosis and kill them through the production of reactive oxygen species (ROS) [39]. Finally, MCs are able to release net-like structures composed of DNA, histones and granule proteins (referred to as „MC extracellular traps“, MCET), which immobilize and degrade large bacteria and parasites. [40]. In addition to their innate functions, MCs also promote and regulate the induction of an adaptive immune response. On the one hand, MCs indirectly enhance T cell priming in the draining lymph node via the modulation of DC functionality in the periphery. On the other hand, MCs were reported to directly modulate T cell activity via the presentation of antigens bound to major-histocompatibillity complex (MHC)-I or MHC-II, as well as T cell proliferation, differentiation and recruitment through the release of specific cytokines (e.g. IL-4, IL-13) [41]. Taken together, MCs play an important role in the initiation of an innate, but also adaptive immune response during infection and inflammation. However, these MC functions are also implicated in the pathophysiology of a variety of allergies.

1.3 Allergic contact dermatitis

Allergic contact dermatitis (ACD) is a common skin disorder that is caused by direct contact with certain metal ions or low-molecular-weight-organic chemicals, also referred to as “haptens”. The acute inflammatory reaction presents as an eczematous rash, usually resolving on its own when triggers are avoided. However, continued exposure to the same hapten can prolong and exacerbate skin inflammation, leading to chronic symptoms such as lichenification, fissuring and scale [42]. As a consequence of changing lifestyles (e.g. common use of cosmetics), the prevalence of ACD has massively increased over the past years. Approximately 20 % of people worldwide are sensitized to at least one hapten [43]. Since ACD is particularly frequent in certain

professions, such as metal workers, hairdressers and health care workers, it represents a major socio-economic health problem [44].

1.3.1 Structure of the skin

The skin is comprised of three major layers including the epidermis, dermis and subcutis. The epidermis forms the outermost layer of the skin and functions as a physical barrier to the external environment. It mainly consists of keratinocytes, which are closely connected by tight junctions [4]. Additionally, Langerhans cells (LCs), which represent a unique subset of tissue-resident macrophages, can be found in the epidermis and constantly surveil the environment [45]. The dermis is located beneath the epidermis and is predominantly comprised of extracellular matrix (ECM). Within the ECM, a dense network of blood and lymphatic vessels is embedded. Moreover, several types of innate immune cells including dermal DCs, macrophages, as well as MCs reside within the dermis [46]. The subcutis represents the lowermost layer of the skin and mainly consists of connective and adipose tissue. It is particularly involved in the regulation of the body temperature but also protects organs from mechanical shock [4].

1.3.2 Haptens

Because of their small size, haptens are not noticed by the immune system and therefore can not elicit an immune response by themselves. However, they rapidly bind to self-proteins in the dermis, due to their negative charge. These modified proteins are then recognized by the immune system and can induce a response [47]. The most frequent hapten in humans is nickel, which is commonly used in jewelry. Furthermore, ingredients of fragrances and cosmetics, such as Myroxylon pereirae, p-phenylenediamine, methylchloroisothiazolinone/methylisothiazolinone, and colophonium often trigger ACD [43]. It is still barely understood, why some people develop ACD while others do not. However, there are certain risk factors known. In particular, other inflammatory skin diseases (e.g. atopic dermatitis) that cause alterations in the epidermal barrier, facilitate the penetration of haptens and thereby increase the risk for ACD. Furthermore, variations in genes, associated with antigen metabolism and uptake, as well as with the induction of an antigen-specific immune response were shown to be correlated with a higher risk for ACD [48].

1.3.3 Pathomechanisms in ACD

Contact hypersensitivity (CHS) represents a widely used mouse model to study the pathophysiological processes in ACD. In general, the immune events during CHS can be divided into two distinct phases: the sensitization and elicitation phase (Figure **2**) [1,49].

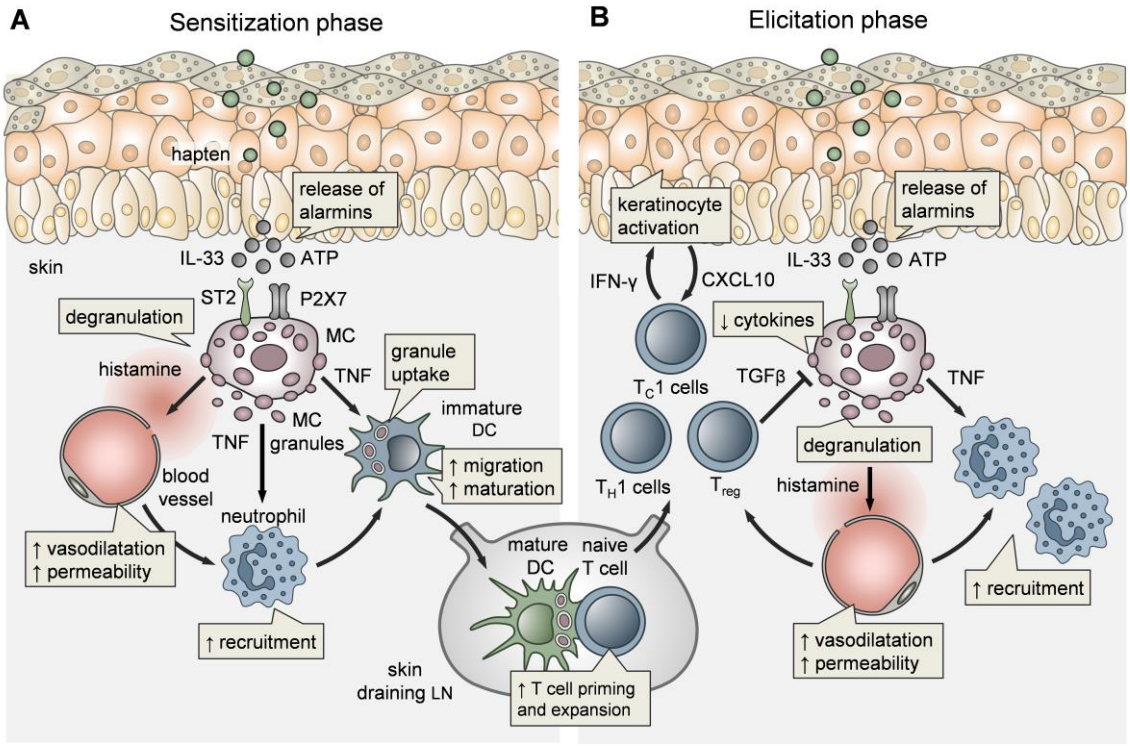

Figure 2| The role of MCs in the pathophysiology of CHS. A| Upon first contact with a hapten (referred to as "sensitization"), keratinocytes are rapidly activated and release alarmins, such as Interleukin-33 (IL-33) and adenosine triphosphate (ATP), which are sensed by MCs through the ST2 and P2X7 receptor, respectively. Subsequently, MCs degranulate and release a plethora of mediators. While histamine induces vasodilatation and an increase in vessel permeability, MC-derived tumor necrosis factor (TNF) facilitates the recruitment of neutrophils. Furthermore, the engulfment of MC secretory granules by DC, as well as MC-derived TNF both promote DC maturation and migration to the draining lymph node, where they prime hapten-specific T cells. **B|** Upon reexposure to the hapten (referred to as "elicitation"), MCs again mediate immediate vascular responses, as well as the recruitment of neutrophils. Additionally, type 1 cytotoxic T cells (T_C1) and type 1 T helper cells (T_H1) infiltrate the skin and amplify the inflammatory response via the release of cytokines. For instance, T_C1-derived interferon-γ (IFN-γ) stimulates keratinocytes, which in turn drive the recruitment of further effector T cells through the release of CXCL10 in a positive feedback loop. During the progression of the inflammatory response, regulatory T cells (T_{reg}) counterregulate MC cytokine production via the release of transforming growth factor-β (TGF-β). (Figure adapted from [1]).

1.3.3.1 Sensitization phase

Upon first contact with a hapten (referred to as "sensitization"), keratinocytes are rapidly activated and start to produce a variety of proinflammatory cytokines (e.g. TNF, IL-1β) and chemokines (e.g. CXCL1, CXCL2) [50]. Furthermore, the hapten induces a stress response in keratinocytes, leading to the release of DAMPs, including ATP and IL-33 [51,52]. Both ATP and IL-33 are directly sensed by tissue-resident MCs through the P2X purinoreceptor 7 (P2RX7) and ST2 receptor, respectively [34,53]. Consequently, MCs degranulate and release their preformed mediators. Our group demonstrated, that MC-derived histamine immediately induces vascular responses, including vasodilatation and a local increase in vessel permeability, leading to edema formation [54]. Moreover, MCs

initiate the early recruitment of neutrophils, which subsequently drive the local inflammatory response through the release of proinflammatory cytokines and ROS [55]. Finally, MCs play a crucial role in the induction of a hapten-specific adaptive immune response, representing a key event in the sensitization phase of CHS. More specifically, the engulfment of MC secretory granules and MC-derived TNF both stimulate DC maturation, as well as their migration from the skin to the draining lymph node, where they prime hapten-specific naïve T cells [2,56]. The effect of MC-derived TNF was restricted to $CD8^+$ DCs (also referred to as “cDC1”), which predominantly activate $CD8^+$ T cells [2]. In addition to MCs, also neutrophils were demonstrated to promote the migration of DCs and thereby the priming of hapten-specific naïve T cells in the draining lymph node. Consequently, these T cells proliferate and differentiate into hapten-specific effector and memory T cells [55].

1.3.3.2 Elicitation phase

Upon re-exposure to the same hapten (referred to as “elicitation”), keratinocytes again activate MCs via the release of ATP and IL-33, which rapidly induce vascular responses through histamine [53]. Moreover, keratinocytes and MCs mediate the early recruitment of neutrophils via the release of chemokines including CXCL1 and CXCL2, as well as TNF [57,58]. In this context, our group could recently demonstrate, that MC-derived TNF directly primes blood circulating neutrophils via binding to TNF receptor 1 (TNFR1) and thereby facilitates the transition from neutrophil rolling to firm adhesion and intravascular crawling and consequently the extravasation into the inflamed tissue. Importantly, perivascular MCs deliver the TNF via directional degranulation into the bloodstream [59]. Following the infiltration of neutrophils, keratinocytes also initiate the recruitment of hapten-specific effector T cells through the release of CXCL9 and CXCL10, which are then reactivated by antigen-presenting cells such as cutaneous DCs. In particular, $CD8^+$ T_C cells drive the inflammatory response in the elicitation phase [60–62]. More specifically, T_C cells stimulate keratinocytes through IFN-γ, which in turn promotes the recruitment of further effector T cells through the secretion of CXCL10 in a positive feedback loop [63,64]. Moreover, T_C cells induce keratinocyte apoptosis via FAS- and perforin-dependent pathways [65]. Recently, Chong *et al.* demonstrated that T_C cells also mediate the recruitment and subsequent activation of TNF/inducible nitric oxide (NO) synthase (iNOS)-producing monocytes through the release of IL-17 and IFN-γ, respectively [66]. In contrast to $CD8^+$ T cells, $CD4^+$ T cells were reported to have regulatory roles in hapten-induced skin inflammation [60,61,67]. Particularly, $CD4^+$ $CD25^+$ regulatory T cells (T_{reg}) can dampen the local inflammatory response via the release of the anti-inflammatory cytokines IL-10 and TGF-β and the expression of the inhibitory surface molecule cytotoxic T-lymphocyte associated protein-4 (CTLA-4) [68].

Additionally, they modulate the influx of leukocytes into the skin by reducing the expression of E-selectin and P-selectin, while also reinforcing junctions on the vascular endothelium [69,70]. These mechanisms may play a critical role in the resolution phase. However, the precise mechanisms governing the resolution of hapten-induced skin inflammation are still not fully understood.

1.4 Resolution of inflammation

In general, an acute inflammatory process can be divided into two distinct phases: induction and resolution [71]. In the induction phase, pathogen or danger signals trigger the activation of tissue-resident cells (e.g. MCs, macrophages) and subsequently the recruitment of effector cells (neutrophils, T cells), which together mount an inflammatory response. Once the activating stimuli have been removed, inflammation is terminated in the resolution phase, which consists of an orchestrated series of events (Figure **3**) [72].

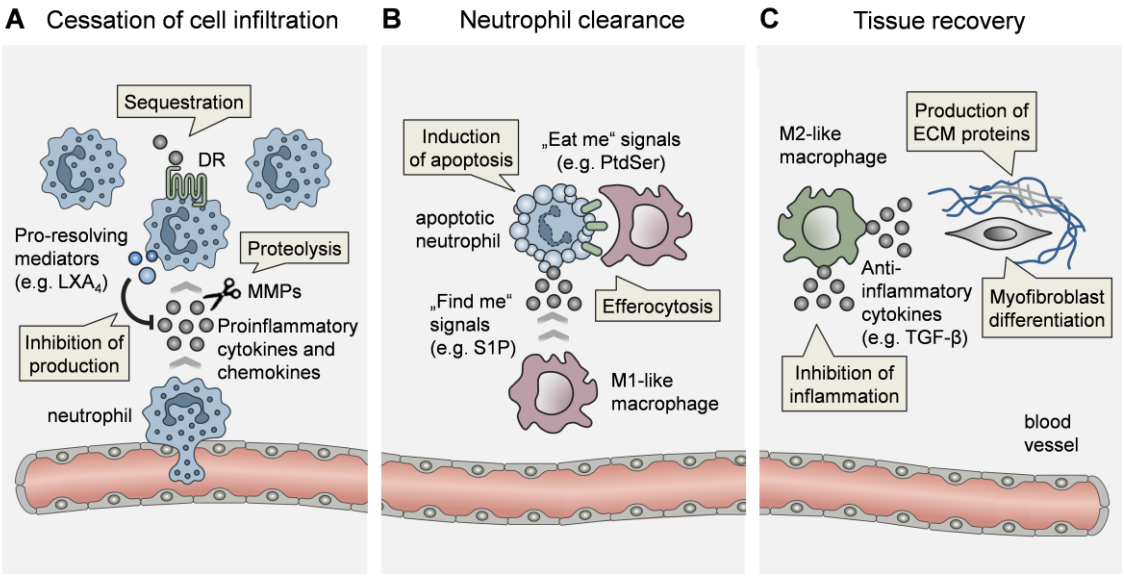

Figure 3| Key events in the resolution of inflammation. A| The resolution of inflammation starts with a switch in lipid mediator synthesis, leading to the production of pro-resolving mediators such as Lipoxin A_4 (LXA_4). These mediators counterregulate the production of proinflammatory cytokines and chemokines, which are subsequently inactivated by matrix metalloproteinases (MMP) through proteolysis or sequestered by decoy receptors (DR). This results in the cessation of immune cell infiltration **B|** As a next step, neutrophils undergo apoptosis and release “find me” signals including Sphingosine-1-phosphate (S1P), which attract macrophages. Additionally, neutrophils expose “eat me” signals such as phosphatidylserine (PtdSer), which promote their engulfment by macrophages, a process termed efferocytosis. **C|** The clearance of apoptotic neutrophils induces a shift in macrophages from a proinflammatory phenotype (referred to as “M1-like macrophage”), to one that is more anti-inflammatory (referred to as “M2-like macrophage”). M2-like macrophages secrete anti-inflammatory cytokines, such as transforming growth factor-β (TGF-β), which i.) inhibit further inflammation, ii.) foster the differentiation of myofibroblasts and iii.) enhance the production of extracellular matrix (ECM) proteins such as collagens, thereby facilitating the restoration of tissue homeostasis.

1.4.1 Initiation of the resolution phase

At the onset of inflammation, lipid mediators including prostaglandins and leukotrienes are rapidly synthesized by tissue-resident immune cells such as MCs and macrophages. While prostaglandins (e.g. PGE_2, PGD_2) induce immediate vascular responses including vasodilatation and an increase in vessel permeability, leukotrienes (e.g. LTB_4) critically promote the recruitment and extravasation of neutrophils into the inflamed tissue [73,74]. Most importantly, prostaglandins also initiate the resolution of inflammation. During the progression of the inflammatory response, PGE_2 and PGD_2 gradually promote a switch in neutrophil lipid mediator synthesis from proinflammatory LTB_4 to pro-resolving lipoxin A_4 (LXA_4), a process termed lipid mediator "class switching" [75]. Subsequently, LXA_4, as well as other pro-resolving lipid mediators such as resolvins, protectins and maresins, attenuate inflammation through the counterregulation of proinflammatory cytokine and chemokine production and thereby initiate the termination sequence [75–78].

1.4.2 Cessation of immune cell infiltration

A first step in the resolution of inflammation is the cessation of immune cell infiltration. To this end, chemokines, which critically promote the recruitment of leukocytes to the inflamed site, are inactivated by matrix metalloproteinases (MMPs) through proteolysis [71,79]. For example, MMP-12 cleaves the ELR amino acid motif of C-X-C chemokines such as CXCL1 and CXCL2, which is essential for receptor binding and thereby limits further neutrophil recruitment [80]. In addition, MMPs process C-C chemokines, which predominantly attract monocytes. More specifically, the cleavage of CCL7 by MMP-2 leads to the generation of an antagonist, which continues to bind to CCR1, -2 and -3, but is not able to induce downstream signalling [81]. Another important process is the sequestration of proinflammatory cytokines and chemokines via decoy receptors, a process termed cytokine/chemokine sequestration [82]. Structural decoy receptors such as IL-1 receptor type II (IL-1RII) and duffy antigen receptor for chemokines (DARC) bind certain cytokines including IL-1α and IL-1β, as well as chemokines including CXCL1, CXCL7, CXCL8, CCL2 and CCL5, respectively. However, they are not able to induce a cellular response due to molecular alterations [83,84]. Furthermore, pro- and anti-inflammatory stimuli (e.g. LPS, IL-10) can induce the uncoupling of classical chemokine receptors, such as CCR3 and CCR5, from intracellular signalling pathways thereby generating functional decoy receptors [85].

1.4.3 Neutrophil apoptosis and clearance by macrophages

During the induction phase, a substantial number of neutrophils is recruited to the site of inflammation, which have to be removed to restore tissue homeostasis. Upon extravasation into the tissue, neutrophil life span is modulated by the inflammatory

micromilieu [86]. For example, the proinflammatory cytokine TNF triggers neutrophil survival at low concentrations, whereas it promotes their apoptosis at high concentrations [87]. Additionally, pro-resolving lipid mediators such as LXA_4 and resolvin E1 initiate neutrophil apoptosis via the phosphorylation of pro-apoptotic mediators including B-cell lymphoma (BCL)-2-associated death promoter (BAD) and the activation of effector caspases, respectively [88,89]. Once apoptosis is induced, neutrophils secrete “find me” signals including lysophosphatidylcholine (LPC), sphingosine-1-phosphate (S1P), C-X3-C chemokine ligand 1 (CX3CL1), as well as nucleotides such as ATP and uridine triphosphate (UTP), which attract macrophages [90–93]. In addition, apoptotic neutrophils expose “eat me” signals on the cell surface, which foster the engulfment by macrophages, a process referred to as “efferocytosis”. One of the best-studied eat-me signal is phosphatidylserine (PtdSer), which is translocated from the inner to the outer leaflet of the plasma membrane after apoptosis induction [94,95]. Macrophages are able to sense PtdSer via several receptors such as T-cell immunoglobulin mucin protein 4 (TIM-4), brain-specific angiogenesis inhibitor 1 (Bai-1) and MER tyrosine kinase (MerTK). While TIM-4 and Bai-1 directly recognize PtdSer, MerTK interacts with serum proteins including growth-arrest specific protein 6 (GAS6) and protein S, which rapidly bind to exposed PtdSer (referred to as “bridging molecules”) [96–98]. Finally, these signals trigger the nonphlogistic clearance of apoptotic neutrophils by macrophages.

1.4.4 Macrophage polarization and tissue recovery

The efferocytosis of apoptotic neutrophils induces a shift in macrophages, from a proinflammatory phenotype (referred to as “M1-like macrophage”) to one, which is more anti-inflammatory (referred to as “M2-like macrophage”) [99,100]. These M2-like macrophages possess increased efferocytosis capacity and therefore play an important role in the removal of apoptotic neutrophils. Moreover, they produce anti-inflammatory cytokines such as IL-10 and TGF-ß, which both limit further inflammation, through the inhibition of proinflammatory cytokine and chemokine production [99]. Additionally, macrophage-derived TGF-ß stimulates the differentiation of fibroblasts to myofibroblasts, as well as the production of ECM proteins, such as collagen I and thereby critically promotes tissue regeneration [71]. However, if released in large amounts, TGF-ß can also drive fibrosis, a pathological process characterized by the excessive deposition of ECM finally leading to a loss of tissue architecture and function (reviewed in [101]). Therefore, tissue regeneration must be tightly regulated.

2 Aim of the study

ACD is a highly socioeconomically relevant skin disease, affecting at least 20 % of people worldwide [43]. The group of Anne Dudeck has substantially contributed to understanding the role of MCs in the pathogenesis of ACD (reviewed in [1]). Due to their capacity to rapidly release preformed mediators by degranulation, MCs play an important role in the initiation of an innate, but also adaptive immune response during hapten-induced skin inflammation. In this context, we recently demonstrated that MC-derived TNF critically promotes the early recruitment of neutrophils in CHS, the mouse model of ACD [59]. Surprisingly, we also found that in the absence of MC-derived TNF, although ear swelling in the induction phase of CHS was reduced, skin thickness did not normalize at later time points (unpublished). This suggests a novel role for MCs and MC-derived TNF in the resolution of inflammation, an aspect that has not been investigated so far. Consequently, this study aimed to decipher the mechanisms underlying the effects of MC-derived TNF on the resolution of hapten-induced skin inflammation.

To address this objective, distinct time points during the course of hapten-induced skin inflammation were depicted for the analysis of immune cell infiltration and the inflammatory micromilieu. Additionally, key events in the resolution phase including the counterregulation of cytokine and chemokine production, the termination of immune cell infiltration, the induction of neutrophil apoptosis, the phenotypical switch of macrophages, as well as the tissue remodeling should be examined.

3 Materials and Methods

3.1 Chemicals and reagents

Table 1| Chemicals and reagents

Chemicals	Source	Cat#
1-fluoro-2,4-dinitrobenzene (DNFB)	Sigma-Aldrich	D1526-25ML
2-propanol (Isopropanol)	Carl Roth	CP41.2
Acetic acid 100 %	Carl Roth	6755.1
Acetone	Fisher Scientific/J.T.Baker	8002
Accutase Cell Detachment Solution	Biolegend	423201
Ammonium chloride (NH_4Cl)	Carl Roth	P726.1
Bovine serum albumin (BSA)	GERBU Biotechnik GmbH	15030500
Chloroform	Sigma-Aldrich	288306
cOmplete™ Protease Inhibitor Cocktail	Merck	04693124001
CountBright™ Absolute Counting Beads	Thermo Fisher Scientific	C36950
Disodium phosphate ($Na_2HPO_4x2H_2O$)	Th. Geyer/CHEMSOLUTE	8622
DNase I, grade II from bovine pancreas	Roche/Sigma-Aldrich	10104159001
Ethanol, 99 % denatured with MEK, IPA and Bitrex® (min. 99.8 %)	Th. Geyer	2212.9010
Ethanol, absolute	Th. Geyer/CHEMSOLUTE	2246.1000
Ethidiumbromid solution 1 % (10 mg/ml)	Carl Roth	2218.1
Ethylenediamine tetraacetic acid disodium salt dehydrate (EDTA)	Carl Roth	8043.2
Fetal bovine serum (FBS)	Pan Biotech	S0615
Gibco™ 2-mercaptoethanol (β-mercaptoethanol)	Thermo Fisher Scientific	21985023
GM-CSF	PeproTech	315-03
Hyaluronidase	Sigma-Aldrich	H3506
Isofluran CP	Cp pharma	G83F20A

Chemicals	Source	Cat#
Isotonic sodium chloride solution (0.9 % NaCl)	Fresenius Kabi	06605514
Liberase™ TM	Roche/Sigma-Aldrich	5401119001
Lipopolysaccharide (LPS S. enterica serotype Minnesota)	Sigma Aldrich	L2137
Methanol	Carl Roth	8388.1
Olive Oil	Sigma-Aldrich	O1514-100ML
Penicillin/Streptomycin	Pan Biotech	P06-07050
Potassium bicarbonate ($KHCO_3$)	Carl Roth	748.1
Potassium chloride (KCl)	Carl Roth	6781.3
Potassium dihydrogen phosphate (KH_2PO_4)	Th. Geyer/CHEMSOLUTE	16480250
Proteinase K	Carl Roth	7528.5
RPMI-1640 Medium	PAN Biotech	P04-18500
Sodium dodecyl sulfate (SDS)	AppliChem GmbH	A2572.0250
Sodium chloride (NaCl)	Th. Geyer/CHEMSOLUTE	13671000
Sodium pyruvate	Pan Biotech	P04-43100
TRIS	Carl Roth	4855.2
Trizol	Life Technologies	15596018
Trypan Blue Solution	Sigma-Aldrich	T8154-100ML
UltraPure™ DNase/RNase-free distilled Water	Thermo Fisher Scientific	10977015

AppliChem GmbH (Darmstadt, Germany), Carl Roth (Karlsruhe, Germany), cp pharma (Burgdorf, Germany), Fisher Scientific/J.T.Baker (Schwerte, Germany), Fresenius Kabi (Bad Homburg, Germany), Merck (Darmstadt, Germany), Invitrogen (Carlsbad, USA), PAN Biotech (Aidenbach, Germany), Peprotech (Hamburg, Germany), quartett (Berlin, Germany), Sigma-Aldrich (Taufkirchen, Germany) Thermo Fisher Scientific (Waltham, USA), Th. Geyer/CHEMSOLUTE (Renningen, Germany)

3.2 Consumables

Table 2| Consumables

Consumable	Specification	Source
Cell strainer	40 µm, 100 µm, Nylon	Corning Inc.
Cell Culture flasks	T75	Greiner BIO-ONE
Cell scraper		SPL Life Sciences
Column for cell separation	LS	Miltenyi Biotec
Insulin syringe	0.5 ml	Braun
Microplates	6-Well flat bottom 96-Well V-bottom	Corning Inc.
Needles	Sterican 27G	Braun
Reaction tubes	0.5 ml 1.5 ml 2.0 ml	Sarstedt
	15 ml 50 ml	Greiner BIO-ONE
Reaction tubes (flow cytometry)	5 ml	Corning
PreCellys® tubes (tissue homogenization)	0.5 ml, 2.0 ml with 14 mm ceramic beads (CK14)	Bertin technologies
Serological pipettes	5 ml 10 ml 25 ml 50 ml	Corning Inc.
Syringe	Injekt-F Luer Solo 1ml	Braun

Bertin technologies (Montigny-le-Bretonneux, France), Braun (Melsungen, Germany), Croning Inc. (Corning, USA), Greiner BIO-ONE (Frickenhausen, Germany), Miltenyi Biotec (Bergisch Gladbach, Germany), Sarstedt (Nümbrecht, Germany), SPL Life Sciences (Myeon, Japan), TPP Techno Plastic Products AG (Trasadingen, Switzerland)

3.3 Devices and software

Table 3| Devices

Device	Specification	Source
Centrifuge	Heraeus Multifuge 3SR+Megafuge ST4R Plus	Thermo Fisher Scientific
Flow cytometer	LSR Fortessa I LSR Fortessa II	BD Biosciences
Gel chamber	Subcell® GT	Bio-Rad
Gel documentation system	Transilluminator with E.A.S.Y B-455-F camera	Herolab GmbH
Haemocytometer	Neubauer	Glaswarenfabrik Karl Hecht GmbH & CO KG
Incubator	Hera Cell 240	Thermo Fisher Scientific
Laminar Flow Workbench	Hera Safe KS18	Thermo Fisher Scientific
Magnetic Separator	QuadroMACS™	Miltenyi Biotec
Microplate Reader (ELISA)	Infinite	Tecan Group Ltd.
Microplate Reader (Multiplex)	Bio-Plex 200	Bio-Rad
Power supply for gel chamber	Power Pac 200 Power Pac Basic	Bio-Rad
Precision thickness gage	7313	Mitutoyo Deutschland
Spectrophotometer	NanoDrop 2000	Thermo Fisher Sientific
Thermocycler	T3000	Biometra GmbH
	Biometra trio	Biometra GmbH
Thermocycler qPCR	ABI Prism 7000	Applied Biosystems
ThermoMixer F1.5	F1.5	Eppendorf
Tissue homogenizer	PreCellys® 24	Bertin technologies
Water purification system	Milli-Q®	Merck Millipore

Applied Biosystems (Waltham, USA), BD Biosciences (Heidelberg, Germany), Bertin technologies (Montigny-le-Bretonneux, France), Biometra GmbH (Göttingen, Germany), Biolegend (San Diego, USA), Bio Rad (Hercules, USA) Eppendorf AG (Hamburg, Germany), Herolab GmbH (Wiesloch, Germany), Glaswarenfabrik Karl Hecht GmbH & CO KG (Sondheim vor der Röhn, Germany), Merck Millipore (Darmstadt, Germany), Miltenyi Biotec (Bergisch Gladbach, Germany), Mitutoyo Deutschland GmbH (Neuss, Germany), Tecan Group Ltd. (Männedorf, Switzerland), Thermo Fisher Scientific (Waltham, USA)

Table 4| Software

Software	Specification	Source
FACSDiva		BD Biosciences
FlowJo™ Software	Version 10	BD Biosciences
GraphPad Prism	Version 9.0.0	Dotmatics Limited
Magellan™		Tecan Group Ltd.
Microsoft Excel	Version 2016	Microsoft
Microsoft Power Point	Version 2016	Microsoft

BD Biosciences (Heidelberg, Germany), Dotmatics Limited (Windhill, UK), Microsoft (Redmond, USA), Tecan Group Ltd. (Männedorf, Switzerland)

3.4 Buffers and Media

Ear digestion medium

- serum-free RPMI-1640 supplemented with:
  - 396 U/ml DNase I
  - 62.5 µg/ml Liberase™ TM
  - 250 µg/ml Hyaluronidase

1x Erythrocyte lysis buffer

- ddH_2O supplemented with:
  - 155 nM NH_4Cl
  - 10 mM $KHCO_3$
  - 0.13 mM EDTA

1x MACS buffer

- 1x PBS supplemented with:
  - 2 mM EDTA
  - 0.5 % (w/v) BSA

Mouse medium

- RPMI-1640 supplemented with:
  - 10 % (w/v) FCS
  - 100 U/ml Penicillin
  - 100 µg/ml Streptomycin
  - 1mM Sodium pyruvate
  - 50 µM β-mercaptoethanol

1x PBS (pH 7.4-7.5)

- ddH_2O supplemented with:
  - 2.68 mM KCL
  - 1.47 mM KH_2PO_4
  - 8.1 mM $Na_2HPO_4x2H_2O$
  - 136.9 mM NaCl

1x TRIS-acetate-EDTA (TAE) buffer

- ddH_2O supplemented with:
  - 40 mM TRIS
  - 1 mM Na_2EDTA
  - 20 mM Acetic acid

Tissue lysis buffer

- ddH_2O supplemented with:
  - 100 mM TRIS (stock 1 M pH 8.5)
  - 5 mM Na_2EDTA (stock 0.5 M pH 8.0)
  - 0.2 % (w/v) SDS (stock 10 % (w/v) pH 7.2)
  - 200 mM NaCl

3.5 Oligonucleotides

Table 5| PCR-primers for genotyping of transgenic mice. Primer sequences are shown in 5' to 3' direction. Primers for genotyping were obtained from Thermo Fisher Scientific.

Target	Primer	Sequence
CD11c-Cre	CD11c-Cre fwd	ACT TGG CAG CTG TCT CCA AG
(200 nM)	CD11c-Cre rev	GCG AAC ATC TTC AGG TTC TG
General Cre	nls Cre UP1	GGA AAT GGT TTC CCG CAG AAC CTG A
(400 nM)	nls Cre DO2	GAT GAG TTG CTT CAA AAA TCC CTT CCA
	cA LoxP3 rev	GGC GAG CTC AGA CCA TAA CTT CG
GFP	oIMR1416	TCC TTG AAG AAG ATG GTG CG
(200 nM)	oIMR0872	AAG TTC ATC TGC ACC ACC G
IL-2	IL-2_fwd	CTA GGC CAC AGA ATT GAA AGA TCT
(200/400 nM)	IL-2_rev	GTA GGT GGA AAT TCT AGC ATC ATC C
Mcpt5-Cre	Mcpt5-Cre UP	ACA GTG GTA TTC CCG GGG AGT GT
(200 nM)	M5/M6-Cre DO	GTC AGT GCG TTC AAA GGC CA
	Mcpt5-Ex1 DO3	TGA GAA GGG CTA TGA GTC CCA
tdRFP	HL15 (RFP mut)	AAG ACC GCG AAG AGT TTG TCC
(400 nM)	HL152 (wt)	AAG GGA GCT GCA GTG GAG TA
	HL154 (mut)	TAA GCC TGC CCA GAA GAC TC
TNF-FL	TNF-fl-fwd	TGA GTC TGT CTT AAC TAA CC
(200 nM)	TNF-fl-rev	CCC TTC ATT CTC AAG GCA CA
TNFR1-FL	TnfR1FL_854	CAA GTG CTT GGG GTT CAG GG
(200 nM)	TnfR1FL_855	CGT CCT GGA GAA AGG GAA AG

Table 6| Primers for qPCR. Primer sequences are shown in 5' to 3' direction. Primers for qPCR were obtained from Invitrogen (Carlsbad, USA).

GOI	Primer	Sequence
Collagen I	forward	CTT CAC CTA CAG CAC CCT TGT G
(Col1a1)	reverse	TGA CTG TCT TGC CCC AAG TTC
Collagen III	forward	AAG GCG AAT TCA AGG CTG AA
(Col3a1)	reverse	TGT GTT TAG TAC AGC CAT CCT CTA GAA
Collagen IV	forward	ACG GGC CAA CGC TTC TTC
(Col4a2)	reverse	CAT GAT CCC AGT CTT TGA GCT CTA
Fibronectin	forward	GTG TAG CAC AAC TTC CAA TTA CGA A
(Fn1)	reverse	GGA ATT TCC GCC TCG AGT CT
Glyceraldehyde-3-phosphat-dehydro-genase (GAPDH)	forward	TGT TCC TAC CCC CAA TGT GT
	reverse	GGT CCT CAG TGT AGC CCA AG
Laminin	forward	TGA GTC TGT CTT AAC TAA CC
(Lama5)	reverse	CCC TTC ATT CTC AAG GCA CA

3.6 Antibodies

Table 7| Antibodies for flow cytometry

Antibody conjugates: Alexa Fluor 647 (AF647), Allophycocyanin (APC), Brilliant Violet™ (BV), Brilliant™ Ultraviolet (BUV), Cyanin™ (Cy), Fluoresceinisothiocyanat (FITC), Pacific Blue™ (PB), Phycoerythrin (PE), Peridinin-Chlorophyll-Protein (PerCP).

Antibody	Fluorophore	Clone	Source	RRID
CD3ε	PE-Cy7	145-2C11	Biolegend	AB_312685
CD4	PerCP-eFluor 710	GK1.5	Thermo Scientific	AB_11150050
CD4	APC	GK1.5	Biolegend	AB_469320
CD8a	eFluor 450	53-6.7	eBioscience	AB_1272198
CD8a	AF488	53-6.7	Biolegend	AB_389304
CD11c	AF488	N418	Biolegend	AB_313775

Antibody	Fluorophore	Clone	Source	RRID
CD11c	BUV496	N418	BD Biosciences	AB_2874611
CD11b	PerCP-Cy5.5	M1/70	Biolgend	AB_893232
CD11b	BUV737	M1/70	BD Biosciences	AB_2738811
CD16/32 (FC Block)		93	Biolegend	AB_1574975
CD31	PE-Cy7	390	Biolegend	AB_830757
CD45	BV570	30-F11	Biolegend	AB_2562612
CD103	PE-Cy7	2E7	Biolegend	AB_2563691
CD115	APC	AFS98	Biolegend	AB_2085222
CD120a (TNFR1)	APC	55R-286	Biolegend	AB_2208779
CD120a (TNFR1)	PE	55R-286	Biolegend	AB_313532
CD192 (CCR2)	PE-Cy7	SA203G11	Biolegend	AB_2616983
CD206	BV421	C068C2	Biolegend	AB_2562232
F4/80	APC-eFluor780	BM8	eBioscience	AB_2735036
gp38	APC	8.11	Biolegend	AB_10613649
Ly6C	PE	HK1.4	eBioscience	AB_10804510
Ly6G	AF488	1A8	Biolegend	AB_2561340
Ly6G	APC	1A8	Biolegend	AB_2227348
Ly6G	BUV395	1A8	BD Biosciences	AB_2716852
MHC-II	AF647	M5/114.15.2	Biolegend	AB_493525
MHC-II	eFluor 450	M5/114.15.2	eBioscience	AB_1272204
MHC-II	PE	M5/114.15.2	Biolegend	AB_313323
NK1.1	APC-Cy7	PK136	Biolegend	AB_830871
NKp46	BV421	29A1.4	Biolegend	AB_2563104

BD Biosciences (Heidelberg, Germany), Biolegend (San Diego, USA), eBioscience/Thermo Fisher Scientific (Waltham, USA),

Table 8| Antibodies for *in vivo* TNF neutralization. (BioXcell Lebanon, USA)

Antibody	Clone	Source	RRID
Anti mouse TNF-α	TN3-19.12	BioXcell	AB_2687725
Polyclonal Armenian hamster IgG	N/A	BioXcell	AB_1107773

3.7 Commercial assays

Table 9| Critical commercial assays

Assay	Source	Cat#
$CD8a^+$ T cell Isolation Kit	Miltenyi Biotec	130-104-075
Cytokine and Chemokine 26-Plex Mouse	Thermo Fisher Scientific	EPX260-26088-901
Dream Taq Green DNA Polymerase	Thermo Fisher Scientific	EP0714
ELISA-Kit for Collagen Type I	Cloud-Clone Corp.	SEA-571Mu
ELISA-Kit for Collagen Type III	Cloud-Clone Corp.	SEA-176Mu
ELISA-Kit for Collagen Type IV	Cloud-Clone Corp.	SEA180Mu
ELISA-Kit for Fibronectin	Cloud-Clone Corp.	SEA037Mu
High-Capacity cDNA Reverse Transcription Kit	Thermo Fisher Scientific	4368814
Mouse IL-17 Quantikine ELISA Kit	R&D Systems	M1700-1
MILLIPLEX® Mouse MMP Magnetic Bead Panel 3	Merck	MMMP2MAG-79K
SYBR® Green PCR Master Mix	Thermo Fisher Scientific	4309155

Cloud-Clone Corp. (Houston, USA), Merck (Darmstadt, Germany), Miltenyi Biotec (Bergisch Gladbach, Germany), R&D Systems (Minneapolis, USA), Thermo Fisher Scientific (Waltham, USA)

3.8 Mice

All mice were bred under specific pathogen-free (SPF) conditions at the central animal facility of the Otto-von-Guericke-University, Magdeburg. Mouse lines are listed in Table **10**. In all experiments, Cre^- littermates served as controls. Mice were used for

experiments at the age of 7-16 weeks. All experimental procedures were approved by the Landesverwaltungsamt Sachsen Anhalt (42502-2-1416UniMD and 203.m-42502-2-1732 UniMD) and were performed in accordance with the guidelines of the animal welfare office of the Otto-von-Guericke-University, Magdeburg.

Table 10| Mouse lines

Mouse line	International nomenclature	Source	Ref
C57BL/6JRj	-	Janvier Labs Cat# JAX 000664	
CD11c-Cre TNFR1-FL x	B6.Cg-Tg(Itgax-cre)1-1Reiz/J x B6.129P2(Cg)-Tnfrsf1atm3.1Gkl/Flmg	In-house breeding	[102]
Mcpt5-Cre x TNF-FL	B6-Tg(Cma1-cre)#Roer x Tnftm1.1Sned	In-house breeding	[2,103,104]
Mcpt5-Cre LysM-GFP x tdRFP x TNF-FL	B6-Tg(Cma1-cre)#Roer x B6.129(Cg)-Lyz2tm1.1Graf/Mmmh x Gt(ROSA)26Sortm1Hjf x Tnftm1.1Sned	In-house breeding	[103–105]
LysM-Cre x TNFR1-FL x	B6.129P2-Lyz2tm1(cre)Ifo/J x B6.129P2(Cg)-Tnfrsf1atm3.1Gkl/Flmg	In-house breeding	[102,106]

3.9 Molecular-biological methods

3.9.1 DNA isolation from ear skin and tail biopsies

For genotyping of transgenic mice, genomic deoxyribonucleic acid (DNA) was isolated from ear skin or tail biopsies. At first, biopsies were resuspended in 300 µl (ear skin biopsies) or 600 µl (tail biopsies) tissue lysis buffer (3.4) containing 2 % Proteinase K and incubated for 2 h in a ThermoMixer (56°C, 800 rpm) to lyse the tissue. Non-lysed tissue was separated by centrifugation (16,000 x g, 10 min, room temperature (RT)) and the supernatant was transferred to a new 1.5 ml reaction tube. Next, the DNA was precipitated by adding equal volumes of Isopropanol and gently inverting the reaction tubes. Samples were centrifuged (16,000 x g, 10 min, RT) and the supernatant was discarded. Then, DNA was washed once with 400 µl (ear skin biopsies) or 800 µl (tail biopsies) 70 % ethanol in nuclease-free water. After centrifugation (16,000 x g, 5 min, RT), the supernatant was discarded and the remaining ethanol was removed by air drying for 2 h. Finally, DNA was eluted in 50 µl (ear skin biopsies) or 100 µl (tail biopsies) nuclease-free water and stored for genotyping at 4°C.

3.9.2 Genotyping of transgenic mice

After DNA isolation, gene regions of interest were amplified using the polymerase chain reaction (PCR). To this end, 2 µl genomic DNA was added to 14 µl reaction mix (Table **11**) containing one of the primer pairs listed in Table **5**. Additionally, 2 µl wildtype (WT) mouse DNA was used as wt control, while 2 µl nuclease-free water served as negative control. PCR reactions were performed in a Thermocycler according to the amplification programs shown in Table **12** and Table **13**.

Table 11 Reaction mix for genotyping. Reagents were obtained from Thermo Fisher Scientific.

Component	Stock concentration	Volume per reaction [µl]	Final concentration
DreamTaq Green-Buffer	10x	1.6	1x
dNTP Mix	10 mM	0.32	0,2 µM
Primer fwd	10 mM	0.32/0.64	0,2/0.4 mM
Primer rev 1	10 mM	0.32/0.64	0.2/0.4 mM
Primer rev 2	10 mM	0.32/0.64	0.2/0.4 mM
DreamTaq DNA Polymerase	5 U/µl	0.06	0.3 U
Nuclease-free water		ad to 14 µl	

Table 12 | Temperature profiles for the general Cre, GFP, IL-2, Mcpt5-Cre and tdRFP genotyping PCR. X: cycle 1-2: 60°C, cycle 3-4: 58°C, cycle 5-6: 56°C

Step	Temperature [°C]	Time [s]	Cycles
Initial denaturation	95	240	
Denaturation	95	30	
Annealing	X	30	6x
Extension	72	45	
Denaturation	95	30	
Annealing	54	30	34x
Extension	72	45	
Final extension	72	600	
Cooling	15	∞	

Table 13| Temperature profiles for the CD11c-Cre genotyping PCR.

Step	Temperature [°C]	Time [s]	Cycles
Initial denaturation	95	120	
Denaturation	95	30	
Annealing	63	45	30x
Extension	72	45	
Final extension	72	300	
Cooling	15	∞	

3.9.3 Agarose gel electrophoresis

In order to separate the amplicons, PCR products were loaded on a 2 % agarose (w/v) gel in 1x TAE buffer (3.4). Additionally, a 100 bp DNA ladder was added to determine the amplicon size later. Subsequently, electrophoresis was performed at 100 V to 135 V. Afterwards, the agarose gel was incubated for 20 min in 1x TAE supplemented with 1 µg/ml ethidium bromide to stain the DNA. Separated amplicons were documented using the Herolab Transilluminator equipped with a Herolab E.A.S.Y B-455-F camera.

3.9.4 RNA extraction from ear skin biopsies

Gene expression analysis of specific genes was performed together with the help of Dr. Yan Fu (Institute of Molecular and Clinical Immunology, Otto-von-Guericke-University, Magdeburg). For extraction of total ribonucleic acid (RNA), murine ear skin biopsies (½ ear) were transferred to 0.5 ml PreCellys® tubes containing 14 mm ceramic beads (CK14) and 350 µl Trizol. Subsequently, the tissue was mechanically homogenized using the PreCellys® 24 tissue homogenizer (program: 2x 30 s at 6500 rpm, 20 s break). Samples were further incubated for 5 min at RT and transferred to 1.5 ml reaction tubes. In order to separate RNA from DNA and proteins, 140 µl chloroform was added and the reaction tubes were gently inverted for 15 s. After centrifugation (15 min, 12,000 x g, 4°C), the aqueous phase (containing the RNA) was carefully transferred to a 1.5 ml reaction tube. RNA was precipitated by the addition of 350 µl Isopropanol and incubated for 10 min at RT. Samples were centrifuged (10 min, 12,000 x g, 4°C) and the supernatant was discarded. Then, RNA was washed once with 700 µl 75 % ethanol in nuclease-free water. After centrifugation (5 min, 12,000 x g, 4°C), the supernatant was discarded and the remaining ethanol was removed by air drying for 10-20 min. Finally, RNA was eluted in 25 µl nuclease-free water. Concentration and purity were measured using the NanoDrop.

3.9.5 Preparation of cDNA

As a next step, purified RNA was converted to complementary DNA (cDNA) using the High-Capacity cDNA Reverse Transcription Kit (Table **9**) according to the manufacturer's instructions. In detail, 100-500 ng RNA per sample was diluted to a volume of 10 µl with sterile nuclease-free water and added to 10 µl reaction mix. Additionally, RT-minus controls were prepared in the same manner while the reverse transcriptase was replaced by nuclease-free water. Samples were incubated for 120 min at 37°C. Then, 2 to 5 µl cDNA from every sample were pooled to prepare standard curves and positive controls. The remaining cDNA was diluted to a concentration of 1 ng/µl and stored at -80°C.

3.9.6 Gene expression analysis by quantitative PCR (qPCR)

For gene expression analysis, 5 µl cDNA template were added to 15 µl qPCR reaction mix containing 10 µl SYBR Green Master mix, 0.6 µl forward and reverse primer (10 µM) for the respective gene (Table **14**) and 4.2 µl nuclease-free water. Samples were run in technical triplicates. qPCR was performed with the ABI Prism 7000 according to the amplification program shown in Table **15**. Afterwards, Ct-values of selected genes were normalized to the expression of the housekeeping gene *Glyceraldehyde-3-phosphat-dehydrogenase (GAPDH)* and further processed according to the ΔΔCT method [107].

Table 14| Primers for qPCR. Primer sequences are shown in the 5' to 3' direction. Primers for qPCR were obtained from Invitrogen (Carlsbad, USA).

GOI	Primer	Sequence
Collagen I	forward	CTT CAC CTA CAG CAC CCT TGT G
(Col1a1)	reverse	TGA CTG TCT TGC CCC AAG TTC
Collagen III	forward	AAG GCG AAT TCA AGG CTG AA
(Col3a1)	reverse	TGT GTT TAG TAC AGC CAT CCT CTA GAA
Collagen IV	forward	ACG GGC CAA CGC TTC TTC
(Col4a2)	reverse	CAT GAT CCC AGT CTT TGA GCT CTA
Fibronectin	forward	GTG TAG CAC AAC TTC CAA TTA CGA A
(Fn1)	reverse	GGA ATT TCC GCC TCG AGT CT
GAPDH	forward	TGT TCC TAC CCC CAA TGT GT
	reverse	GGT CCT CAG TGT AGC CCA AG
Laminin	forward	TGA GTC TGT CTT AAC TAA CC
(Lama5)	reverse	CCC TTC ATT CTC AAG GCA CA

Table 15| Temperature profiles for gene expression analysis

step	temperature [°C]	time [s]	cycles
denaturation	95	15	40x
annealing/extension	60	60	
dissociation	95	15	
	60	20	
	95	15	

3.10 Animal based-methods

3.10.1 Contact hypersensitivity

CHS represents a well-established murine model of delayed-type hypersensitivity and was induced as described previously [54]. In brief, mice (Table **10**) were sensitized by an epicutaneous application of 100 µl 0.5 % DNFB (v/v) in acetone/olive oil (4:1) on the shaved back skin. Six days later, mice were challenged by an epicutaneous application of 10 µl 0.2 % DNFB (v/v) in acetone/olive oil (4:1) on both sides of the right ear. Mice treated only with the solvent (acetone/olive oil) served as vehicle (veh) control. The inflammatory response was assessed by means of ear swelling. In detail, ear thickness was measured before and several times after DNFB challenge with a precision thickness gauge and ear swelling was calculated as percent increase compared to pre-challenged ear thickness. Furthermore, immune cell infiltration (3.13.2) and the release of specific mediators (3.13.3) was quantified in ear skin.

3.10.2 Adoptive Transfer of hapten-primed $CD8^+$ T cells

A total of $4.0*10^6$ $CD8^+$ T cells in 50 µl sterile 1x PBS were intravenously (i.v.) injected to sensitized Mcpt5-Cre^+ x $TNF^{fl/fl}$ mice by retro-orbital injection using an insulin syringe. Injection of PBS only served as a control. Subsequently, mice were challenged with DNFB (3.10.1).

3.10.3 TNF depletion

In order to deplete TNF, 70 µl sterile 1x PBS containing 500 µg anti-TNF-antibody were i.v. injected to C57BL/6JRj mice by retro-orbital injection using an insulin syringe 2 h after DNFB-sensitization (3.10.1). Mice, that were injected with 70 µl 1x PBS containing 500 µg Immunoglobulin G isotype served as a control.

3.11 Surgical methods and murine cell isolation

At different time points after DNFB challenge (3.10.1), mice were euthanized with an overdose of isoflurane in accordance with the legislative of the German Federal Republic (TierSchVersV, Anlage 2). Subsequently, mice were fixed on a surgical board, disinfected with 70 % ethanol and different organs were prepared.

3.11.1 Blood collection and preparation

In order to collect blood, the thoracic cavity was opened by the use of surgical scissors and forceps and the left ventricle of the heart was punctured with a 27G needle and a 1 ml syringe. For analysis of immune cell numbers, 40 µl of the blood was mixed thoroughly with 20 µl heparin (500 U/ml), to avoid clotting. Then, red blood cells were lysed by incubating for 3 min at RT in 3 ml erythrocyte lysis buffer (3.4). After incubation, cells were washed once with 13 ml 1x PBS and stained with the respective antibodies for flow cytometry (3.13.2). In order to quantify cytokines and chemokines (3.13.3), the remaining blood was incubated for 20 min at room temperature and then centrifuged (20 min, 400 x g). Afterwards, the serum was transferred to a 1.5 ml reaction tube and stored for further analysis at -80°C.

3.11.2 Preparation of single-cell suspensions from ear skin

For the analysis of cell subsets in ear skin (3.13.2), the ear pinnae was removed by the use of a surgical scissor and carefully separated into the dorsal and ventral layers. Both layers were dissected into small pieces by the use of a scalpel and transferred to a 2.0 ml reaction with 0.5 ml serum-free RPMI-1640 on ice. In order to dissolve the tissue, 0.5 ml ear digestion medium (3.4) was added and samples were incubated in a thermomixer (37°C, 1400 rpm). After an incubation of 1 hr, the enzymatic reaction was stopped by transferring the samples on ice. Subsequently, the cell suspension was filtered through a 100 µm cell strainer to remove non-lysed tissue and washed once with 1 ml 1x PBS. After centrifugation (365 x g, 5 min, 4°C), cells were resuspended in 100 µl MACS buffer and transferred to a 96-V-Well microplate for antibody staining.

3.11.3 Preparation of tissue homogenates from ear skin

For the preparation of tissue homogenates from ear skin, biopsies were transferred to 0.5 ml (1/2 ear) or 2.0 ml PreCellys® tubes (1 ear) and weighed. Subsequently, 14 mm ceramic beads (CK14) and 250 µl (1/2 ear) or 500 µl (1 ear) 1x PBS containing complete protease Inhibitor were added. The tissue was mechanically homogenized using the PreCellys® 24 tissue homogenizer (program: 2x 30 s at 6500 rpm, 20 s break). Afterwards, extracts were filtered through a 40 µm cell strainer and stored at -80°C until use (3.13.3).

3.11.4Preparation of single-cell suspensions from spleen

For the analysis of immune cell subsets in the spleen (3.13.2), the organ was carefully isolated by the use of surgical scissors and forceps and gently mashed through a 100 µm cell strainer placed in a 6-well plate with 5 ml 1x PBS. Afterwards, the single-cell suspension was centrifuged (365 x g, 5 min, 4°C), the supernatant was discarded and the cells resuspended in 1 ml erythrocyte lysis buffer (3.4). After an incubation of 1 min, cells were washed once with 14 ml 1x PBS and resuspended in 5 ml 1x PBS. 100 µl of the cell suspension was used for flow cytometry analysis of immune cell subsets.

3.11.5Preparation of single suspensions from bone marrow

For the analysis of immune cell subsets in the BM (3.13.2), or the generation of bone-marrow-derived DCs (BMDCs) (3.12.1), one femur (immune cell analysis) or both femurs and tibias (BMDC generation) were dissected and carefully removed by dislocating the hip joints. Under sterile conditions, the condyles were cut off and the bones of one leg were transferred into a 0.5 ml reaction tube with a hole, placed in a 1.5 ml reaction tube with 100 µl 1x PBS. Subsequently, the BM was flushed out by centrifugation (16,000 x g, 15 sec, RT), resuspended in 1 ml 1x PBS and filtered through a cell strainer (100 µm). In order to eliminate red blood cells, the single-cell suspension was centrifuged (365 x g, 5 min, 4°C) and cells were resuspended in 1 ml erythrocyte lysis buffer (3.4). After an incubation of 1 min, cells were washed once with 14 ml 1x PBS.

3.11.6Preparation of single-cell suspensions from inguinal lymph node

For adoptive transfer of $CD8^+$ T cells (3.10.2), both inguinal lymph nodes were carefully isolated by the use of surgical scissors and gently mashed under sterile conditions through a 40 µm cell strainer, placed in a 6-well plate containing 5 ml sterile 1x PBS. The resulting single-cell suspensions were pooled, centrifuged (365 x g, 5 min, 4°C) and the cells were resuspended in 1 ml sterile 1x PBS after discarding the supernatant. Afterwards, cells were counted (3.11.7) and $CD8^+$ T cells were isolated using magnetic cell separation (3.13).

3.11.7Cell counting

In order to count the cells, 10 µl of the cell suspension was mixed with 10 µl trypan blue solution and transferred to a Neubauer hemocytometer. The absolute cell number was calculated according to the following equation:

$$absolute\ cell\ number = \frac{number\ of\ cells * volume * dilution * 10.000}{number\ of\ biq\ squares}$$

3.12 Cell-biological methods

3.12.1 Generation of BMDCs

For the generation of BMDCs, BM cells (3.11.5) were resuspended in 20 ml mouse medium supplemented with 10 ng/ml recombinant murine GM-CSF, seeded into a T75 cell culture flask and incubated at 37°C and 5% carbon dioxide (CO_2) under humid atmosphere. On the next day, non-adherent cells were removed and 20 ml mouse medium supplemented with 10 ng/ml recombinant murine GM-CSF was added. On day 4 of culture, the medium was replaced by 20 ml fresh mouse medium supplemented with 5 ng/ml recombinant murine GM-CSF. BMDCs were used for experiments on day seven of cell culture.

3.12.2 Lipopolysaccharide (LPS) stimulation of BMDCs

To detach the cells, BMDCs were washed once with 10 ml sterile 1x PBS and incubated for 15 min with Accutase Cell Detachment Solution (5 ml/T75 cell culture flask) at 37 °C and 5 % CO_2. Subsequently, the reaction was stopped by adding 10 ml mouse medium and the remaining adherent cells, were gently detached with a cell scraper. The cell suspension was transferred to a 50 ml reaction tube, centrifuged (365 x g, 5 min, 4°C) and the supernatant was discarded. BMDCs were resuspended in 1 ml mouse medium and counted. For the stimulation with LPS, BMDCs ($3{,}3*10^5$ cells/well) were seeded into 6-well cell culture plates containing 2 ml mouse medium supplemented with 5 ng/ml recombinant murine GM-CSF and incubated at 37°C and 5% CO_2. The next day, BMDCs were stimulated with 100 ng/ml LPS for 6 hr. Afterwards, cells were washed once with 1x PBS and incubated for 15 min with Accutase Cell Detachment Solution (1 ml/well) at 37°C and 5 % CO_2. The reaction was stopped by adding 2 ml mouse medium and the remaining adherent cells were gently detached with a cell scraper. The cell suspension was transferred to a 50 ml reaction tube, centrifuged (365 x g, 5 min, 4°C) and the supernatant was discarded. Finally, BMDCs were analysed via flow cytometry (3.13.2).

3.13 Immunological methods

3.13.1 Magnetic cell separation (MACS)

$CD8^+$ T cells from single-cell suspensions of inguinal lymph nodes (3.11.6) were purified by negative selection using a $CD8a^+$ T cell Isolation Kit (Table **9**) according to the manufacturer's instructions. In detail, lymph node cells were resuspended in MACS buffer (40 µl per 10^7 cells) supplemented with a biotin antibody cocktail (10 µl per 10^7 cells) and incubated for 10 min at 4°C. Subsequently, MACS buffer (30 µl per 10^7 cells) containing anti-Biotin-Microbeads (20 µl per 10^7 cells) was added and cells were further

incubated for 10 min at 4°C. In order to isolate the $CD8^+$ T cells, the cell suspension was transferred to a LS-Column, placed in the QuadroMACS® separator and the flow through containing the $CD8^+$ T cells was collected. Afterwards, the column was rinsed with 3 ml MACS buffer and cells were counted (3.11.7). Purity (> 95 %) was always confirmed by flow cytometry (3.13.2).

3.13.2Flow cytometry

Flow cytometry represents a key method in immunological research, facilitating the phenotypical identification and characterization of different cell populations in single-cell suspensions [108]. For analysis of immune cell subsets in different organs, 100 µl of the respective single-cell suspensions (3.11) were transferred to a 96-well V-plate, centrifuged (365 x g, 5 min, 4°C) and the supernatant was discarded. Cells were resuspended in 50 µl MACS buffer containing 1 µg/µl Fc-block to prevent unspecific binding of fluorescently-labeled antibodies. After an incubation of 20 min at 4°C, samples were centrifuged (365 x g, 5 min, 4°C) and the supernatant was discarded. Subsequently, cells were resuspended in 50 µl MACS buffer containing fluorescently-labeled antibodies (Table **7**) and incubated for 30 min at 4°C. Then, cells were washed once with 150 µl MACS buffer centrifuged (365 x g, 5 min, 4°C) and resuspended in 100 µl MACS buffer. In order to calculate absolute cell numbers, 10 µl CountBright™ Absolute Counting Beads were added to each sample. Finally, specimens were collected with a BD LSR Fortessa I or II and analysed using FlowJo™ software.

3.13.3 Quantification of cytokines, chemokines and MMPs using ELISA and multiplex approaches

For the quantification of cytokines, chemokines, MMPs and matrix proteins in ear skin homogenates (3.11.3) and serum (3.11.1), sandwich enzyme-linked immunosorbent assays (ELISAs), as well as bead-based multiplex assays were used. Both methods are based on the same principle. At first, one (ELISA) or multiple analytes of interest (multiplex) are immobilized at the surface of a plate (ELISA) or fluorescently-labeled beads (multiplex) via specific capture antibodies. The different bead/capture antibody complexes can be distinguished by means of fluorescence intensity. Afterwards, biotinylated detection antibodies specifically bind to the analyte/s of interest, which subsequently interact either with streptavidin-horseradish peroxidase (HRP) conjugates (ELISA) or streptavidin-PE (multiplex). Finally, the turnover of a HRP-substrate such as tetramethylbenzidine (TMB) or the fluorescence intensity of PE is measured, in order to calculate the concentration of the analyte/s of interest.

The different immunoassays (Table **9**) were performed according to the manufacturer's instructions and measured with the Tecan infinite (ELISA) or Bio-Plex 200 (multiplex).

3.14 Data analysis and statistics

No statistical methods were used to predetermine sample size, but similar sample sizes as in previous studies were used [2,53,54,59]. Statistical analysis and graphing were performed using GraphPad Prism Software 9.5.1 and Microsoft Excel 2016. Results are presented as mean (radar charts), mean +/- standard deviation (SD) (bar/line graphs), or minimum to maximum range with lines at median and interquartile range (box plots). The number of independent experiments and biological replicates (n) for each panel is indicated in the figure legends. Outliers were identified using the Grubbs' or ROUT method and excluded from the analysis. Finally, statistical significance was determined by a two-tailed Mann-Whitney test for two groups or one way, as well as a two-way analysis of variance (ANOVA) with Tukey's multiple-comparison test for multiple groups.

4 Results

4.1 Impaired CHS response in the absence of MC-derived TNF

The research group of Prof. Anne Dudeck recently demonstrated that MCs facilitate the recruitment of neutrophils in the elicitation phase of CHS through the release of TNF and thereby critically promote the onset of hapten-induced skin inflammation [59]. Importantly, it has been shown, that the hapten-induced ear swelling, as a measure of skin inflammation, is reduced at the initial stages upon CHS elicitation, but not resolved to basal ear thickness at later time points in the absence of MC-derived TNF (unpublished). This suggests a novel role for MC-derived TNF in the resolution of hapten-induced skin inflammation.

To validate these previous observations and investigate the underlying mechanisms, Mcpt5-Cre^{+} TNF$^{fl/fl}$ mice (referred to as "MC$^{\Delta TNF}$"), which lack the expression of TNF in CTMCs, and respective Cre^{-} littermates (referred to as "MC^{WT}") were sensitized by an epicutaneous application of the hapten DNFB on the shaved back skin and challenged six days later at the ear (Figure **4A**). Administration of DNFB resulted in a substantial increase in ear swelling in sensitized MC^{WT} mice compared to the veh-treated controls (w/o DNFB), reaching its peak at 48 h after DNFB challenge and then gradually declining until 120 h (Figure **4B**, blue line). Consistently with the previous results, MC$^{\Delta TNF}$ mice showed a strong decrease in ear swelling during the initial stages of CHS, followed by an increase in ear thickness at later time points (Figure **4B**, red line).

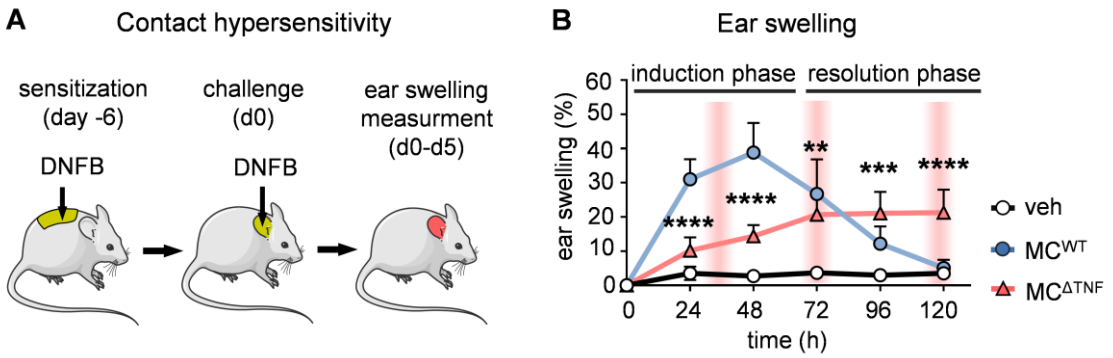

Figure 4| Impaired CHS response in absence of MC-derived TNF. A| Contact hypersensitivity response was induced by the application of the hapten dinitrofluorobenzene (DNFB). After DNFB sensitization on the shaved back skin and challenge six days later at the ear, skin inflammation was measured as ear swelling response. Vehicle (veh)-treated mice served as a negative control. B| Ear swelling of MC$^{\Delta TNF}$ mice and respective MC^{WT} littermates at indicated time points after DNFB challenge shown as percent (%) increase. Graphs depict the mean + SD. Statistical significance between the MC^{WT} and MC$^{\Delta TNF}$ groups was determined using a two-way ANOVA with Tukey's multiple-comparison test (two independent experiments, n=15-16 per group and n=5 for veh). ns p>0.1; # p<0.1; * p<0.05; ** p<0.01; *** p<0.001; **** p<0.0001

According to the inflammatory response observed in MC^{WT} mice, the period from 0 to 72 h after DNFB challenge was designated as the “induction phase”, while the interval from 72 to 120 h was defined as the “resolution phase”. In order to further characterize the induction (section **4.2**) and resolution phase (section **4.4**) in the absence of MC-derived TNF, three distinct time points were selected. These time points mark the peak of the induction phase (36 h), the transition to resolution (72 h), and the end of the resolution phase (120 h) (Figure **4B**, red bars).

4.2 Characterization of the induction phase

4.2.1 Reduced infiltration of monocytes and T cells in absence of MC-derived TNF

Upon hapten exposure, keratinocytes as well as MCs release a plethora of chemokines and cytokines that subsequently initiate the recruitment of neutrophils, monocytes and T cells to the site of inflammation [49]. Given the reduced ear swelling during the induction phase in the absence of MC-derived TNF (Figure **4B**), I first determined the numbers of immune cells within ear skin at 36 h post-DNFB challenge using flow cytometry. Application of DNFB induced a massive infiltration of $CD45^+$ leukocytes in MC^{WT} mice as compared to veh-treated controls, which was strongly reduced in $MC^{\Delta TNF}$ mice (Figure **5A**).

As a next step, the different leukocyte subsets were identified according to the gating strategy shown in Figure **5B.** For the analysis of myeloid cell subsets, leukocytes were first separated into $Ly6C^-$ $Ly6G^-$ cells (P1), $Ly6C^+$ $Ly6G^-$ cells (P2) and $Ly6C^{int}$ $Ly6G^+$ neutrophils. Within the population P1, $CD11b^+$ $F4/80^+$ cells were defined as macrophages and $F4/80^-$ $CD11c^+$ $MHC\text{-}II^+$ cells as DCs. The population P2 was further analysed for the co-expression of CD11b and CCR2 to identify monocytes. For the analysis of T cell subsets, $CD3^+$ cells were subsequently separated into $CD4^+$ and $CD8^+$ T cells. In order to illustrate the difference, the normalized cell counts of skin leukocyte subsets in $MC^{\Delta TNF}$ mice and veh-treated controls were calculated as a percentage of those in MC^{WT} mice, with the latter set as 100 %. I found that particularly the quantities of skin monocytes and $CD4^+$, as well as $CD8^+$ T cells were decreased within the ear skin of $MC^{\Delta TNF}$ compared to MC^{WT} mice at 36 h after DNFB challenge. On the other hand, skin numbers of DCs, macrophages and neutrophils exhibited only minor alterations in the absence of MC-derived TNF (Figure **5C**).

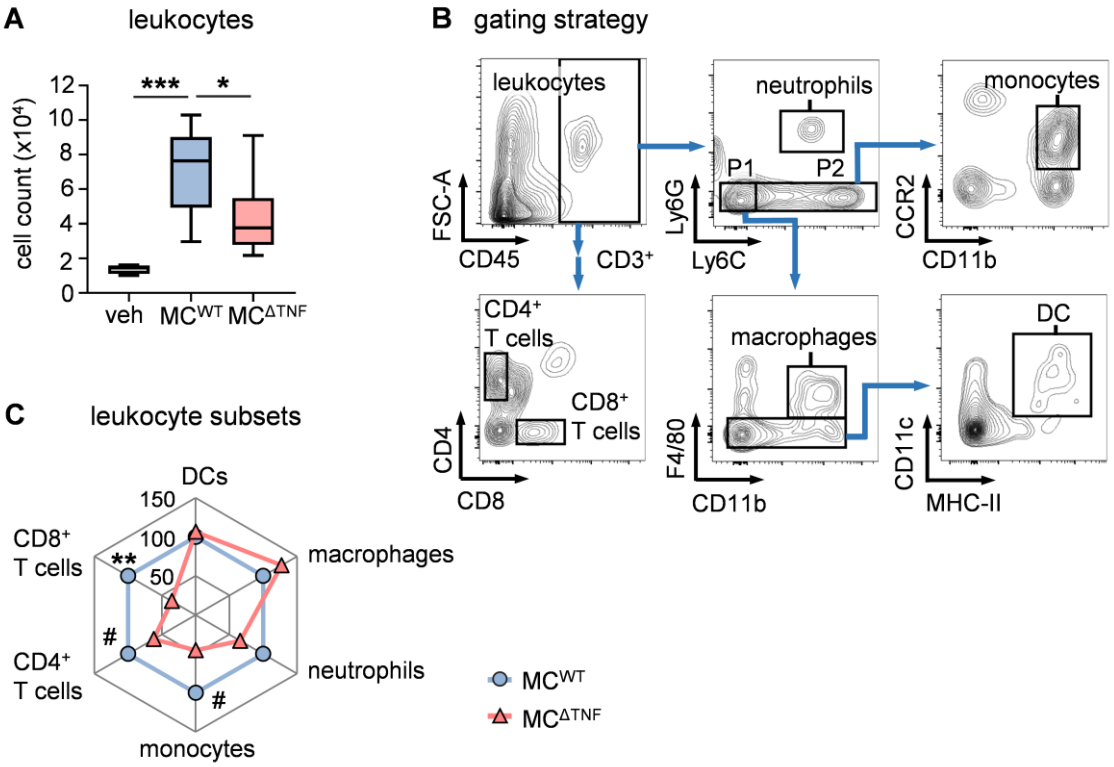

Figure 5| Reduced recruitment of monocytes and T cells in the absence of MC-derived TNF during the induction phase. $MC^{\Delta TNF}$ mice and respective MC^{WT} littermates were sensitized on the back skin and challenged six days later at the ear with DNFB. Vehicle (veh) mice were only treated with the solvent (w/o DNFB). **A|** Skin leukocyte numbers were quantified 36 h post-DNFB challenge using flow cytometry and normalized to the total cell count. The box-whisker plot indicates the median (horizontal line), interquartile range (box) and minimum to maximum range (whisker) of the values. **B|** Representative contour plots illustrating the gating strategy for the identification of the indicated skin leukocyte subsets following gating on singlets. **C|** Radar plot showing the normalized numbers of indicated subsets 36 h after challenge in ear skin of $MC^{\Delta TNF}$ as percentage compared to MC^{WT} mice, which were set as 100 %. (**A-C** two independent experiments, n=8-9 per group and n=4 for veh). Statistical significance was determined using a one-way ANOVA with Tukey's multiple-comparison test (**A**) or a two-tailed Mann-Whitney test (**C**). ns p>0.1; # p<0.1; * p<0.05; ** p<0.01; *** p<0.001; **** p<0.0001

Based on the expression of specific surface markers, gene expression profiles and functional analyses, Tamoutounour *et al*. defined three distinct skin monocyte subsets [109]. $Ly6C^{hi}$ $MHC\text{-}II^{-}$ dermal monocytes (dMonocytes) represent newly infiltrated monocytes, which subsequently can differentiate into $Ly6C^{hi}$ $MHC\text{-}II^{+}$ monocyte-derived DC1 (moDC)1 and consequently to $Ly6C^{low}$ $MHC\text{-}II^{+}$ moDC2 (Figure **6A**) [109].

In order to determine, whether monocyte recruitment and/or differentiation was affected in $MC^{\Delta TNF}$ mice, the numbers of skin monocyte subsets were quantified 36 h after DNFB challenge using flow cytometry. Intriguingly, the number of dMonocytes was significantly decreased, while the number of moDC1 was only slightly reduced in the absence of MC-derived TNF (Figure **6B,** left and middle). On the other hand, the number of moDC2 was not altered within the ear skin of $MC^{\Delta TNF}$ compared to MC^{WT} mice (Figure **6B,** right).

Taken together, these results indicate that MC-derived TNF is crucial for early monocyte infiltration during hapten-induced skin inflammation.

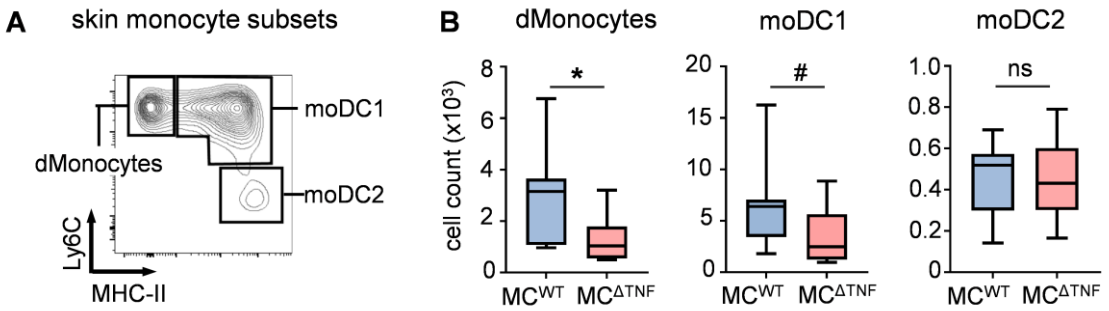

Figure 6| MC-derived TNF promotes the infiltration of dMonocytes. $MC^{\Delta TNF}$ mice and respective MC^{WT} littermates were sensitized on the back skin and challenged six days later at the ear with DNFB. **A|** Representative contour plot of skin monocyte subsets including $Ly6C^{hi}$ MHC-II^{-} dermal monocytes (dMonocytes), $Ly6C^{hi}$ MHC-II^{+} monocyte-derived dendritic cells (moDC) 1 and $Ly6C^{lo}$ MHC-II^{+} moDC2 following gating on singlets and $CD45^{+}$ $Ly6C^{+}$ $Ly6G^{-}$ $CD11b^{+}$ $CCR2^{+}$ cells. **B|** The numbers of skin monocyte subsets were quantified 36 h post-DNFB challenge using flow cytometry and normalized to the total cell count (two independent experiments, n=8-9 per group). Box-whisker plots indicate the median (horizontal line), interquartile range (box) and minimum to maximum range (whisker) of the values. Statistical significance was determined using a two-tailed Mann-Whitney test. ns $p>0.1$; # $p<0.1$; * $p<0.05$; ** $p<0.01$; *** $p<0.001$; **** $p<0.0001$

4.2.2 Altered inflammatory micromilieu in the absence of MC-derived TNF

During CHS, monocytes and T cells critically promote the inflammatory response through the release of effector cytokines [49,66]. While monocytes predominantly produce proinflammatory cytokines, T cells are able to secrete distinct patterns of cytokines (referred to as “signature cytokines”), depending on their stage of polarization [12,110].

Regarding the reduced skin infiltration of monocytes, as well as $CD4^{+}$ and $CD8^{+}$ T cells in the absence of MC-derived TNF, protein levels of selected cytokines were quantified within ear skin of MC^{WT} and $MC^{\Delta TNF}$ mice at 36 h after DNFB challenge using multiplex approaches. To illustrate the difference, the normalized protein levels of skin cytokines in $MC^{\Delta TNF}$ mice and veh-treated controls were calculated as a percentage of those in MC^{WT} mice, which were set as 100 %. Compared to veh controls, DNFB-treated MC^{WT} mice exhibited elevated skin protein levels of IL-1β, IL-6, TNF, IFN-γ, IL-4, and IL-5, while IL-17 and IL-22 showed only minor alterations. (Figure **7A**). In line with the reduced monocyte infiltration in the absence of MC-derived TNF, the levels of the proinflammatory cytokines IL-6 and TNF were reduced within the ear skin of $MC^{\Delta TNF}$ compared to MC^{WT} mice (Figure **7B**, left and middle). Additionally, the level of the T_H2-cytokine IL-4 was significantly reduced in the absence of MC-derived TNF (Figure **7B**, right). Protein levels of the other analysed cytokines (Figure **7A**) were not significantly changed within the ear skin of $MC^{\Delta TNF}$ compared to MC^{WT} mice.

These results indicate, that MC-derived TNF critically promotes inflammation in the induction phase of CHS through the early recruitment of monocytes and T cells.

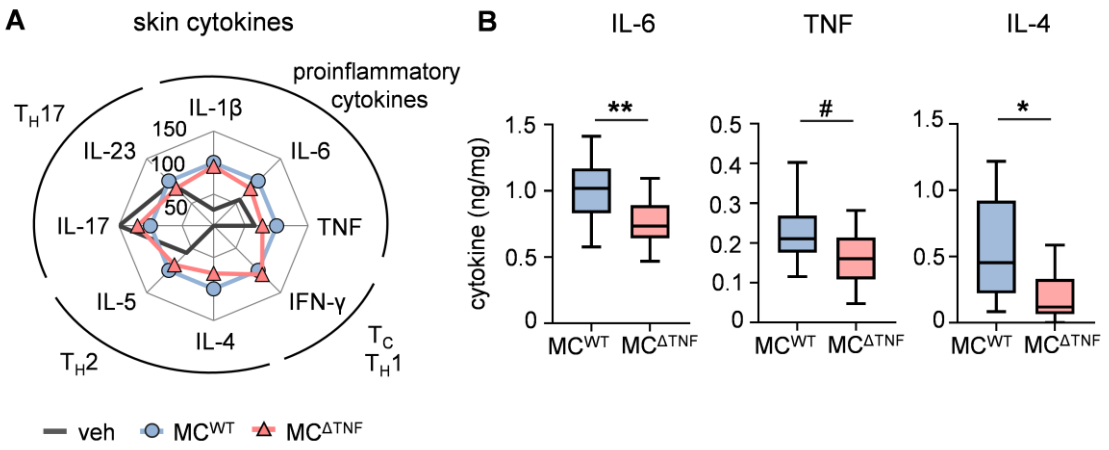

Figure 7| Reduced levels of IL-6, TNF and IL-4 in $MC^{\Delta TNF}$ mice at 36 h post challenge. $MC^{\Delta TNF}$ mice and respective MC^{WT} littermates were sensitized on the back skin and challenged six days later at the ear with DNFB. Vehicle (veh) mice were only treated with the solvent (w/o DNFB). **A-B|** Protein levels of proinflammatory cytokines, as well as cytotoxic T cell (T_C) and T helper cell (T_H) signature cytokines were quantified in ear skin at 36 h post-DNFB challenge using multiplex approaches and normalized to the skin biopsy weight (two independent experiments, n=12-13 per group and n=5-6 for veh). The radar chart (**A**) depicts the percentage difference in protein levels of cytokines in $MC^{\Delta TNF}$ and veh mice compared to MC^{WT} mice (set to 100 %). Box-whisker plots (**B**) indicate the median (horizontal line), interquartile range (box) and minimum to maximum range (whisker) of the values. Statistical significance was determined using a two-tailed Mann-Whitney test. ns p>0.1; # p<0.1; * p<0.05; ** p<0.01; *** p<0.001; **** p<0.0001

4.3 Analysis of the mechanism of MC-derived TNF effects on early monocyte recruitment to the skin

4.3.1 MC-derived TNF is dispensable for monocyte mobilization

Next, I investigated the mechanisms of MC-derived TNF effects on early monocyte recruitment. In peripheral tissues like the spleen, monocytes are divided based on the expression of Ly6C into $Ly6C^{low}$ patrolling monocytes (pMonocytes) and $Ly6C^{hi}$ inflammatory monocytes (iMonocytes) (Figure **8A**). During infection and inflammation, predominantly iMonocytes are mobilized from reservoirs such as the BM and spleen and recruited via the bloodstream [111].

To determine, whether the mobilization of monocytes was reduced in the absence of MC-derived TNF, iMonocyte numbers were quantified in BM, spleen and blood at 36 h after DNFB challenge using flow cytometry. Total numbers of BM, splenic and blood iMonocytes were not significantly increased at 36 h post-DNFB challenge in the absence of MC-derived TNF. Nonetheless, there was a clear tendency for increased iMonocyte numbers in the spleen and blood of $MC^{\Delta TNF}$ compared to MC^{WT} mice (Figure **8B**).

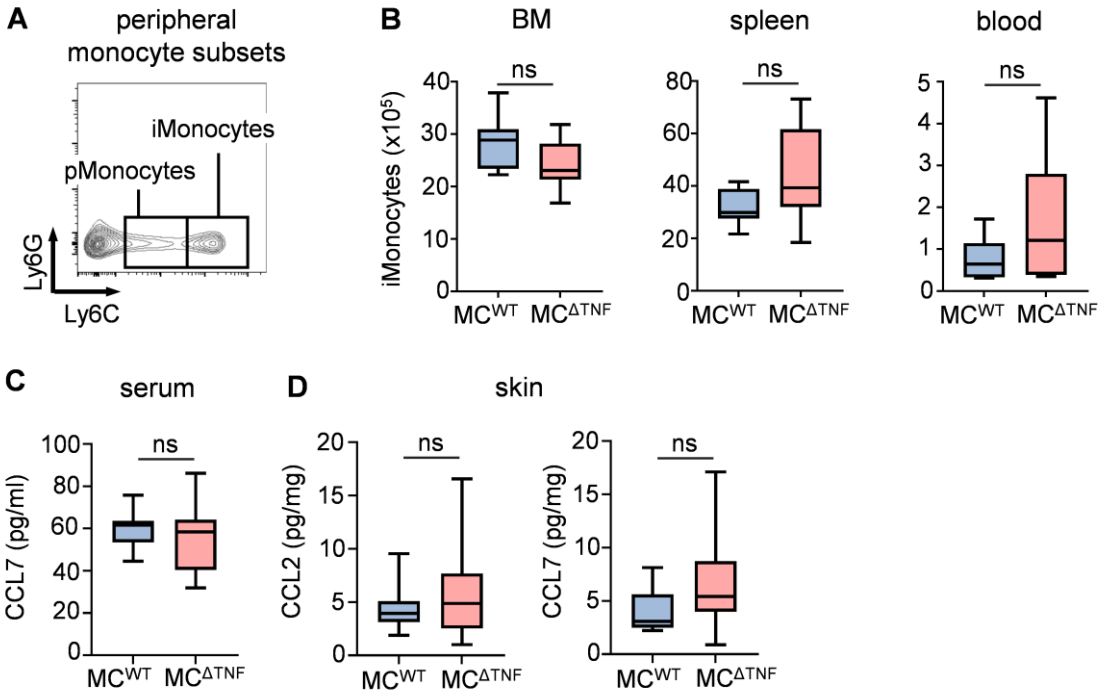

Figure 8| MC-derived TNF is dispensable for iMonocyte mobilization during the induction phase of CHS. $MC^{\Delta TNF}$ mice and respective MC^{WT} littermates were sensitized on the back skin and challenged six days later at the ear with DNFB. **A|** Representative contour plot of splenic monocyte subsets including $Ly6G^{-}$ $Ly6C^{low}$ patrolling monocytes (pMonocytes) and $Ly6G^{-}$ $Ly6C^{hi}$ inflammatory monocytes (iMonocytes) following gating on singlets. **B|** iMonocyte numbers in bone marrow (BM), spleen and blood were determined 36 h after DNFB challenge using flow cytometry. **C|** Serum and **D|** skin protein levels of CCL2 and CCL7 were quantified 36 h after DNFB challenge using multiplex approaches and normalized to the skin biopsy weight (only **D**). (two independent experiments, n=7-9 (**B, C**) and n=13-15 per group (**D**)). Box-whisker plots indicate the median (horizontal line), interquartile range (box) and minimum to maximum range (whisker) of the values. Statistical significance was determined using a two-tailed Mann-Whitney test. ns $p>0.1$; # $p<0.1$; * $p<0.05$; ** $p<0.01$; *** $p<0.001$; **** $p<0.0001$

Both, iMonocyte mobilization from the BM or spleen and subsequent recruitment to the site of infection/inflammation is predominantly mediated by the chemoattractants CCL2 and CCL7, which bind to the CCR2 receptor on monocytes [111]. Therefore, protein levels of both chemoattractants were analysed in the serum and skin of $MC^{\Delta TNF}$ and MC^{WT} mice at 36 h post-DNFB challenge using multiplex approaches. In serum, only CCL7 could be detected. The concentration of CCL7 was not decreased in the absence of MC-derived TNF (Figure **8C**). In line with this, protein levels of CCL2 and CCL7 were not reduced within the ear skin of $MC^{\Delta TNF}$ compared to MC^{WT} mice (Figure **8D**). Taken together, these results indicate that MC-derived TNF is dispensable for monocyte mobilization, as well as the upregulation of the monocyte-attracting chemokines CCL2 and CCL7.

4.3.2 MC-derived TNF indirectly promotes monocyte skin infiltration

Importantly, TNF was also shown to directly regulate the recruitment of monocytes by activating TNFR1 in a cutaneous wound healing model [112]. Mechanistically, Lim *et al.* found, that TNF-TNFR1 signalling in monocytes enhances their Ras homolog family member A (RhoA)-dependent transmigratory activity [113].

Therefore, I next investigated a direct effect of MC-derived TNF on monocyte skin infiltration using a mouse line with a conditional inactivation of the *Tnfrsf1a* gene in monocytes, macrophages and neutrophils (LysM-Cre^{+} x TNFR1$^{fl/fl}$, referred to as "Mo$^{\Delta TNFR1}$") [102,106]. Mo$^{\Delta TNFR1}$ mice and respective Cre^{-} littermates (referred to as "Mo^{WT}") were sensitized on the shaved back skin and challenged six days later at the ear with the contact allergen DNFB. However, total skin leukocyte numbers were not reduced at 36 h after DNFB challenge in Mo$^{\Delta TNFR1}$ compared to Mo^{WT} mice (Figure **9A**). Moreover, the numbers of monocyte subsets including dMonocytes, as well as moDC1 and moDC2 were not decreased in the absence of TNFR1 signalling in LysM-expressing cells (Figure **9B**). This indicates that TNFR1 signalling in monocytes is not required for their recruitment during the induction phase of hapten-induced skin inflammation.

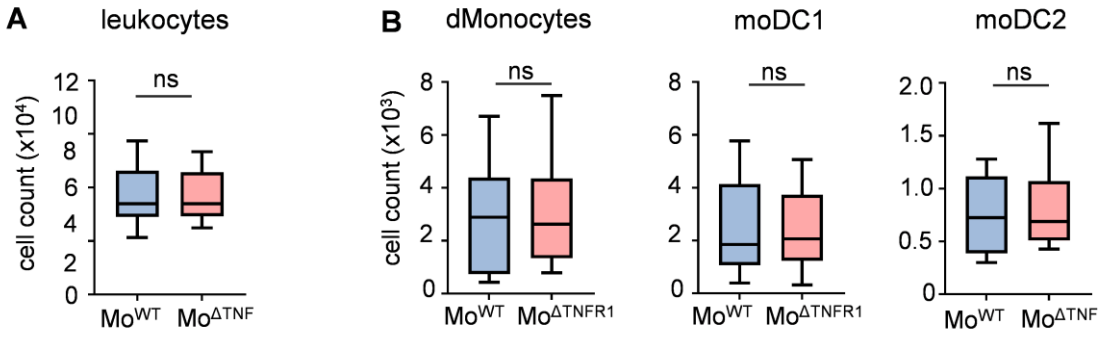

Figure 9| TNFR1 signalling in monocytes is dispensable for their early recruitment during CHS. Mo$^{\Delta TNFR1}$ mice and respective Mo^{WT} littermates were sensitized on the shaved back and challenged six days later at the ear with DNFB. The numbers of **A|** leukocytes and **B|** monocyte subsets including dermal monocytes (dMonocytes), monocyte-derived DC (moDC)1 and moDC2 were quantified in ear skin 36 h after DNFB challenge using flow cytometry (see Figure **5** and **6** for gating) and normalized to the total cell count (two independent experiments, n=10-12 per group). Box-whisker plots indicate the median (horizontal line), interquartile range (box) and minimum to maximum range (whisker) of the values. Statistical significance was determined using a two-tailed Mann-Whitney test. ns p>0.1; # p<0.1; * p<0.05; ** p<0.01; *** p<0.001; **** p<0.0001

4.3.3 MC-derived TNF indirectly promotes early monocyte recruitment and tissue recovery via an adequate priming of CD8$^+$ T cells

It has been recently reported by Chong *et al*. that in hapten-induced skin inflammation, CD8$^+$ effector T cells mediate the infiltration of CD11b$^+$ Ly6C$^+$ monocytes (here referred to as “dMonocytes”) via the release of IL-17 and consequently their differentiation towards CD11b$^+$ Ly6C$^+$ MHC-II$^+$ monocytes (here referred to as “moDC1”) through the secretion of IFN-γ [66]. Furthermore, the group of Anne Dudeck could previously demonstrate, that CD8$^+$ T cell priming and their recruitment to the challenged site are reduced in the absence of MC-derived TNF, as a consequence of an impaired activation of cDC1 in the sensitization phase [2]. Consistent with this finding, I also found strongly reduced numbers of CD8$^+$ T cells within the ear skin of MC$^{\Delta TNF}$ compared to MC^{WT} mice at 36 h after DNFB challenge (4.2.1).

In order to assess, whether the reduced monocyte infiltration resulted from an inefficient CD8$^+$ T cell priming in the absence of MC-derived TNF, an adoptive transfer of adequately primed CD8$^+$ T cells was performed. More specifically, CD8$^+$ T cells were purified from back skin (= sensitization site) draining inguinal lymph nodes of C57BL/6Jrj donor mice at day three post-DNFB sensitization using magnetic cell separation. Afterwards, equal amounts of CD8$^+$ T cells were adoptively transferred into sensitized MC$^{\Delta TNF}$ recipient mice at day six post-sensitization, which were subsequently challenged with DNFB at the ear. PBS-injected MC^{WT} and MC$^{\Delta TNF}$ mice served as controls. Immune cell numbers were quantified 24 h post-DNFB challenge, representing the peak of monocyte infiltration in hapten-induced skin inflammation [66]. Indeed, the numbers of leukocytes (Figure **10A**) and particularly of dMonocytes (Figure **10B**, left) were significantly increased within the ear skin of MC$^{\Delta TNF}$ mice transferred with CD8$^+$ T cells, as compared to PBS-injected control mice, to the level of MC^{WT} mice. Furthermore, the numbers of skin moDC1 (Figure **10B**, middle) were significantly increased in MC$^{\Delta TNF}$ mice that received adequately primed CD8$^+$ T cells compared to PBS-injected ones, while the numbers of moDC2 were not affected by the adoptive transfer (Figure **10B**, right). This indicates that MC-derived TNF indirectly promotes the recruitment of monocytes via an efficient priming of CD8$^+$ T cells in the sensitization phase.

Intriguingly, skin CD8$^+$ T cell numbers were not decreased in PBS-injected MC$^{\Delta TNF}$ compared to MC^{WT} mice and also not increased in MC$^{\Delta TNF}$ mice transferred with CD8$^+$ T cells at 24 h post-DNFB challenge (Figure **10C**). In addition to the numbers of skin CD8$^+$ T cells, the concentration of IL-17 was analysed in serum at 24 and 36 h post-DNFB challenge, as well as in ear skin at 36 h post-DNFB challenge using ELISA approaches. However, IL-17 protein levels in both, serum and ear skin were below the detection limit (< 5 pg/ml) of the assay.

Finally, the inflammatory course of CHS upon transfer of adequately primed CD8$^+$ T cells was investigated. In line with the restored monocyte skin infiltration, ear swelling in MC$^{\Delta TNF}$ mice transferred with CD8$^+$ T cells was equivalent to MC^{WT} mice at early time points of hapten-induced skin inflammation. Most importantly, the transfer of primed CD8$^+$ T cells also prevented the persistent ear swelling at later stages in the absence of MC-derived TNF, indicating a connection between CD8$^+$ T cells, monocyte recruitment and proper tissue recovery (Figure **10D**).

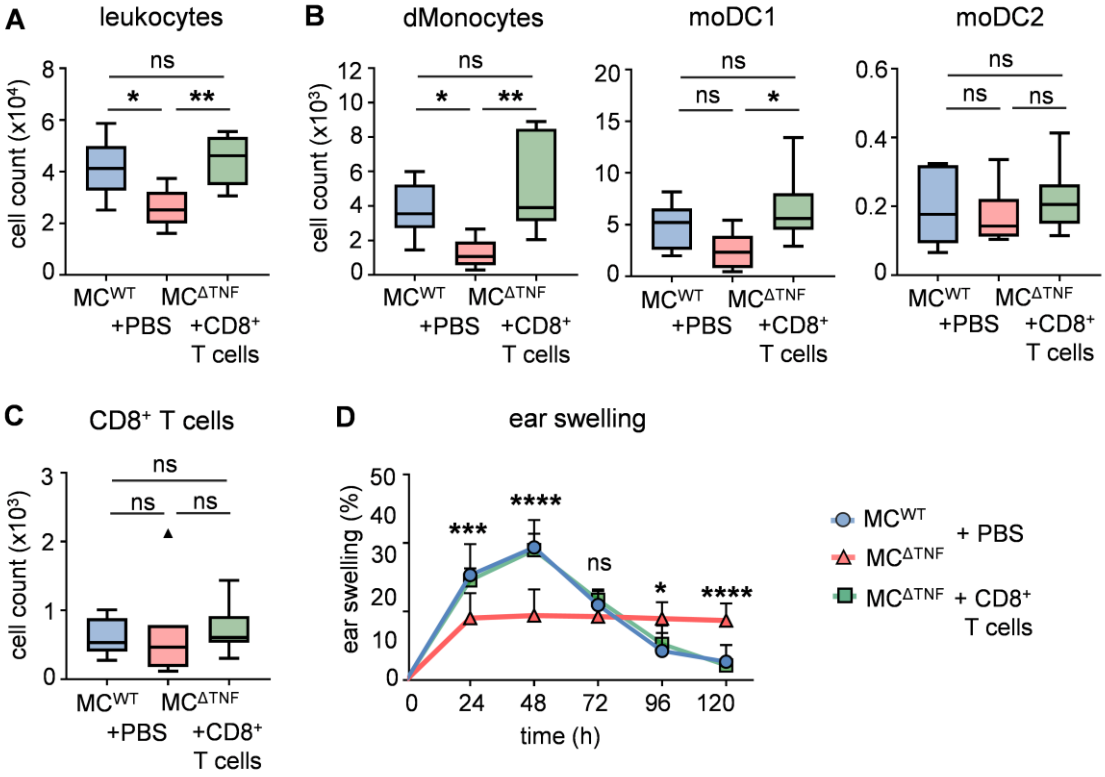

Figure 10| MC-derived TNF promotes early monocyte recruitment and tissue recovery via its impact on efficient priming of CD8$^+$ T cells. Adequately primed CD8$^+$ T cells were purified from inguinal lymph nodes of C57BL/6Jrj mice at day three post-sensitization and adoptively transferred into sensitized MC$^{\Delta TNF}$ mice (+CD8$^+$ T cells), which were challenged with DNFB at the ear 30 min later. MC^{WT} and MC$^{\Delta TNF}$ mice injected with PBS (+PBS) served as a control. The numbers of **A|** leukocytes**, B|** dermal monocytes (dMonocyte) and monocyte-derived DCs (moDC), as well as **C|** CD8$^+$ T cells within ear skin were quantified 24 h after challenge using flow cytometry (see Figure **5** and **6** for gating) and normalized to the total cell count. **D|** Ear swelling at indicated time points after DNFB challenge shown as percent (%) increase (**A-D** two independent experiments, n=7-10 per group). Box-whisker plots (**A-C**) indicate the median (horizontal line), interquartile range (box) and minimum to maximum range (whisker) of the values. The graph (**D**) depicts the mean + SD. Statistical significance was determined using a one-way ANOVA (**A-C**) or a two-way ANOVA with Tukey's multiple-comparison test for the comparison between MC$^{\Delta TNF}$ and MC$^{\Delta TNF}$+CD8$^+$ T cells (**D**). ns p>0.1; # p<0.1; * p<0.05; ** p<0.01; *** p<0.001; **** p<0.0001

4.3.4 MC-derived TNF promotes tissue recovery, but not monocyte recruitment via TNFR1 signalling in cDCs

In order to further prove the indirect effect of MC-derived TNF on monocyte recruitment via the early activation of cDC1 in hapten-induced skin inflammation, a mouse line with a conditional knockout of the *Tnfrsf1a* gene in DCs (referred to as $DC^{\Delta TNFR1}$) was generated by crossing CD11c-Cre mice with $TNFR1^{fl/fl}$ mice [102]. At first, surface expression of TNFR1 on DCs from $DC^{\Delta TNFR1}$ mice, as well as Cre^- littermates (referred to as DC^{WT}) was analysed by means of median fluorescence intensity (MFI) using flow cytometry, to validate the conditional knockout. However, no specific TNFR1 expression could be detected on skin and splenic DCs from both $DC^{\Delta TNFR1}$, as well as DC^{WT} mice, at steady-state conditions (Figure **11A**). Therefore, BMDCs were generated and stimulated with LPS, which has been previously shown to increase TNFR1 levels [114]. Surface expression of TNFR1 was significantly lower in untreated (Figure **11B**) and LPS-treated BMDCs (Figure **11C**) derived from $DC^{\Delta TNFR1}$ as compared to $DC^{\Delta WT}$ mice, but not completely absent, when compared to the antibody isotype (Iso) control. Hence, $DC^{\Delta TNFR1}$ mice may possess only a partial knockout of the *Tnfrsf1a* gene in DC, which should be determined in further experiments.

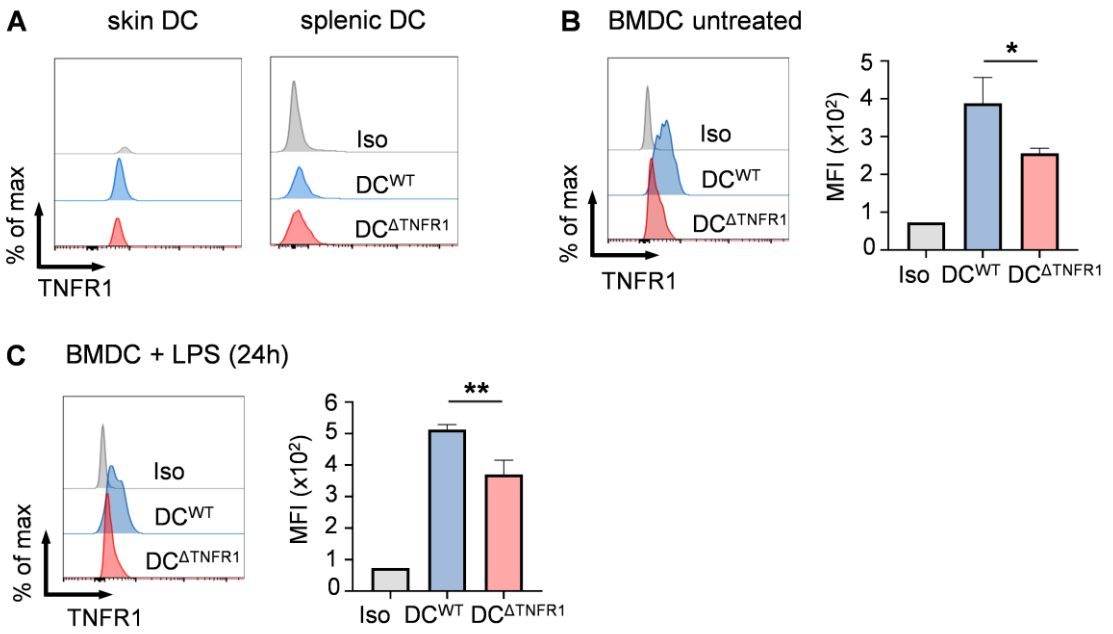

Figure 11| TNFR1 surface expression is reduced in BMDCs derived from $DC^{\Delta TNFR1}$ mice. TNF receptor 1 (TNFR1) surface expression was analysed by means of median fluorescence intensity (MFI) using flow cytometry. **A-C|** Representative histograms and bar graphs (only **B-C**) showing MFI of TNFR1 surface expression by **A|** skin and splenic $CD11c^+$ MHC^+ DCs, as well as **B|** untreated and **C|** lipopolysaccharide (LPS)-treated bone marrow-derived DCs (BMDCs) from DC^{WT} and $DC^{\Delta TNFR1}$ mice. The fluorescence minus one (FMO) or antibody isotype control (Iso) served as negative controls (background fluorescence). The graphs (**B-C**) depict the mean + SD. Statistical significance was determined using a two-tailed Student's t-test. ns p>0.1; # p<0.1; * p<0.05; ** p<0.01; *** p<0.001; **** p<0.0001

Beside DCs, also monocytes, macrophages and NK cells express CD11c to a certain extent (www.imgen.org) and therefore may be affected by the conditional knockout. Since TNFR1 signalling is crucial for the regulation of apoptosis, the numbers of these immune cells were determined within the spleen and ear skin of $DC^{\Delta TNFR1}$ and DC^{WT} mice under steady-state conditions using flow cytometry. In spleen, the numbers of $CD11c^+$ $MHC\text{-}II^+$ DCs, $F4/80^+$ macrophages, $Ly6G^-$ $Ly6C^{lo}$ pMonocytes, $Ly6G^-$ $Ly6C^{hi}$ iMonocytes and $NK1.1^+$ $NKp46^+$ NK cells were not altered in the absence of TNFR1-signalling in CD11c-expressing cells (Figure **12A**). Furthermore, I found no alterations in the numbers of skin immune cell subsets including DCs, macrophages, dMonocytes, moDC1 and moDC2 in the ear skin of $DC^{\Delta TNFR1}$ as compared to DC^{WT} mice (Figure **12B**).

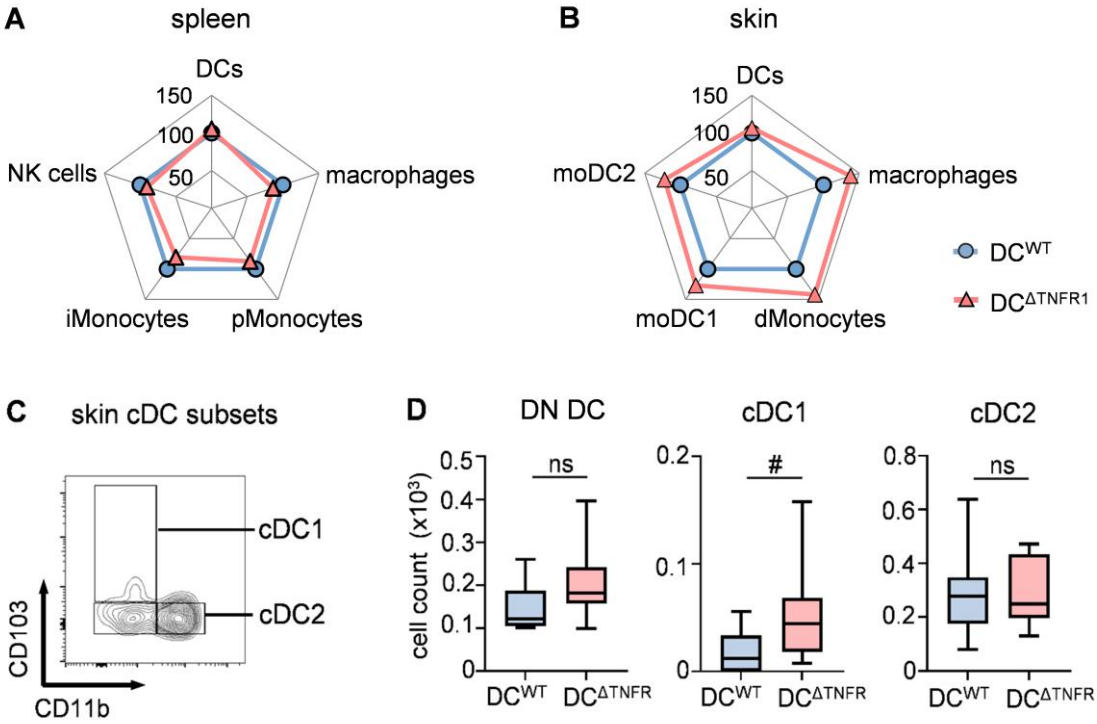

Figure 12| Splenic and skin immune cell subsets are not changed in $DC^{\Delta TNFR1}$ mice under physiologic conditions. The numbers of immune cell subsets within **A|** spleen and **B|** ear skin of $DC^{\Delta TNFR1}$ and DC^{WT} mice were quantified using flow cytometry. Cell subsets were identified by the expression of the following markers: dendritic cells (DC): $CD11c^+$ $MHC\text{-}II^+$, macrophages: $F4/80^+$, patrolling monocytes (pMonocyte): $Ly6G^-$ $Ly6C^{lo}$, inflammatory monocytes (iMonocytes): $Ly6G^-$ $Ly6C^{hi}$, NK cells: $CD3^-$ $NK1.1^+$ $NKp46^+$, dermal monocytes (dMonocytes): $Ly6G^-$ $Ly6C^{hi}$ $MHC\text{-}II^-$, monocyte derived DC (moDC)1: $Ly6C^{hi}$ $MHC\text{-}II^+$, moDC2: $Ly6C^{lo}$ $MHC\text{-}II^+$. **C|** Representative contour plot of skin cDC subsets including $CD11b^-$ $CD103^-$ double negative (DN) DC, $CD103^+$ $CD11b^-$ cDC1 and $CD11b^+$ $CD103^-$ cDC2. **D|** Numbers of cDC subsets were quantified in the ear skin of $DC^{\Delta TNFR1}$ mice and DC^{WT} littermates using flow cytometry and normalized to the total cell count. Radar plots (**A-B**) show the normalized numbers of indicated immune cell subsets in $DC^{\Delta TNFR1}$ as percentage compared to DC^{WT} mice, which were set to 100 %. Box-whisker plots (**D**) indicate the median (horizontal line), interquartile range (box) and minimum to maximum range (whisker) of the values. Statistical significance was determined using a two-tailed Mann-Whitney test. ns $p>0.1$; # $p<0.1$; * $p<0.05$; ** $p<0.01$; *** $p<0.001$; **** $p<0.0001$

With respect to the crucial role of skin cDC1 during the initiation of hapten-induced skin inflammation [2], I further investigated the numbers of cDC subsets at steady-state within ear skin, which can be divided based on the differential expression of CD103 and CD11b (Figure **12C**). Intriguingly, the number of cDC1 ($CD103^+$ $CD11b^-$) was slightly increased in the ear skin of $DC^{\Delta TNFR1}$ as compared to DC^{WT} mice (Figure **12D**, middle), while the numbers of $CD103^-$ $CD11b^-$ double negative (DN) DC and $CD103^-$ $CD11b^+$ cDC2 were not affected by the absence of TNFR1 singnalling in CD11c-expressing cells (Figure **12D**, left and right).

Taken together, these results suggest that $DC^{\Delta TNFR1}$ mice represent an appropriate transgenic mouse model to study the role of TNFR1 signalling in DCs during hapten-induced skin inflammation.

Finally, the recruitment of monocytes during hapten-induced skin inflammation, as well as the inflammatory course were investigated in the absence of TNFR1 signalling in DCs. To this end, $DC^{\Delta TNFR1}$ and DC^{WT} mice were sensitized by an epicutaneous application of DNFB on the shaved back skin and challenged six days later at the ear. Skin infiltration of monocytes was determined 36 h after DNFB challenge using flow cytometry. Neither the numbers of leukocytes (Figure **13A**) nor of dMonocytes and moDC1 (Figure **13B,** left and middle) were reduced in the absence of TNFR1 signalling in CD11c-expressing cells. Surprisingly, I observed a significantly increased number of moDC2 in the ear skin of $DC^{\Delta TNFR1}$ compared to DC^{WT} mice (Figure **13B,** right), whereas the number of $CD8^+$ T cells was also not affected by the absence of TNFR1 signalling in CD11c-expressing cells (Figure **13C**). These findings suggest that MC-derived TNF effects on $CD8^+$ T cell priming and subsequent monocyte recruitment are independent of TNFR1-signalling in DCs.

Despite the adequate recruitment of leukocytes and particularly of monocytes and $CD8^+$ T cells, ear swelling in the induction phase of CHS was significantly reduced in $DC^{\Delta TNFR1}$ compared to DC^{WT} mice. Furthermore, $DC^{\Delta TNFR1}$ mice exhibited also a prolonged ear swelling at later time points of CHS as observed in the absence of MC-derived TNF (Figure **13D**).

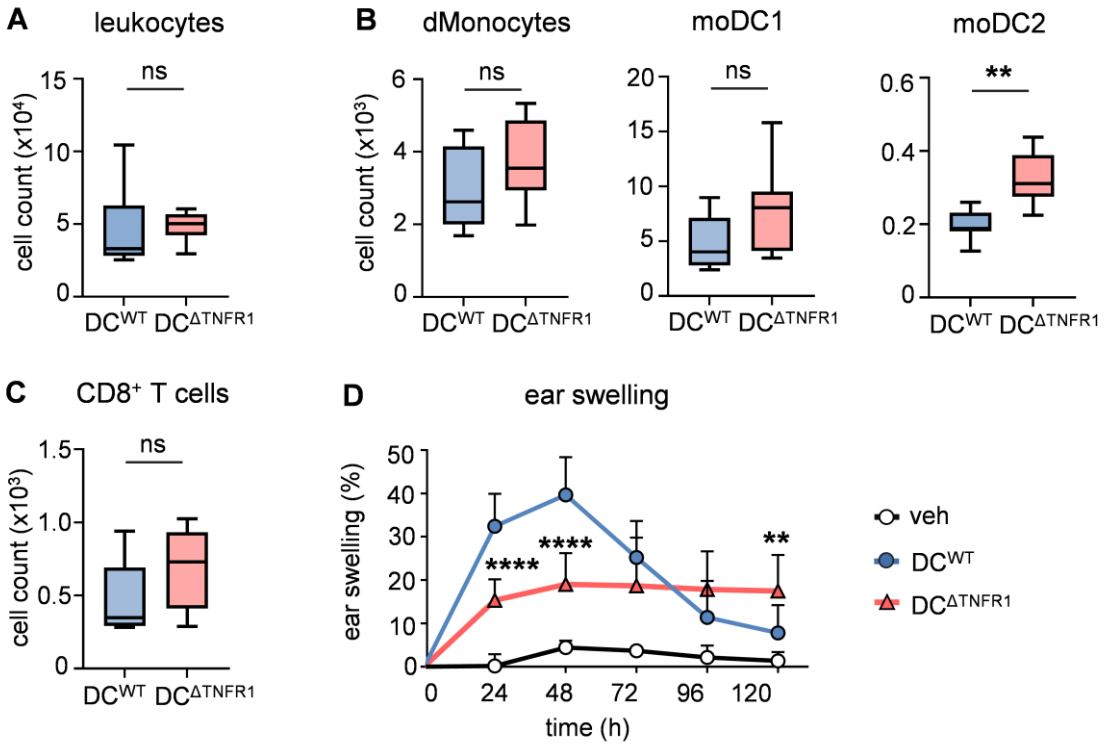

Figure 13| Monocyte recruitment is not affected by the absence of TNFR1 signalling DCs. $DC^{\Delta TNFR1}$ mice and respective DC^{WT} littermates were sensitized on the shaved back skin and challenged six days later at the ear with DNFB. The numbers of **A|** total leukocytes and **B|** monocyte subsets including dermal monocytes (dMonocytes), monocyte-derived dendritic cells (moDC)1, moDC2 and $CD8^+$ T cells were quantified in ear skin 36 h after DNFB challenge using flow cytometry (see Figure **5** and **6** for gating) and normalized to the total cell count (two independent experiments, n=7-8 per group). **D|** Ear swelling at indicated time points after DNFB challenge shown as percent (%) increase (two independent experiments, n=8-15 per group and n=4 for veh). Box-whisker plots (**A-C**) indicate the median (horizontal line), interquartile range (box) and minimum to maximum range (whisker) of the values. The graph (**D**) depicts the mean +SD. Statistical significance was determined using a two-tailed Mann-Whitney test (**A-C**) or a two-way ANOVA with Tukey's multiple-comparison test for the comparison between the DC^{WT} and $DC^{\Delta TNFR1}$ groups (**D**). ns p>0.1; # p<0.1; * p<0.05; ** p<0.01; *** p<0.001; **** p<0.0001

4.4 Characterization of the resolving phase

4.4.1 The continuing ear thickness is not associated with ongoing inflammation

A first step in the resolution of inflammation is the counterregulation of proinflammatory chemokine and cytokine production subsequently leading to the abrogation of immune cell recruitment and activation [79].

In order to determine, whether the persistent ear swelling at later time points of CHS in the absence of MC-derived TNF (Figure **4B**) resulted from ongoing inflammatory processes, chemokine and cytokine protein levels, as well as leukocyte numbers were quantified within ear skin of $MC^{\Delta TNF}$ and MC^{WT} mice at the onset (72 h after DNFB challenge) and towards the end of the resolution phase (120 h after DNFB challenge)

using multiplex approaches and flow cytometry, respectively. Of note, protein levels of chemokines such as CXCL1, CXCL2, CCL3, CCL4 and CCL5 (Figure **14A**), as well as proinflammatory cytokines including IL-1ß and TNF (Figure **14B**) were strongly reduced in $MC^{\Delta TNF}$ compared to MC^{WT} mice at 72 h post-DNFB challenge. Subsequently, skin chemokine and cytokine protein levels regularly decreased in $MC^{\Delta TNF}$ mice and were not altered at 120 h post-DNFB challenge as compared to MC^{WT} mice (Figure **14A/B**). In line with this, total leukocyte numbers were not increased at 72 h and 120 h post-DNFB challenge in the absence of MC-derived TNF and declined over time to equal levels in $MC^{\Delta TNF}$ compared to MC^{WT} mice (Figure **14C**).

These results indicate that the non-resolving ear thickness at later time points of CHS in the absence of MC-derived TNF does not result from persistent inflammation.

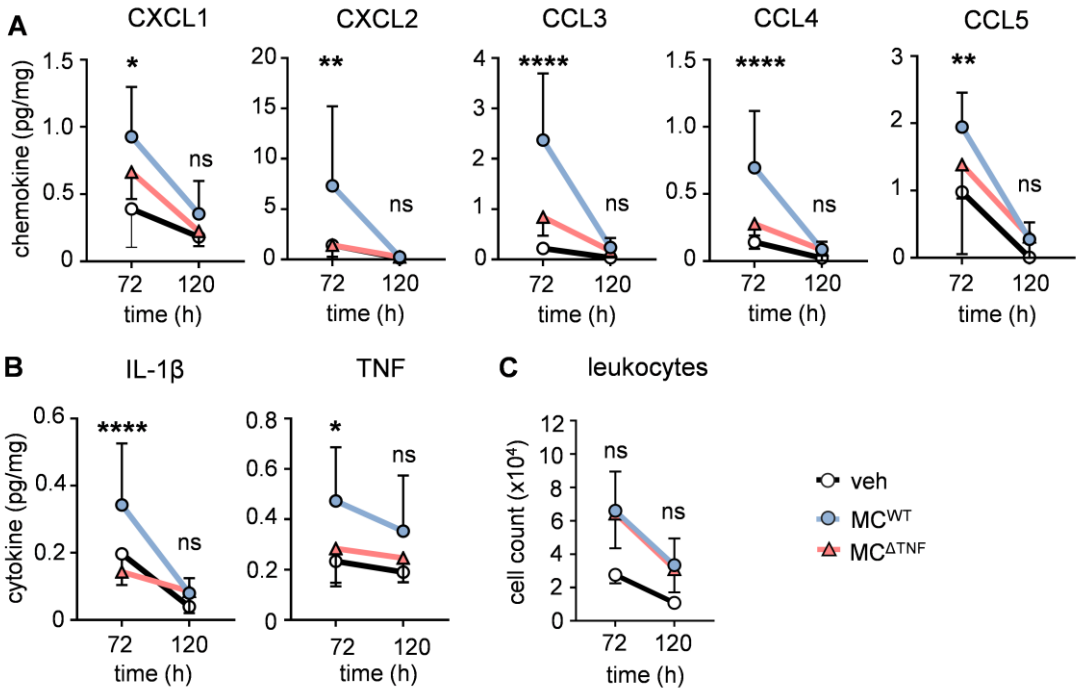

Figure 14| The absence of MC-derived TNF does not lead to ongoing inflammatory processes. $MC^{\Delta TNF}$ mice and respective MC^{WT} littermates were sensitized on the back skin and challenged six days later at the ear with DNFB. Vehicle (veh) mice were only treated with the solvent (w/o DNFB). Protein levels of **A|** chemokines and **B|** cytokines were quantified in ear skin at indicated time points after DNFB challenge using multiplex approaches and normalized to the skin biopsy weight (two independent experiments, n=7-14 per group and n=3-4 for veh). **C|** The numbers of $CD45^+$ leukocytes (pregated on singlets) within ear skin were determined at indicated time points after DNFB challenge using flow cytometry and normalized to the total cell count (two independent experiments, n=12-15 per group and n=4-5 for veh). Graphs depict the mean +/- SD. Statistical significance between the MC^{WT} and $MC^{\Delta TNF}$ groups was determined using a two-way ANOVA with Tukey's multiple-comparison test. ns p>0.1; # p<0.1; * p<0.05; ** p<0.01; *** p<0.001; **** p<0.0001

4.4.2 Adequate induction of neutrophil apoptosis in absence of MC-derived TNF

As a next step during the resolution of inflammation, neutrophil apoptosis in the tissue is triggered by pro-resolving lipid mediators and cytokines such as TNF. Subsequently, these apoptotic neutrophils are removed by macrophages through a process known as “efferocytosis”. [79].

With respect to this, I next examined, whether the persistent ear thickness at later time points of CHS was caused by an accumulation of neutrophils resulting from a diminished induction of apoptosis or impaired clearance by macrophages. To this end, frequencies of living and apoptotic neutrophils (Figure **15A**) were determined in the ear skin of $MC^{\Delta TNF}$ and MC^{WT} mice at 72 h post-DNFB challenge using flow cytometry in combination with AnnexinV-7AAD staining. However, the percentages of living ($AnnexinV^{-}$ $7AAD^{-}$), early apoptotic ($AnnexinV^{+}$ $7AAD^{-}$) and late apoptotic neutrophils ($AnnexinV^{+}$ $7AAD^{+}$) were not altered in the absence of MC-derived TNF (Figure **15B**). Furthermore, neutrophil numbers were not increased at 72 h and 120 h post-DNFB challenge in the ear skin of $MC^{\Delta TNF}$ compared to MC^{WT} mice and regularly decreased to the level of veh-treated controls (Figure **15C**).

In summary, these results indicate that MC-derived TNF is dispensable for the induction of neutrophil apoptosis in the resolution phase of hapten-induced skin inflammation.

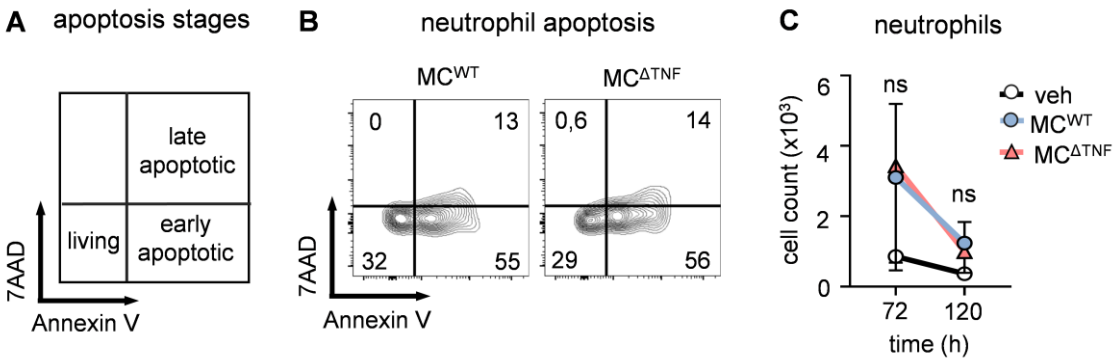

Figure 15| MC-derived TNF is dispensable for the induction of neutrophil apoptosis. $MC^{\Delta TNF}$ mice and respective MC^{WT} littermates were sensitized on the back skin and challenged six days later at the ear with DNFB. Vehicle (veh) mice were only treated with the solvent (w/o DNFB). **A|** The frequency of living ($AnnexinV^{-}$ $7AAD^{-}$), early ($AnnexinV^{+}$ $7AAD^{-}$) and late apoptotic neutrophils ($AnnexinV^{+}$ $7AAD^{-}$) within ear skin was determined using flow cytometry **B|** Representative contour plots from two independent experiments showing the percentages of living and apoptic $CD11b^{+}$ $Ly6G^{+}$ neutrophils following gating on singlets and $CD45^{+}$ $F4/80^{-}$ cells at 72 h post-DNFB challenge. **C|** The numbers of $CD11b^{+}$ $Ly6G^{+}$ neutrophils (pregated on singlets and $CD45^{+}$ $F4/80^{-}$) were quantified at indicated time points after DNFB challenge using flow cytometry and normalized to the total cell count (two independent experiments, n=10-14 per group and n=4-7 for veh). The graph depicts the mean +/- SD. Statistical significance between the MC^{WT} and $MC^{\Delta TNF}$ groups was determined using a two-way ANOVA with Tukey’s multiple-comparison test. ns p>0.1; # p<0.1; * p<0.05; ** p<0.01; *** p<0.001; **** p<0.0001

4.4.3 MC-derived TNF promotes the polarization of M2-like macrophages

The efferocytosis of apoptotic neutrophils together with other pro-resolution signals, induces a shift in macrophages from a proinflammatory (referred to as “M1-like macrophage”) to an anti-inflammatory (referred to as “M2-like macrophage”) phenotype [79]. The different macrophage subsets can be identified according to their differential expression of surface molecules, such as MHC-II and CD206 (Figure **16A**).

While the numbers of MHC-II^{+} CD206^{-} M1-like macrophages and the intermediate stage (MHC-II^{+} CD206^{lo}) were not altered in the absence of MC-derived TNF (Figure **16B**, left and middle), the number of MHC-II^{-} CD206^{hi} M2-like macrophages was significantly decreased at 120 h post-DNFB challenge within the ear skin of MC$^{\Delta TNF}$ compared to MC^{WT} mice (Figure **16B**, right).

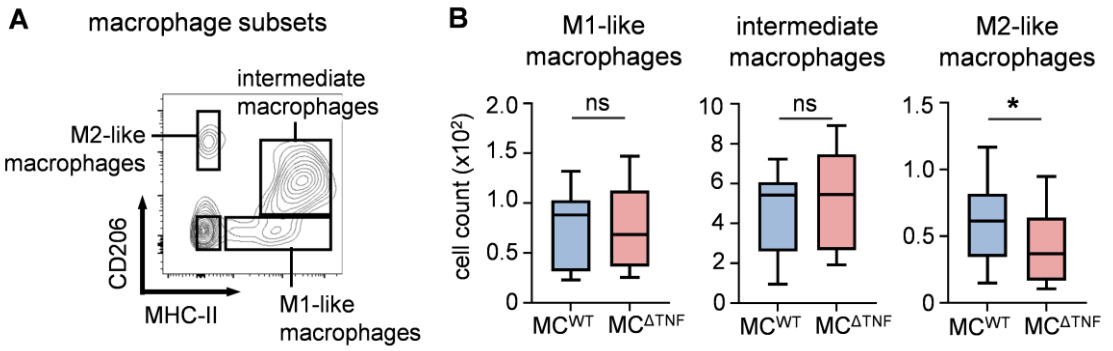

Figure 16| Reduced numbers of M2-like macrophages in the absence of MC-derived TNF. MC$^{\Delta TNF}$ mice and respective MC^{WT} littermates were sensitized on the back skin and challenged six days later at the ear with DNFB. Vehicle (veh) mice were only treated with the solvent (w/o DNFB). **A|** Representative contour plot of skin macrophage subsets including MHC-II^{+} CD206^{-} M1-like, MHC-II^{+} CD206^{lo} intermediate and MHC-II^{-} CD206^{hi} M2-like macrophages following gating on singlets and CD45^{+} Ly6G^{-} F4/80^{+} cells. **B|** Numbers of skin macrophage subsets were quantified 120 h after DNFB challenge using flow cytometry and normalized to the total cell count (two independent experiments, n=13-15 per group). Box-whisker plots indicate the median (horizontal line), interquartile range (box) and minimum to maximum range (whisker) of the values. Statistical significance was determined using a two-tailed Mann-Whitney test. ns p>0.1; # p<0.1; * p<0.05; ** p<0.01; *** p<0.001; **** p<0.0001

4.4.4 MC-derived TNF is essential for proper tissue recovery

Following the resolution of inflammation, a final step is the restoration of tissue integrity through remodeling processes. These include the degradation of ECM components (mainly collagen) as well as their synthesis. A balance between those two processes is essential for proper tissue recovery and the maintenance or restoration of tissue integrity. Both, monocytes and M2-like macrophages critically promote the degradation of ECM through the release of MMPs [115].

To determine, whether the persistent ear thickness at later time points of hapten-induced skin inflammation in the absence of MC-derived TNF resulted from a dysregulated ECM degradation, protein levels of different MMPs were quantified using multiplex approaches. At 72 h post-DNFB challenge, protein levels of MMP-8 and proMMP-9, but not of MMP-2, -3 and -12, were strongly increased within the ear skin of MC^{WT} mice compared to veh-treated controls (Figure **17A**). In contrast, protein expression of MMP-8 and proMMP-9 was completely missing in $MC^{\Delta TNF}$ mice (Figure **17B**). While MMP-8 degrades collagen type I and III (most abundant collagen subforms in the skin), MMP-9 cleaves collagen type IV, V and XI [115]. Therefore, I next determined the protein levels of collagen type I, III and IV in ear skin homogenates using ELISA approaches. According to the reduced amount of MMP-8, the protein level of collagen type I was increased at 120 h post-DNFB challenge in $MC^{\Delta TNF}$ compared to MC^{WT} mice (Figure **17C**, left). In contrast, protein levels of collagen type III and IV were not changed at 72 h and 120 h post-DNFB challenge in the absence of MC-derived TNF (Figure **17C**, middle and right).

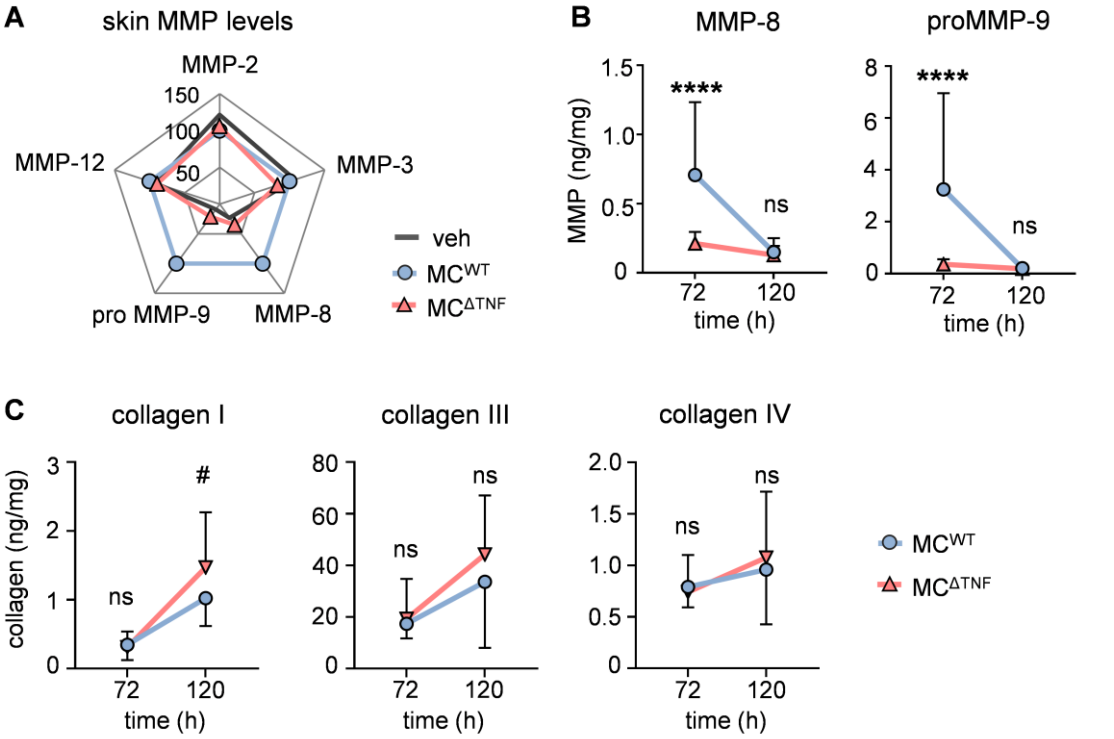

Figure 17| MC-derived TNF promotes collagen degradation in the resolution phase. $MC^{\Delta TNF}$ mice and respective MC^{WT} littermates were sensitized on the back skin and challenged 6 days later at the ear with DNFB. Vehicle (veh) mice were only treated with the solvent (w/o DNFB). **A-B|** Protein levels of matrix metalloproteinases (MMP) in ear skin were quantified at indicated time points after DNFB challenge using multiplex approaches and normalized to the skin biopsy weight. The radar plot (**A**) show the protein levels of MMPs in $MC^{\Delta TNF}$ and veh mice as percentage compared to MC^{WT} mice (set to 100 %). **C|** Protein levels of collagen subforms were determined at indicated time points after DNFB challenge using ELISA and normalized to the skin biopsy weight. (Two independent experiments, n=7-14 per group and n=3-4 for veh). Graphs depict the mean +/- SD. Statistical significance was determined using a two-way ANOVA with Tukey's multiple-comparison test. ns p>0.1; # p<0.1; * p<0.05; ** p<0.01; *** p<0.001; **** p<0.0001

Additionally, M2-like macrophages promote the synthesis of new ECM by myofibroblasts through the release of the profibrotic factor TGF-ß [71]. In order to examine, whether matrix production was also affected by the absence of MC-derived TNF, gene expression of major ECM components was measured using qRT-PCR. Gene expression of *Collagen 1a1*, *3a1* and *4a1* was not increased at 120 h post-DNFB challenge in the ear skin of $MC^{\Delta TNF}$ compared to MC^{WT} mice (Figure **18A**). Interestingly, I observed an increased gene expression of *Fibronectin* in the absence of MC-derived TNF (Figure **18B**). Fibronectin is predominantly expressed by fibroblasts and crosslinks collagen fibrils, thereby increasing tissue strength [116]. However, neither the numbers of $CD31^{-}$ $gp38^{+}$ fibroblastic reticular cells (Figure **18C**), nor protein levels of fibronectin were increased within the ear skin of $MC^{\Delta TNF}$ compared to MC^{WT} mice at 120 h post-DNFB challenge (Figure 18**D**).

Taken together, these results suggest that the persistent ear thickness at later time points of hapten-induced skin inflammation in the absence of MC-derived TNF may be associated with a dysregulated collagen degradation.

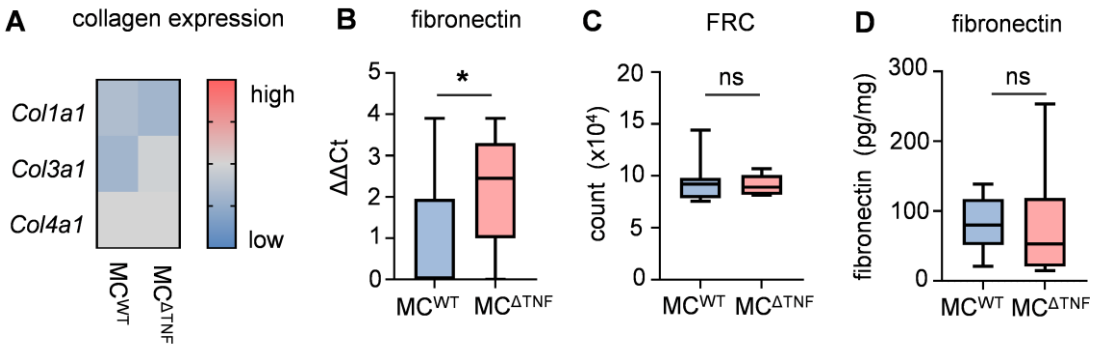

Figure 18| MC-derived TNF does not affect collagen production. $MC^{\Delta TNF}$ mice and respective MC^{WT} littermates were sensitized on the back skin and challenged 6 days later at the ear with DNFB. Gene expression of **A|** *collagen* (Col) subforms and **B|** *fibronectin* was quantified 120 h after DNFB challenge using quantitative (q)PCR. **C|** Numbers of $CD31^{-}$ $gp38^{+}$ fibroblastic reticular cells (FRC) (pregated on singlets and $CD45^{-}$ cells) in ear skin were quantified 120 h post-DNFB challenge using flow cytometry and normalized to the total cell count. **D|** Protein levels of fibronectin were determined 120 h after DNFB challenge using ELISA and normalized to the skin biopsy weight. Box-whisker plots indicate the median (horizontal line), interquartile range (box) and minimum to maximum range (whisker) of the values (**A-D** two independent experiments, n=10-12 per group). Statistical significance was determined using a two-tailed Mann-Whitney test. ns p>0.1; # p<0.1; * p<0.05; ** p<0.01; *** p<0.001; **** p<0.0001

4.5 The total depletion of TNF alters the resolution of CHS

Given the importance of MC-derived TNF for the proper onset of hapten-induced skin inflammation and subsequent tissue recovery, I questioned whether an anti-inflammatory TNF therapy might have a similar effect on the inflammatory course in CHS. This therapy is commonly used in humans for the treatment of several autoimmune diseases such as rheumatoid arthritis [117].

In order to investigate this, a murine anti-TNF antibody was i.v. injected into C57BL/6Jrj mice two hours before DNFB sensitization. C57BL6Jrj mice injected with the antibody isotype served as a control. Six days later, mice were challenged and the inflammatory response was analysed by means of ear swelling measurement (Figure **19A**). Indeed, C57BL/6Jrj mice treated with the anti-TNF antibody mirrored the same phenotype as $MC^{\Delta TNF}$ mice with a reduced ear swelling in the induction phase and a non-resolving ear thickness at later time points of hapten-induced skin inflammation (Figure **19B**).

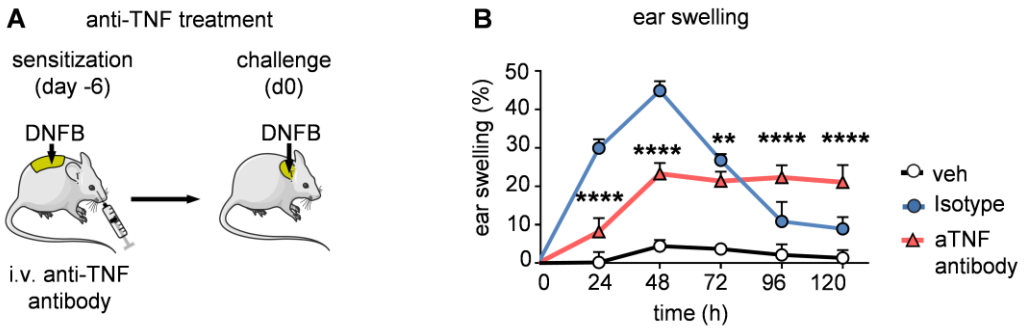

Figure 19| Impaired CHS response after TNF depletion in the sensitization phase. A| C57BL/6Jrj mice were intravenously (i.v.) injected with a murine anti-tumor necrosis factor (TNF) antibody and sensitized two hours later on the shaved back. C57BL/6Jrj mice injected with the antibody isotype served as a control. Six days later, mice were challenged with DNFB at the ear. Vehicle (veh) mice were only treated with the solvent (w/o DNFB). **B|** Ear swelling at indicated time points after DNFB challenge shown as percent (%) increase (one experiment, n=5 per group and n=4 for veh). The graph depicts the mean +/- SD. Statistical significance between the isotype and aTNF antibody-treated groups was determined using a two-way ANOVA with Tukey's multiple-comparison test. ns p>0.1; # p<0.1; * p<0.05; ** p<0.01; *** p<0.001; **** p<0.0001

5 Discussion

Due to their location at interface organs such as the skin and their capacity, to rapidly release preformed mediators by degranulation, MCs play an important role in the initiation of hapten-induced skin inflammation (reviewed in [1]). However, the relevance of MCs in the resolution phase was not investigated so far. We recently found that in the absence of MC-derived TNF, although inflammation in the induction phase of CHS was reduced, the skin did not adequately recover at later time points. This suggests, that MC-derived TNF is essential for the resolution of hapten-induced skin inflammation or the complete restoration of the physiological tissue integrity after an inflammatory challenge.

Upon contact with a hapten, MCs are rapidly activated by alarmins such as ATP and IL-33 [34], which are for instance released by stressed keratinocytes [51,52]. Subsequently, they secrete a variety of preformed mediators via degranulation [21]. The group of Anne Dudeck demonstrated that MCs initiate immediate vascular responses in hapten-induced skin inflammation. MC-derived histamine enhances vasodilatation and vessel permeability, leading to endothelial barrier disruption and edema formation. Furthermore, MCs induce the activation of vessel endothelium, thereby promoting neutrophil and T cell recruitment to the hapten-challenged site [54]. Beside vascular effects, MCs critically promote the activation and transmigration of circulating neutrophils. More specifically, we could recently prove, that MC-derived TNF regulates the transition from rolling to firm adhesion and intravascular crawling of neutrophils [59]. Moreover, MCs promote the maturation and migration of DCs in acute skin inflammation, partially again via TNF, thereby increasing T cell priming and enhancing the T cell response [2,19,118].

While the effects of MCs on neutrophils and DCs have been extensively studied, our understanding of their impact on monocytes and macrophages remains limited [8]. In general, MCs are known as important producers of the chemokines CCL2 and CCL7, which effectively attract monocytes [119]. However, an influence on monocyte recruitment during hapten-induced skin inflammation was not investigated thus far. In my study, I found a strong decrease in the numbers of skin monocytes at early time points of hapten-induced skin inflammation in the absence of MC-derived TNF. According to phenotypical and functional properties, skin monocytes can be divided into three distinct subsets. Ly6C^{hi} MHC-II^{-} dMonocytes represent newly infiltrated Ly6C^{hi} blood iMonocytes, which can differentiate for instance into Ly6C^{hi} MHC-II^{+} moDC1 and consequently to Ly6C^{hi} MHC-II^{+} moDC2 [109]. In particular, the number of dMonocytes was reduced whereas moDC1 numbers were only slightly decreased in the absence of MC-derived TNF. Taken together, these results indicate a crucial role for MC-derived TNF in the recruitment of monocytes during hapten-induced skin inflammation.

During infection and inflammation, Ly6C^{hi} iMonocytes are mobilized from reservoirs, such as the spleen and BM, as well as the blood [120]. Subsequently, emergency myelopoiesis, involving the local proliferation of myeloid progenitors, is rapidly induced to replenish these reservoirs of myeloid cells. Surprisingly, iMonocyte numbers in the spleen and BM were not increased in the absence of MC-derived TNF 36 h after hapten challenge. Therefore, MC-derived TNF seems to have no effect on monocyte mobilization, or any potential effects on monocyte numbers in the spleen and BM may already be diminished at this time point [121]. The influence of MC-derived TNF on myeloid cell mobilization and emergency myelopoiesis in the spleen and BM are therefore studied in detail and at even earlier time points after DNFB challenge in a separate and ongoing project in the Dudeck research group. Both, iMonocyte mobilization and subsequent recruitment to sites of infection and inflammation are predominantly mediated by the chemokines CCL2 and CCL7, which bind to the respective receptor CCR2 on monocytes [120]. During the elicitation of hapten-induced skin inflammation, CCL2 is initially released in small amounts by skin resident cells including keratinocytes fibroblasts and endothelial cells. Afterwards, fibroblasts and newly infiltrating monocytes become the primary source of this chemokine, resulting in a peak of CCL2 protein expression around 24 h after hapten challenge [122]. Regarding the production, kinetics and role of CCL7 in hapten-induced skin inflammation, our current understanding is still limited. Despite the reduced skin infiltration of dMonocytes, skin and serum levels of CCL2 and CCL7 were not changed in the absence of MC-derived TNF at 36 h post-DNFB challenge. This implies that MC-derived TNF is dispensable for the upregulation of CCL2 and CCL7 production and that other cells, such as fibroblasts, may compensate for the production of CCL2 by monocytes. Most importantly, these results also indicate that monocyte recruitment during hapten-induced skin inflammation is only partially mediated by the chemokines CCL2 and CCL7 with MC-derived TNF initiating an additional process.

Notably, TNF was also reported to directly modulate monocyte/macrophage recruitment via the activation of TNFR1 in a cutaneous wound healing model [112]. In this context, Lim *et al.* demonstrated that TNF-TNFR1 signalling in monocytes potentiates their RhoA-mediated transmigratory capacity *in vitro*. Furthermore, they found that the elevation of TNF serum levels through the intraperitoneal injection of mouse-specific TNF resulted in an increased CCL2-dependent recruitment of monocytes to the intraperitoneal cavity *in vivo*. This led them to conclude that TNF present in the bloodstream may prime the RhoA-dependent activities of circulating monocytes, thus enhancing their recruitment to inflammatory sites [113]. We recently demonstrated a similar effect of MC-derived TNF on neutrophil recruitment and extravasation during hapten-induced skin inflammation. Moreover, we found that MCs can deliver the TNF via directional degranulation into the

bloodstream [59]. Therefore, I next examined a direct influence of MC-derived TNF on monocyte recruitment using conditional knockout mice, which lack TNFR1 expression in monocytes. However, the results ruled out a direct receptor-ligand signalling-driven effect of MC-derived TNF on monocyte recruitment via TNFR1 during hapten-induced skin inflammation.

Previously, Chong *et al.* demonstrated that during the elicitation of hapten-induced skin inflammation, particularly $CD8^+$ T cells mediate the recruitment of monocytes via IL-17, as well as their differentiation towards moDC1 through IFN-γ [66]. In this context, Anne Dudeck and her former colleagues showed, that $CD8^+$ T cell priming and recruitment to the skin are reduced in the absence of MC-derived TNF, as a consequence of a decreased functionality of cDC1. In line with the latter study, I found a reduced skin infiltration of $CD8^+$ T cells at 36 h post-DNFB challenge in the absence of MC-derived TNF, supporting the crucial role of MC-derived TNF in the induction of a hapten-specific T cell response. Therefore, I hypothesized that the reduced skin infiltration of monocytes after hapten challenge may result from an inefficient $CD8^+$ T cell priming in the absence of MC-derived TNF. Indeed, the adoptive transfer of adequately primed $CD8^+$ T cells from sensitized wildtype mice restored monocyte skin infiltration at 24 h post-DNFB challenge in the absence of MC-derived TNF and even slightly enhanced the differentiation of moDC1. Notably, skin $CD8^+$ T cell numbers were not significantly decreased at this time point in the absence of MC-derived TNF. This might be related to the early stage of $CD8^+$ T cell infiltration, which typically starts around 18 h to 24 h after hapten challenge [123]. Additionally, a minor skin infiltration of $CD8^+$ T cells was observed even in the absence of MC-derived TNF [2]. Taken together, these results prove that MC-derived TNF indirectly facilitates monocyte recruitment during the elicitation of hapten-induced skin inflammation by ensuring an adequate priming of $CD8^+$ T cells in the sensitization phase.

Interestingly, Kish *et al.* found that the reactivation of primed $CD8^+$ T cells and the subsequent expression of IL-17 and IFN-γ are initiated by hapten-presenting endothelial cells at the challenged site. This suggests that $CD8^+$ T cells license the recruitment and extravasation of monocytes already within the circulation before they enter the skin. In order to prove this, serum levels of IL-17, which was shown to be crucial for monocyte recruitment, were analysed at 24 and 36 h after DNFB challenge. However, IL-17 protein levels were not detectable at these time points using ELISA approaches. In this context, employing more sensitive techniques such as qRT-PCR to assess IL-17 expression may be helpful to further validate the process. To date, the molecular mechanism by which IL-17 promotes monocyte recruitment and/or transmigration remains unknown.

Most importantly, I found that the adoptive transfer of adequately primed $CD8^+$ T cells also restored adequate tissue recovery to physiologic ear thickness at later time points of CHS. This indicates that the priming of $CD8^+$ T cells together with the early recruitment of monocytes to the skin are crucial events for the induction of an effective resolution program during CHS-induced skin inflammation.

In order to further examine an indirect effect of MC-derived TNF on monocyte recruitment via the modulation of cDC1 functionality to effectively prime $CD8^+$ T cells (see Figure **20**), a conditional knockout mouse lacking TNFR1 signalling in CD11c-expressing cells was generated. Surface expression of TNFR1 on BMDCs from these mice was significantly reduced at steady-state and inflammatory conditions (LPS stimulation), but not completely absent, when compared to the antibody isotype control. This observation could be linked to an insufficient antibody specificity. However, it may also be that the deletion of the *Tnfrsfa1* gene in BMDCs is only partial. In order to further verify the knockout, more sensitive methods for the analysis of gene deletions such as single-cell PCR may be helpful. Additionally, I proved that these mice do not possess alterations in the numbers of skin resident and splenic immune cell subsets, except for a slight increase in the numbers of skin cDC1. Since TNFR1 is critically implicated in the regulation of apoptosis [124], this increase might be related to a reduced apoptosis. As described before, cDC1 promote the priming of hapten-specific $CD8^+$ T cells in the sensitization phase [2]. However, it is likely that the small increase in numbers is negligible with respect to $CD8^+$ T cell priming.

Intriguingly, when investigating the CHS response in $DC^{\Delta TNFR1}$ mice, the ear swelling was reduced at initial stages after DNFB challenge, but not resolved at later time points in the absence of TNFR1 signalling in DCs, similar to the findings observed in the absence of MC-derived TNF. In contrast, neither the numbers of skin infiltrating $CD8^+$ T cells nor of dMonocytes were significantly reduced. This controversy may suggest that reduced TNF-TNFR1 signalling in DCs affects the $CD8^+$ T cell priming more than their recruitment to the skin, while, as outlined above, effective $CD8^+$ T cell priming is also more relevant than their infiltration into the skin. Importantly, we and others have shown for neutrophils, that proper activation of these cells, while being still in blood circulation, is as critical for the extravasation and functions as recruiting signals from the tissues [59]. This dependency on priming effects within the circulation time frame may be similar for monocytes. Hence, the skin infiltrating cell numbers alone provide no information about their functionality and efficiency in triggering or terminating an inflammatory reaction. Importantly, despite the discrepancy, and although the mechanism is not yet fully understood, the data prove that TNF-TNFR1 signalling in DCs is critical for the induction, but also the termination of the hapten-induced inflammation.

Already in 2001, Mizumoto *et al.* demonstrated a crucial role for monocytes in the pathophysiology of hapten-induced skin inflammation. More specifically, they found that transgenic mice, which overexpress the monocyte-attracting chemokine CCL2, possess an increased CHS response, whereas the depletion of this chemokine reduces disease severity [125]. However, the specific effector function of monocytes has long been an enigma. More than 10 years later, Chong *et al.* revealed that $Ly6C^+$ $CD11b^+$ monocytic cells are key producers of TNF and iNOS in hapten-induced skin inflammation [66], which were both found to critically promote the inflammatory response [126,127]. In line with the latter study, I found reduced levels of TNF at early time points of CHS in the absence of MC-derived TNF. This decline could be attributed to either the lack of MC-derived TNF or the reduced infiltration of monocytes. Importantly, MCs store preformed and fully active TNF in their secretory granules, which can be rapidly released upon activation through degranulation [16]. In this context, we demonstrated that MCs secrete TNF as early as 2 h upon hapten challenge and thereby critically promote the early recruitment of neutrophils [59]. Afterwards, also other skin-resident cells such as macrophages and DCs along with newly infiltrating monocytes participate in the synthesis of TNF at the hapten-challenged site [49,66]. Given the substantial influx of monocytes, the decline in TNF protein levels at 36 h after DNFB challenge is more likely attributed to the reduced recruitment of monocytes than to the lack of MC-derived TNF. In addition to TNF, I found strongly reduced protein levels of IL-6 at the hapten-challenged site in the absence of MC-derived TNF. The proinflammatory cytokine IL-6 can be produced by a variety of immune and non-immune cells, but the primary contributors at the site of inflammation are thought to be monocytes and macrophages [128]. Therefore, it is likely that the decreased levels of IL-6 at the hapten-challenged site are also a consequence of the reduced monocyte skin infiltration in the absence of MC-derived TNF. Taken together, these results support the effector role of monocytes in the induction phase of hapten-induced skin inflammation and also suggest monocytes as important producers of IL-6.

Beside their important role in the induction phase, monocytes also play a crucial role in the resolution of inflammation (reviewed in [129]). Upon infiltration into the tissue, monocytes can differentiate into macrophages, and under the influence of cytokines such as IFN-γ or IL-4, respectively, these macrophages can adopt either a classically activated phenotype (M1-like) or an alternatively activated phenotype (M2-like) [110]. While M1-like macrophages are potent pro-inflammatory cells, M2-like macrophages critically promote the resolution of inflammation through the clearance of apoptotic neutrophils and tissue repair [79]. Accordingly, an inflammatory process is often accompanied by a switch in macrophage plasticity from M1-like in early phases to M2-like in later phases. In order to elucidate the link between $CD8^+$ T cells, monocytes and the adequate resolution of inflammation, key events during the resolution phase were investigated.

A first step in the resolution of inflammation is the counterregulation of chemokine and proinflammatory cytokine production which is mainly driven by M1-like macrophages. This counterregulation represents a prerequisite for the subsequent termination of immune cell infiltration and precedes the phenotypic switch from M1-like to M2-like macrophages [71,79]. Interestingly, I observed a strong decrease in skin protein levels of chemokines, including CXCL1, CXCL2, CCL3 and CCL5, as well as proinflammatory cytokines such as IL-1β and TNF at the onset of the resolution phase (72 h after DNFB challenge) in the absence of MC-derived TNF. At the same time, total numbers of leukocytes and neutrophils were not altered in the absence of MC-derived TNF. Thus, it is likely that the decreased levels of these mediators are a consequence of an attenuated inflammatory response in the induction phase. Most importantly, protein levels of chemokines and proinflammatory cytokines, as well as total numbers of leukocytes regularly decreased in the absence of MC-derived TNF. These results indicate that the defective recovery of ear swelling at later time points of CHS in the absence of MC-derived TNF does not result from persistent inflammation.

As a next step during the resolution of inflammation, neutrophils undergo apoptosis and are removed by macrophages [7,71]. The induction of neutrophil apoptosis is tightly regulated by the proinflammatory micromilieu [86]. The cytokine TNF was shown to have divergent effects on neutrophil life span during this phase. While high concentrations induce neutrophil apoptosis, low concentrations were demonstrated to promote neutrophil survival [87]. Once apoptosis is induced, neutrophils release “find me” and “eat me” signals, which promote their non-phlogistic clearance by macrophages in a process termed “efferocytosis” [79]. With respect to the impaired recruitment of monocytes, as well as the reduced levels of TNF at the onset of the resolution phase, I questioned whether the persistent ear thickness at later time points of CHS in the absence of MC-derived TNF resulted from an accumulation of neutrophils as a consequence of a prolonged life span and/or reduced clearance by monocytes/macrophages. However, I found that MC-derived TNF is dispensable for the timely induction of neutrophil apoptosis, as well as their removal by macrophages during hapten-induced skin inflammation.

The efferocytosis of apoptotic neutrophils, pro-resolving lipid mediators and specific cytokines such as IL-4 induce a switch in macrophages from the proinflammatory M1-like to the anti-inflammatory M2-like phenotype [79]. Despite the regular clearance of neutrophils, I observed significantly reduced numbers of M2-like macrophages within ear skin at 120 h after DNFB challenge in the absence of MC-derived TNF. Due to the substantial differentiation of infiltrating monocytes into macrophages throughout an inflammatory process [110], the reduced number of M2-like macrophages is likely a

consequence of the decreased infiltration of monocytes at early stages of CHS in the absence of MC-derived TNF. This hypothesis is supported by a study from Arnold *et al.*, demonstrating that infiltrating Ly6C^{hi} monocytes predominantly differentiate into CD206^{+} macrophages during sterile inflammation, which they referred to as “repair macrophages”, but reflect the herein explained M2-like macrophages [130]. Additionally, I showed strongly reduced levels of IL-4 in the induction phase, which may also affect the M2-like macrophage polarization at later time points of CHS. Further studies on the intercellular crosstalk between MCs and macrophages and its effect on macrophage polarization, also with regard to soluble MC mediators vs. MC granules and physical contacts, are currently being carried out in the research group of Anne Dudeck.

Infiltrating monocytes and M2-like macrophages critically promote the restoration of tissue functionality via the induction of processes restructuring the ECM (reviewed in [131]). This restoration is essential for reestablishing skin barrier function, maintaining the composition and localization of resident immune cells, and ensuring the overall integrity and stability of the tissue [46]. Both M2-like macrophages and monocytes secrete a variety of MMPs, including MMP-8, MMP-9 and MMP-12, which facilitate the timely and precise degradation of collagen during the induction and resolution phase [132]. In the induction phase, the degradation of collagen is essential for facilitating the correct tissue migration of infiltrating cells, whereas, during the resolution phase, it plays a crucial role in restoring the physiological tissue architecture [115,133]. Additionally, M2-like macrophages activate resident fibroblasts through the release of TGF-β and growth factors such as platelet-derived growth factor (PDGF) and VEGF, resulting in the increased production and deposition of collagen [134]. Of note, protein expression of MMP-8 and pro-MMP-9 was completely missing at the onset of the resolution phase (72 h post-DNFB challenge) in the absence of MC-derived TNF, which may be attributed to the impaired skin infiltration of monocytes during the induction phase [132]. Conversely, collagen I protein levels were elevated at 120 h post-DNFB challenge, without a corresponding increase in gene expression. Thus, the persistent ear thickness at later time points of CHS presumably results from a decreased collagen degradation, due to an impaired monocyte skin infiltration in the absence of MC-derived TNF. This hypothesis is supported by a study from Wang *et al.*, which demonstrated that MMP-9 deficiency prolongs the ear swelling response in DNFB-induced skin inflammation [135]. Moreover, MMP-8 and MMP-9 were both reported to possess potent anti-fibrotic activities in lung [136] and liver fibrosis [136–138] through the degradation of ECM. In addition to the increased protein levels of collagen, I found an elevated gene expression of the collagen crosslinking protein fibronectin in the absence of MC-derived TNF, which was also demonstrated to be critical for fibrogenesis [139]. However, protein levels of fibronectin and the number of fibroblastic reticular cells were not changed in the absence

of MC-derived TNF, thus suggesting a minor role of enhanced fibronectin gene expression to the persistence of ear swelling.

In summary, I aim to illustrate the aforementioned findings in alignment with existing studies, depicted within the following model (Figure **20**).

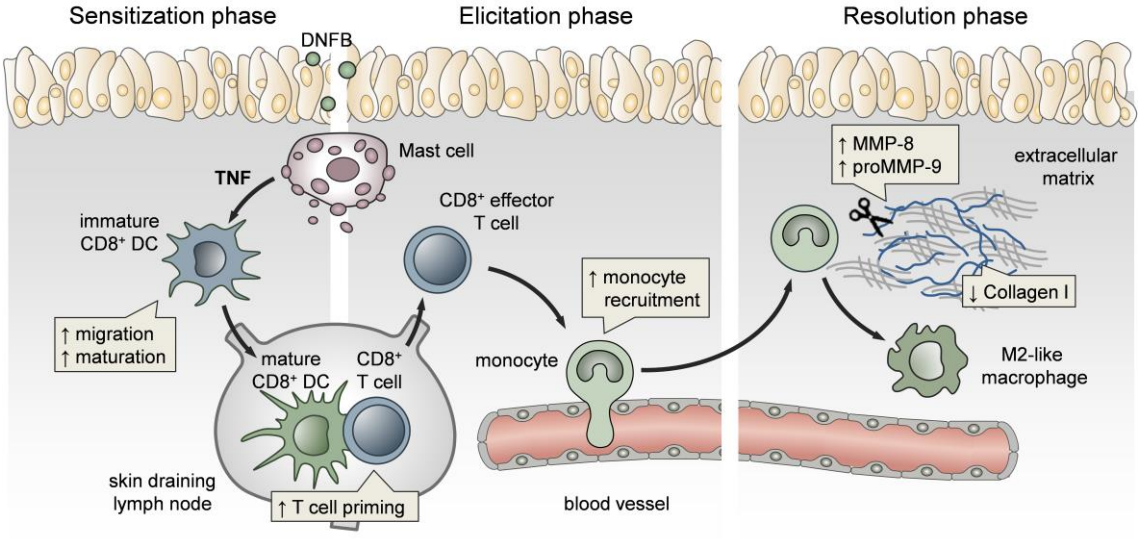

Figure 20| MC-derived TNF indirectly promotes monocyte recruitment and subsequent tissue recovery by enduring an adequate priming of CD8⁺ T cells. Conventional dendritic cell (cDC)-1, Dinitrofluorobenzene (DNFB) Interleukin-17 (IL-17), Matrix metalloproteinase (MMP)

In the sensitization phase, MC-derived TNF critically promotes cDC1 maturation and migration to the draining lymph node and consequently the effective priming of $CD8^+$ T cells [2]. During the elicitation phase, primed $CD8^+$ T cells then mediate the recruitment and skin infiltration of monocytes, presumably via the release of IL-17 upon reactivation by endothelial cells at the challenged site [66,140]. In turn, monocytes release MMP-8 and proMMP-9, which are crucial for ECM degradation, particularly collagen I, in the resolving phase. Moreover, proinflammatory monocytes become polarized towards alternatively activated (M2-like) macrophages. Taken together, these results indicate, that a timely and precise initiation of hapten-induced skin inflammation by MC-derived TNF is crucial for subsequent tissue recovery.

Based on these findings, a pivotal question arises regarding whether the effects of MC-derived TNF on tissue recovery in hapten-induced skin inflammation extend to other inflammatory disorders characterized by significant involvement of $CD8^+$ T cells and monocytes. To address this, experiments investigating the role of MC-derived TNF (using Mcpt5-Cre^+ $TNF^{fl/fl}$ mice) during both the induction and resolution phase of unilateral ureteral obstruction, a murine kidney fibrosis model, are currently being conducted in cooperation with Dr. Sabine Brandt (Institute of Experimental Nephrology, Otto-von-Guericke University Magdeburg).

With respect to the important function of MC-derived TNF in the initiation of hapten-induced skin inflammation and consequently for adequate tissue recovery, I also questioned, whether an anti-TNF therapy, which is often used for the treatment of inflammatory autoimmune diseases including Crohn's disease, rheumatoid arthritis and psoriasis [117], may also impair the resolution of hapten-induced skin inflammation. Of note, the total depletion of TNF via the injection of a murine anti-TNF antibody immediately before DNFB sensitization caused a reduced inflammation in the initiation phase, but also the persistence of ear swelling at later time points of CHS, as it has been shown for MC-derived TNF. These results prove the essential role of TNF in the initiation of hapten-induced skin inflammation. In contrast, no effect of an anti-TNF treatment on the development of the human disease ACD and on patch test responses was shown [141–143]. Most importantly, these findings also suggest that a therapeutic depletion of TNF may have an adverse impact on the resolution of ACD, an aspect that has not yet been investigated. However, further research is needed to confirm the mechanism, described before, including the analysis of monocyte skin infiltration at early time points, as well as the quantification of MMP-8, proMMP-9 and collagen I protein levels at later stages upon total depletion of TNF.

As mentioned before, TNF inhibitors are commonly used to treat autoimmune diseases such as Crohn's disease and rheumatoid arthritis [117]. In both conditions, monocytes and macrophages also play an important role in the pathophysiology [144,145]. While several studies have proven the effectiveness of TNF inhibitors in reducing acute inflammation, only a few have investigated their effect on the resolution of these diseases [146,147]. Importantly, Schaeffer *et al.* found, that TNF-inhibition during Chron's disease caused an increase in submucosal hyaline fibrosis [148]. Another recent study confirmed heightened intestinal fibrosis during TNF treatment of Crohn's disease, highlighting a potential side effect of TNF inhibitors [149]. The exact pathophysiological mechanisms remain unclear. Scheaffer *et al.* suggested that the increased fibrosis may result from an imbalance between TNF and the profibrogenic factor TGF-β. Consequently, inhibiting TNF could amplify the profibrotic signalling cascade [148]. However, it may also result from a dysregulated collagen degradation at later stages, as observed in the absence of MC-derived TNF. This aspect warrants further investigation to better understand the effects and potential side effects of TNF inhibitors.

In conclusion, the results obtained in this study reveal an intricate series of cellular events initiated by MC-derived TNF that is essential for adequate tissue recovery. Notably, these findings are clinically relevant in the context of anti-TNF therapies, which efficiently inhibit acute inflammation, but may affect tissue remodeling in late phases or long term.

6 References

[1] Voss M, Kotrba J, Gaffal E, Katsoulis-Dimitriou K, Dudeck A. Mast cells in the skin: Defenders of integrity or offenders in inflammation? Int J Mol Sci 2021;22. https://doi.org/10.3390/ijms22094589.

[2] Dudeck J, Ghouse SM, Lehmann CHK, Hoppe A, Schubert N, Nedospasov SA, et al. Mast-Cell-Derived TNF Amplifies CD8+ Dendritic Cell Functionality and CD8+ T Cell Priming. Cell Rep 2015;13:399–411. https://doi.org/10.1016/j.celrep.2015.08.078.

[3] Murphy K, Weaver C. Janeway Immunologie. Berlin, Heidelberg: Springer Berlin Heidelberg; 2018. https://doi.org/10.1007/978-3-662-56004-4.

[4] Kabashima K, Honda T, Ginhoux F, Egawa G. The immunological anatomy of the skin. Nat Rev Immunol 2019;19:19–30. https://doi.org/10.1038/s41577-018-0084-5.

[5] Mahlapuu M, Håkansson J, Ringstad L, Björn C. Antimicrobial Peptides: An Emerging Category of Therapeutic Agents. Front Cell Infect Microbiol 2016;6. https://doi.org/10.3389/fcimb.2016.00194.

[6] Di Nardo A, Yamasaki K, Dorschner RA, Lai Y, Gallo RL. Mast Cell Cathelicidin Antimicrobial Peptide Prevents Invasive Group A Streptococcus Infection of the Skin. The Journal of Immunology 2008;180:7565–73. https://doi.org/10.4049/jimmunol.180.11.7565.

[7] Soehnlein O, Lindbom L. Phagocyte partnership during the onset and resolution of inflammation. Nat Rev Immunol 2010;10:427–39. https://doi.org/10.1038/nri2779.

[8] Dudeck A, Köberle M, Goldmann O, Meyer N, Dudeck J, Lemmens S, et al. Mast cells as protectors of health. Journal of Allergy and Clinical Immunology 2019;144:S4–18. https://doi.org/10.1016/j.jaci.2018.10.054.

[9] Li D, Wu M. Pattern recognition receptors in health and diseases. Signal Transduct Target Ther 2021;6:291. https://doi.org/10.1038/s41392-021-00687-0.

[10] Eisenbarth SC. Dendritic cell subsets in T cell programming: location dictates function. Nat Rev Immunol 2019;19:89–103. https://doi.org/10.1038/s41577-018-0088-1.

[11] Kambayashi T, Laufer TM. Atypical MHC class II-expressing antigen-presenting cells: can anything replace a dendritic cell? Nat Rev Immunol 2014;14:719–30. https://doi.org/10.1038/nri3754.

[12] Jiang S, Dong C. A complex issue on CD4+ T-cell subsets. Immunol Rev 2013;252:5–11. https://doi.org/10.1111/imr.12041.

[13] Kaech SM, Cui W. Transcriptional control of effector and memory CD8+ T cell differentiation. Nat Rev Immunol 2012;12:749–61. https://doi.org/10.1038/nri3307.

[14] Kaech SM, Wherry EJ, Ahmed R. Effector and memory T-cell differentiation: implications for vaccine development. Nat Rev Immunol 2002;2:251–62. https://doi.org/10.1038/nri778.

[15] Crivellato E, Beltrami CA, Mallardi F, Ribatti D. Paul Ehrlich's doctoral thesis: a milestone in the study of mast cells. Br J Haematol 2003;123:19–21. https://doi.org/10.1046/j.1365-2141.2003.04573.x.

[16] Abraham SN, St. John AL. Mast cell-orchestrated immunity to pathogens. Nat Rev Immunol 2010;10:440–52. https://doi.org/10.1038/nri2782.

[17] Chia SL, Kapoor S, Carvalho C, Bajénoff M, Gentek R. Mast cell ontogeny: From fetal development to life-long health and disease. Immunol Rev 2023;315:31–53. https://doi.org/10.1111/imr.13191.

[18] Leist M, Sünder CA, Drube S, Zimmermann C, Geldmacher A, Metz M, et al. Membrane-bound stem cell factor is the major but not only driver of fibroblast-induced murine skin mast cell differentiation. Exp Dermatol 2017;26:255–62. https://doi.org/10.1111/exd.13206.

[19] Dudeck J, Medyukhina A, Fröbel J, Svensson CM, Kotrba J, Gerlach M, et al. Mast cells acquire MHC II from dendritic cells during skin inflammation. Journal of Experimental Medicine 2017;214:3791–811. https://doi.org/10.1084/jem.20160783.

[20] Frossi B, Mion F, Sibilano R, Danelli L, Pucillo CEM. Is it time for a new classification of mast cells? What do we know about mast cell heterogeneity? Immunol Rev 2018;282:35–46. https://doi.org/10.1111/imr.12636.

[21] Wernersson S, Pejler G. Mast cell secretory granules: armed for battle. Nat Rev Immunol 2014;14:478–94. https://doi.org/10.1038/nri3690.

[22] Jiménez M, Cervantes-García D, Córdova-Dávalos LE, Pérez-Rodríguez MJ, Gonzalez-Espinosa C, Salinas E. Responses of Mast Cells to Pathogens: Beneficial and Detrimental Roles. Front Immunol 2021;12. https://doi.org/10.3389/fimmu.2021.685865.

[23] Dwyer DF, Barrett NA, Austen KF. Expression profiling of constitutive mast cells reveals a unique identity within the immune system. Nat Immunol 2016;17:878–87. https://doi.org/10.1038/ni.3445.

[24] Akula, Paivandy, Fu, Thorpe, Pejler, Hellman. Quantitative In-Depth Analysis of the Mouse Mast Cell Transcriptome Reveals Organ-Specific Mast Cell Heterogeneity. Cells 2020;9:211. https://doi.org/10.3390/cells9010211.

[25] Haase P, Voehringer D. Regulation of the humoral type 2 immune response against allergens and helminths. Eur J Immunol 2021;51:273–9. https://doi.org/10.1002/eji.202048864.

[26] Bischoff SC. Role of mast cells in allergic and non-allergic immune responses: comparison of human and murine data. Nat Rev Immunol 2007;7:93–104. https://doi.org/10.1038/nri2018.

[27] McNeil BD, Pundir P, Meeker S, Han L, Undem BJ, Kulka M, et al. Identification of a mast-cell-specific receptor crucial for pseudo-allergic drug reactions. Nature 2015;519:237–41. https://doi.org/10.1038/nature14022.

[28] Mukai K, Tsai M, Saito H, Galli SJ. Mast cells as sources of cytokines, chemokines, and growth factors. Immunol Rev 2018;282:121–50. https://doi.org/10.1111/imr.12634.

[29] Halova I, Draberova L, Draber P. Mast Cell Chemotaxis – Chemoattractants and Signaling Pathways. Front Immunol 2012;3. https://doi.org/10.3389/fimmu.2012.00119.

[30] Gaudenzio N, Sibilano R, Marichal T, Starkl P, Reber LL, Cenac N, et al. Different activation signals induce distinct mast cell degranulation strategies. Journal of Clinical Investigation 2016;126:3981–98. https://doi.org/10.1172/JCI85538.

[31] Dvorak A, Tepper R, Weller P, Morgan E, Estrella P, Monahan-Earley R, et al. Piecemeal degranulation of mast cells in the inflammatory eyelid lesions of interleukin-4 transgenic mice. Evidence of mast cell histamine release in vivo by diamine oxidase-gold enzyme-affinity ultrastructural cytochemistry. Blood 1994;83:3600–12. https://doi.org/10.1182/blood.V83.12.3600.3600.

[32] Andrade M V., Iwaki S, Ropert C, Gazzinelli RT, Cunha-Melo JR, Beaven MA. Amplification of cytokine production through synergistic activation of NFAT and AP-1 following stimulation of mast cells with antigen and IL-33. Eur J Immunol 2011;41:760–72. https://doi.org/10.1002/eji.201040718.

[33] Bando T, Fujita S, Nagano N, Yoshikawa S, Yamanishi Y, Minami M, et al. Differential usage of COX-1 and COX-2 in prostaglandin production by mast cells

and basophils. Biochem Biophys Rep 2017;10:82–7. https://doi.org/10.1016/j.bbrep.2017.03.004.

[34] Jordan PM, Andreas N, Groth M, Wegner P, Weber F, Jäger U, et al. ATP/IL-33-triggered hyperactivation of mast cells results in an amplified production of pro-inflammatory cytokines and eicosanoids. Immunology 2021;164:541–54. https://doi.org/10.1111/imm.13386.

[35] T K, G. A-H. Degranulation and regranulation of human mast cells. An electron microscopic study of the whealing reaction in urticaria pigmentosa. Acta Derm Venereol 1969;49:369–81. https://doi.org/10.2340/0001555549369381.

[36] Iskarpatyoti JA, Shi J, Abraham MA, Rathore APS, Miao Y, Abraham SN. Mast cell regranulation requires a metabolic switch involving mTORC1 and a glucose-6-phosphate transporter. Cell Rep 2022;40:111346. https://doi.org/10.1016/j.celrep.2022.111346.

[37] Friend DS, Ghildyal N, Austen KF, Gurish MF, Matsumoto R, Stevens RL. Mast cells that reside at different locations in the jejunum of mice infected with Trichinella spiralis exhibit sequential changes in their granule ultrastructure and chymase phenotype. Journal of Cell Biology 1996;135:279–90. https://doi.org/10.1083/jcb.135.1.279.

[38] St. John AL, Rathore APS, Ginhoux F. New perspectives on the origins and heterogeneity of mast cells. Nat Rev Immunol 2023;23:55–68. https://doi.org/10.1038/s41577-022-00731-2.

[39] Malaviya R, Ross EA, MacGregor JI, Ikeda T, Little JR, Jakschik BA, et al. Mast cell phagocytosis of FimH-expressing enterobacteria. J Immunol 1994;152:1907–14.

[40] von Köckritz-Blickwede M, Goldmann O, Thulin P, Heinemann K, Norrby-Teglund A, Rohde M, et al. Phagocytosis-independent antimicrobial activity of mast cells by means of extracellular trap formation. Blood 2008;111:3070–80. https://doi.org/10.1182/blood-2007-07-104018.

[41] Katsoulis-Dimitriou K, Kotrba J, Voss M, Dudeck J, Dudeck A. Mast Cell Functions Linking Innate Sensing to Adaptive Immunity. Cells 2020;9. https://doi.org/10.3390/cells9122538.

[42] Litchman G, Nair PA, Atwater AR, Bhutta BS. Contact Dermatitis. 2024.

[43] Alinaghi F, Bennike NH, Egeberg A, Thyssen JP, Johansen JD. Prevalence of contact allergy in the general population: A systematic review and meta-analysis. Contact Dermatitis 2019;80:77–85. https://doi.org/10.1111/cod.13119.

[44] Continentale-Studie zur Berufsunfähigkeit: Berufsunfähigkeit - das unterschätzte Risiko 2011:31–3.

[45] Clayton K, Vallejo AF, Davies J, Sirvent S, Polak ME. Langerhans Cells—Programmed by the Epidermis. Front Immunol 2017;8. https://doi.org/10.3389/fimmu.2017.01676.

[46] Nguyen A V., Soulika AM. The Dynamics of the Skin's Immune System. Int J Mol Sci 2019;20:1811. https://doi.org/10.3390/ijms20081811.

[47] Chipinda I, Hettick JM, Siegel PD. Haptenation: Chemical Reactivity and Protein Binding. J Allergy (Cairo) 2011;2011:1–11. https://doi.org/10.1155/2011/839682.

[48] Peiser M, Tralau T, Heidler J, Api AM, Arts JHE, Basketter DA, et al. Allergic contact dermatitis: epidemiology, molecular mechanisms, in vitro methods and regulatory aspects. Cellular and Molecular Life Sciences 2012;69:763–81. https://doi.org/10.1007/s00018-011-0846-8.

[49] Honda T, Egawa G, Grabbe S, Kabashima K. Update of Immune Events in the Murine Contact Hypersensitivity Model: Toward the Understanding of Allergic Contact Dermatitis. Journal of Investigative Dermatology 2013;133:303–15. https://doi.org/10.1038/jid.2012.284.

[50] Watanabe H, Gaide O, Pétrilli V, Martinon F, Contassot E, Roques S, et al. Activation of the IL-1β-Processing Inflammasome Is Involved in Contact Hypersensitivity. Journal of Investigative Dermatology 2007;127:1956–63. https://doi.org/10.1038/sj.jid.5700819.

[51] Weber FC, Esser PR, Müller T, Ganesan J, Pellegatti P, Simon MM, et al. Lack of the purinergic receptor P2X7 results in resistance to contact hypersensitivity. Journal of Experimental Medicine 2010;207:2609–19. https://doi.org/10.1084/jem.20092489.

[52] Imai Y, Yasuda K, Sakaguchi Y, Futatsugi-Yumikura S, Yoshimoto T, Nakanishi K, et al. Immediate-type contact hypersensitivity is reduced in interleukin-33 knockout mice. J Dermatol Sci 2014;74:159–61. https://doi.org/10.1016/j.jdermsci.2014.01.009.

[53] Hoppe A, Katsoulis-Dimitriou K, Edler HJ, Dudeck J, Drube S, Dudeck A. Mast cells initiate the vascular response to contact allergens by sensing cell stress. Journal of Allergy and Clinical Immunology 2020;145:1476-1479.e3. https://doi.org/10.1016/j.jaci.2020.01.036.

[54] Dudeck A, Dudeck J, Scholten J, Petzold A, Surianarayanan S, Köhler A, et al. Mast Cells Are Key Promoters of Contact Allergy that Mediate the Adjuvant Effects

of Haptens. Immunity 2011;34:973–84. https://doi.org/10.1016/j.immuni.2011.03.028.

[55] Weber FC, Németh T, Csepregi JZ, Dudeck A, Roers A, Ozsvári B, et al. Neutrophils are required for both the sensitization and elicitation phase of contact hypersensitivity. Journal of Experimental Medicine 2015;212:15–22. https://doi.org/10.1084/jem.20130062.

[56] Dudeck J, Froebel J, Kotrba J, Lehmann CHK, Dudziak D, Speier S, et al. Engulfment of mast cell secretory granules on skin inflammation boosts dendritic cell migration and priming efficiency. Journal of Allergy and Clinical Immunology 2019;143:1849-1864.e4. https://doi.org/10.1016/j.jaci.2018.08.052.

[57] Dilulio NA, Engeman T, Armstrong D, Tannenbaum C, Hamilton TA, Fairchild RL. Groα-mediated recruitment of neutrophils is required for elicitation of contact hypersensitivity. Eur J Immunol 1999;29:3485–95. https://doi.org/10.1002/(SICI)1521-4141(199911)29:11<3485::AID-IMMU3485>3.0.CO;2-B.

[58] Biedermann T, Kneilling M, Mailhammer R, Maier K, Sander CA, Kollias G, et al. Mast Cells Control Neutrophil Recruitment during T Cell–Mediated Delayed-Type Hypersensitivity Reactions through Tumor Necrosis Factor and Macrophage Inflammatory Protein 2. Journal of Experimental Medicine 2000;192:1441–52. https://doi.org/10.1084/jem.192.10.1441.

[59] Dudeck J, Kotrba J, Immler R, Hoffmann A, Voss M, Alexaki VI, et al. Directional mast cell degranulation of tumor necrosis factor into blood vessels primes neutrophil extravasation. Immunity 2021;54:468-483.e5. https://doi.org/10.1016/j.immuni.2020.12.017.

[60] Gocinski BL, Tigelaar RE. Roles of CD4+ and CD8+ T cells in murine contact sensitivity revealed by in vivo monoclonal antibody depletion. The Journal of Immunology 1990;144:4121–8. https://doi.org/10.4049/jimmunol.144.11.4121.

[61] Bour H, Peyron E, Gaucherand M, Garrigue J-L, Desvignes C, Kaiserlian D, et al. Major histocompatibility complex class I-restricted CD8+ T cells and class II-restricted CD4+ T cells, respectively, mediate and regulate contact sensitivity to dinitrofluorobenzene. Eur J Immunol 1995;25:3006–10. https://doi.org/10.1002/eji.1830251103.

[62] Vocanson M, Hennino A, Cluzel-Tailhardat M, Saint-Mezard P, Benetiere J, Chavagnac C, et al. CD8+ T Cells Are Effector Cells of Contact Dermatitis to

Common Skin Allergens in Mice. Journal of Investigative Dermatology 2006;126:815–20. https://doi.org/10.1038/sj.jid.5700174.

[63] Abe M, Kondo T, Xu H, Fairchild RL. Interferon-γ Inducible Protein (IP-10) Expression Is Mediated by CD8+ T Cells and Is Regulated by CD4+ T Cells During the Elicitation of Contact Hypersensitivity. Journal of Investigative Dermatology 1996;107:360–6. https://doi.org/10.1111/1523-1747.ep12363337.

[64] Tokuriki A, Seo N, Ito T, Kumakiri M, Takigawa M, Tokura Y. Dominant expression of CXCR3 is associated with induced expression of IP-10 at hapten-challenged sites of murine contact hypersensitivity: a possible role for interferon-γ-producing CD8+ T cells in IP-10 expression. J Dermatol Sci 2002;28:234–41. https://doi.org/10.1016/S0923-1811(01)00172-4.

[65] Trautmann A, Akdis M, Kleemann D, Altznauer F, Simon H-U, Graeve T, et al. T cell–mediated Fas-induced keratinocyte apoptosis plays a key pathogenetic role in eczematous dermatitis. Journal of Clinical Investigation 2000;106:25–35. https://doi.org/10.1172/JCI9199.

[66] Chong SZ, Tan KW, Wong FHS, Chua YL, Tang Y, Ng LG, et al. CD8 T Cells Regulate Allergic Contact Dermatitis by Modulating CCR2–Dependent TNF/iNOS–Expressing Ly6C + CD11b + Monocytic Cells. Journal of Investigative Dermatology 2014;134:666–76. https://doi.org/10.1038/jid.2013.403.

[67] Saint-Mezard P, Chavagnac C, Vocanson M, Kehren J, Rozières A, Bosset S, et al. Deficient Contact Hypersensitivity Reaction in CD4−/− Mice Is Because of Impaired Hapten-Specific CD8+ T Cell Functions. Journal of Investigative Dermatology 2005;124:562–9. https://doi.org/10.1111/j.0022-202X.2005.23567.x.

[68] Ring S, Schäfer SC, Mahnke K, Lehr H-A, Enk AH. CD4+CD25+ regulatory T cells suppress contact hypersensitivity reactions by blocking influx of effector T cells into inflamed tissue. Eur J Immunol 2006;36:2981–92. https://doi.org/10.1002/eji.200636207.

[69] Ring S, Inaba Y, Da M, Bopp T, Grabbe S, Enk A, et al. Regulatory T Cells Prevent Neutrophilic Infiltration of Skin during Contact Hypersensitivity Reactions by Strengthening the Endothelial Barrier. Journal of Investigative Dermatology 2021;141:2006–17. https://doi.org/10.1016/j.jid.2021.01.027.

[70] Ring S, Oliver SJ, Cronstein BN, Enk AH, Mahnke K. CD4+CD25+ regulatory T cells suppress contact hypersensitivity reactions through a CD39, adenosine-

dependent mechanism. Journal of Allergy and Clinical Immunology 2009;123:1287-1296.e2. https://doi.org/10.1016/j.jaci.2009.03.022.

[71] Ortega-Gómez A, Perretti M, Soehnlein O. Resolution of inflammation: an integrated view. EMBO Mol Med 2013;5:661–74. https://doi.org/10.1002/emmm.201202382.

[72] Schett G, Neurath MF. Resolution of chronic inflammatory disease: universal and tissue-specific concepts. Nat Commun 2018;9:3261. https://doi.org/10.1038/s41467-018-05800-6.

[73] WILLIAMS TJ, PECK MJ. Role of prostaglandin-mediated vasodilatation in inflammation. Nature 1977;270:530–2. https://doi.org/10.1038/270530a0.

[74] Pouliot M, Fiset M-E, Massé M, Naccache PH, Borgeat P. Adenosine Up-Regulates Cyclooxygenase-2 in Human Granulocytes: Impact on the Balance of Eicosanoid Generation. The Journal of Immunology 2002;169:5279–86. https://doi.org/10.4049/jimmunol.169.9.5279.

[75] Levy BD, Clish CB, Schmidt B, Gronert K, Serhan CN. Lipid mediator class switching during acute inflammation: signals in resolution. Nat Immunol 2001;2:612–9. https://doi.org/10.1038/89759.

[76] Serhan CN, Clish CB, Brannon J, Colgan SP, Chiang N, Gronert K. Novel Functional Sets of Lipid-Derived Mediators with Antiinflammatory Actions Generated from Omega-3 Fatty Acids via Cyclooxygenase 2–Nonsteroidal Antiinflammatory Drugs and Transcellular Processing. J Exp Med 2000;192:1197–204. https://doi.org/10.1084/jem.192.8.1197.

[77] Hong S, Gronert K, Devchand PR, Moussignac R-L, Serhan CN. Novel Docosatrienes and 17S-Resolvins Generated from Docosahexaenoic Acid in Murine Brain, Human Blood, and Glial Cells. Journal of Biological Chemistry 2003;278:14677–87. https://doi.org/10.1074/jbc.M300218200.

[78] Serhan CN, Yang R, Martinod K, Kasuga K, Pillai PS, Porter TF, et al. Maresins: novel macrophage mediators with potent antiinflammatory and proresolving actions. Journal of Experimental Medicine 2009;206:15–23. https://doi.org/10.1084/jem.20081880.

[79] Sugimoto MA, Sousa LP, Pinho V, Perretti M, Teixeira MM. Resolution of Inflammation: What Controls Its Onset? Front Immunol 2016;7. https://doi.org/10.3389/fimmu.2016.00160.

[80] Dean RA, Cox JH, Bellac CL, Doucet A, Starr AE, Overall CM. Macrophage-specific metalloelastase (MMP-12) truncates and inactivates ELR+ CXC

chemokines and generates CCL2, -7, -8, and -13 antagonists: potential role of the macrophage in terminating polymorphonuclear leukocyte influx. Blood 2008;112:3455–64. https://doi.org/10.1182/blood-2007-12-129080.

[81] McQuibban GA, Gong J-H, Wong JP, Wallace JL, Clark-Lewis I, Overall CM. Matrix metalloproteinase processing of monocyte chemoattractant proteins generates CC chemokine receptor antagonists with anti-inflammatory properties in vivo. Blood 2002;100:1160–7. https://doi.org/10.1182/blood.V100.4.1160.h81602001160_1160_1167.

[82] Mantovani A, Bonecchi R, Locati M. Tuning inflammation and immunity by chemokine sequestration: decoys and more. Nat Rev Immunol 2006;6:907–18. https://doi.org/10.1038/nri1964.

[83] Colotta F, Re F, Muzio M, Bertini R, Polentarutti N, Sironi M, et al. Interleukin-1 Type II Receptor: A Decoy Target for IL-1 That Is Regulated by IL-4. Science (1979) 1993;261:472–5. https://doi.org/10.1126/science.8332913.

[84] Gardner L, Patterson AM, Ashton BA, Stone MA, Middleton J. The human Duffy antigen binds selected inflammatory but not homeostatic chemokines. Biochem Biophys Res Commun 2004;321:306–12. https://doi.org/10.1016/j.bbrc.2004.06.146.

[85] D'Amico G, Frascaroli G, Bianchi G, Transidico P, Doni A, Vecchi A, et al. Uncoupling of inflammatory chemokine receptors by IL-10: generation of functional decoys. Nat Immunol 2000;1:387–91. https://doi.org/10.1038/80819.

[86] El Kebir D, Filep JG. Modulation of Neutrophil Apoptosis and the Resolution of Inflammation through β2 Integrins. Front Immunol 2013;4. https://doi.org/10.3389/fimmu.2013.00060.

[87] van den Berg JM, Weyer S, Weening JJ, Roos D, Kuijpers TW. Divergent effects of tumor necrosis factor alpha on apoptosis of human neutrophils. J Leukoc Biol 2001;69:467–73.

[88] El Kebir D, József L, Pan W, Wang L, Petasis NA, Serhan CN, et al. 15-Epi-lipoxin A4 Inhibits Myeloperoxidase Signaling and Enhances Resolution of Acute Lung Injury. Am J Respir Crit Care Med 2009;180:311–9. https://doi.org/10.1164/rccm.200810-1601OC.

[89] El Kebir D, Gjorstrup P, Filep JG. Resolvin E1 promotes phagocytosis-induced neutrophil apoptosis and accelerates resolution of pulmonary inflammation. Proceedings of the National Academy of Sciences 2012;109:14983–8. https://doi.org/10.1073/pnas.1206641109.

[90] Truman LA, Ford CA, Pasikowska M, Pound JD, Wilkinson SJ, Dumitriu IE, et al. CX3CL1/fractalkine is released from apoptotic lymphocytes to stimulate macrophage chemotaxis. Blood 2008;112:5026–36. https://doi.org/10.1182/blood-2008-06-162404.

[91] Lauber K, Bohn E, Kröber SM, Xiao Y, Blumenthal SG, Lindemann RK, et al. Apoptotic Cells Induce Migration of Phagocytes via Caspase-3-Mediated Release of a Lipid Attraction Signal. Cell 2003;113:717–30. https://doi.org/10.1016/S0092-8674(03)00422-7.

[92] Gude DR, Alvarez SE, Paugh SW, Mitra P, Yu J, Griffiths R, et al. Apoptosis induces expression of sphingosine kinase 1 to release sphingosine-1-phosphate as a "come-and-get-me" signal. The FASEB Journal 2008;22:2629–38. https://doi.org/10.1096/fj.08-107169.

[93] Elliott MR, Chekeni FB, Trampont PC, Lazarowski ER, Kadl A, Walk SF, et al. Nucleotides released by apoptotic cells act as a find-me signal to promote phagocytic clearance. Nature 2009;461:282–6. https://doi.org/10.1038/nature08296.

[94] Fadok VA, de Cathelineau A, Daleke DL, Henson PM, Bratton DL. Loss of Phospholipid Asymmetry and Surface Exposure of Phosphatidylserine Is Required for Phagocytosis of Apoptotic Cells by Macrophages and Fibroblasts. Journal of Biological Chemistry 2001;276:1071–7. https://doi.org/10.1074/jbc.M003649200.

[95] Liu G, Wang J, Park Y-J, Tsuruta Y, Lorne EF, Zhao X, et al. High Mobility Group Protein-1 Inhibits Phagocytosis of Apoptotic Neutrophils through Binding to Phosphatidylserine. The Journal of Immunology 2008;181:4240–6. https://doi.org/10.4049/jimmunol.181.6.4240.

[96] Miyanishi M, Tada K, Koike M, Uchiyama Y, Kitamura T, Nagata S. Identification of Tim4 as a phosphatidylserine receptor. Nature 2007;450:435–9. https://doi.org/10.1038/nature06307.

[97] Park D, Tosello-Trampont A-C, Elliott MR, Lu M, Haney LB, Ma Z, et al. BAI1 is an engulfment receptor for apoptotic cells upstream of the ELMO/Dock180/Rac module. Nature 2007;450:430–4. https://doi.org/10.1038/nature06329.

[98] Scott RS, McMahon EJ, Pop SM, Reap EA, Caricchio R, Cohen PL, et al. Phagocytosis and clearance of apoptotic cells is mediated by MER. Nature 2001;411:207–11. https://doi.org/10.1038/35075603.

[99] Fadok VA, Bratton DL, Konowal A, Freed PW, Westcott JY, Henson PM. Macrophages that have ingested apoptotic cells in vitro inhibit proinflammatory cytokine production through autocrine/paracrine mechanisms involving TGF-beta, PGE2, and PAF. Journal of Clinical Investigation 1998;101:890–8. https://doi.org/10.1172/JCI1112.

[100] Filardy AA, Pires DR, Nunes MP, Takiya CM, Freire-de-Lima CG, Ribeiro-Gomes FL, et al. Proinflammatory Clearance of Apoptotic Neutrophils Induces an IL-12lowIL-10high Regulatory Phenotype in Macrophages. The Journal of Immunology 2010;185:2044–50. https://doi.org/10.4049/jimmunol.1000017.

[101] Frangogiannis NG. Transforming growth factor–β in tissue fibrosis. Journal of Experimental Medicine 2020;217. https://doi.org/10.1084/jem.20190103.

[102] Van Hauwermeiren F, Armaka M, Karagianni N, Kranidioti K, Vandenbroucke RE, Loges S, et al. Safe TNF-based antitumor therapy following p55TNFR reduction in intestinal epithelium. Journal of Clinical Investigation 2013;123:2590–603. https://doi.org/10.1172/JCI65624.

[103] Scholten J, Hartmann K, Gerbaulet A, Krieg T, Müller W, Testa G, et al. Mast cell-specific Cre/loxP-mediated recombination in vivo. Transgenic Res 2008;17:307–15. https://doi.org/10.1007/s11248-007-9153-4.

[104] Grivennikov SI, Tumanov A V., Liepinsh DJ, Kruglov AA, Marakusha BI, Shakhov AN, et al. Distinct and Nonredundant In Vivo Functions of TNF Produced by T Cells and Macrophages/Neutrophils. Immunity 2005;22:93–104. https://doi.org/10.1016/j.immuni.2004.11.016.

[105] Faust N, Varas F, Kelly LM, Heck S, Graf T. Insertion of enhanced green fluorescent protein into the lysozyme gene creates mice with green fluorescent granulocytes and macrophages. Blood 2000;96:719–26.

[106] Clausen BE, Burkhardt C, Reith W, Renkawitz R, Förster I. Conditional gene targeting in macrophages and granulocytes using LysMcre mice. Transgenic Res 1999;8:265–77. https://doi.org/10.1023/A:1008942828960.

[107] Livak KJ, Schmittgen TD. Analysis of Relative Gene Expression Data Using Real-Time Quantitative PCR and the 2−ΔΔCT Method. Methods 2001;25:402–8. https://doi.org/10.1006/meth.2001.1262.

[108] Luttmann W, Bratke K, Küpper M, Myrtek D. Der Experimentator: Immunologie. Berlin, Heidelberg: Springer Berlin Heidelberg; 2014. https://doi.org/10.1007/978-3-642-41899-0.

[109] Tamoutounour S, Guilliams M, Montanana Sanchis F, Liu H, Terhorst D, Malosse C, et al. Origins and Functional Specialization of Macrophages and of Conventional and Monocyte-Derived Dendritic Cells in Mouse Skin. Immunity 2013;39:925–38. https://doi.org/10.1016/j.immuni.2013.10.004.

[110] Italiani P, Boraschi D. From Monocytes to M1/M2 Macrophages: Phenotypical vs. Functional Differentiation. Front Immunol 2014;5. https://doi.org/10.3389/fimmu.2014.00514.

[111] Shi C, Pamer EG. Monocyte recruitment during infection and inflammation. Nat Rev Immunol 2011;11:762–74. https://doi.org/10.1038/nri3070.

[112] MORI R, KONDO T, OHSHIMA T, ISHIDA Y, MUKAIDA N. Accelerated wound healing in tumor necrosis factor receptor p55-deficient mice with reduced leukocyte infiltration. The FASEB Journal 2002;16:963–74. https://doi.org/10.1096/fj.01-0776com.

[113] Lim S, Ryu J, Shin J-A, Shin M-J, Ahn YK, Kim JJ, et al. Tumor Necrosis Factor-α Potentiates RhoA-Mediated Monocyte Transmigratory Activity In Vivo at a Picomolar Level. Arterioscler Thromb Vasc Biol 2009;29:2138–45. https://doi.org/10.1161/ATVBAHA.109.195735.

[114] Leeuwenberg JF, Dentener MA, Buurman WA. Lipopolysaccharide LPS-mediated soluble TNF receptor release and TNF receptor expression by monocytes. Role of CD14, LPS binding protein, and bactericidal/permeability-increasing protein. The Journal of Immunology 1994;152:5070–6. https://doi.org/10.4049/jimmunol.152.10.5070.

[115] Webster NL, Crowe SM. Matrix metalloproteinases, their production by monocytes and macrophages and their potential role in HIV-related diseases. J Leukoc Biol 2006;80:1052–66. https://doi.org/10.1189/jlb.0306152.

[116] Olsen KC, Sapinoro RE, Kottmann RM, Kulkarni AA, Iismaa SE, Johnson GVW, et al. Transglutaminase 2 and Its Role in Pulmonary Fibrosis. Am J Respir Crit Care Med 2011;184:699–707. https://doi.org/10.1164/rccm.201101-0013OC.

[117] Jang D, Lee A-H, Shin H-Y, Song H-R, Park J-H, Kang T-B, et al. The Role of Tumor Necrosis Factor Alpha (TNF-α) in Autoimmune Disease and Current TNF-α Inhibitors in Therapeutics. Int J Mol Sci 2021;22:2719. https://doi.org/10.3390/ijms22052719.

[118] Dudeck A, Suender CA, Kostka SL, von Stebut E, Maurer M. Mast cells promote Th1 and Th17 responses by modulating dendritic cell maturation and function. Eur J Immunol 2011;41:1883–93. https://doi.org/10.1002/eji.201040994.

[119] Nakajima T. Marked increase in CC chemokine gene expression in both human and mouse mast cell transcriptomes following Fcepsilon receptor I cross-linking: an interspecies comparison. Blood 2002;100:3861–8. https://doi.org/10.1182/blood-2002-02-0602.

[120] Shi C, Pamer EG. Monocyte recruitment during infection and inflammation. Nat Rev Immunol 2011;11:762–74. https://doi.org/10.1038/nri3070.

[121] Schultze JL, Mass E, Schlitzer A. Emerging Principles in Myelopoiesis at Homeostasis and during Infection and Inflammation. Immunity 2019;50:288–301. https://doi.org/10.1016/j.immuni.2019.01.019.

[122] Ishimoto T, Takei Y, Yuzawa Y, Hanai K, Nagahara S, Tarumi Y, et al. Downregulation of Monocyte Chemoattractant Protein-1 Involving Short Interfering RNA Attenuates Hapten-induced Contact Hypersensitivity. Molecular Therapy 2008;16:387–95. https://doi.org/10.1038/sj.mt.6300360.

[123] Kish DD, Li X, Fairchild RL. CD8 T Cells Producing IL-17 and IFN-γ Initiate the Innate Immune Response Required for Responses to Antigen Skin Challenge. The Journal of Immunology 2009;182:5949–59. https://doi.org/10.4049/jimmunol.0802830.

[124] Micheau O, Tschopp J. Induction of TNF Receptor I-Mediated Apoptosis via Two Sequential Signaling Complexes. Cell 2003;114:181–90. https://doi.org/10.1016/S0092-8674(03)00521-X.

[125] Mizumoto N, Iwabichi K, Nakamura H, Ato M, Shibaki A, Kawashima T, et al. Enhanced Contact Hypersensitivity in Human Monocyte Chemoattractant Protein-1 Transgenic Mouse. Immunobiology 2001;204:477–93. https://doi.org/10.1078/0171-2985-00057.

[126] Ross R. Involvement of NO in contact hypersensitivity. Int Immunol 1998;10:61–9. https://doi.org/10.1093/intimm/10.1.61.

[127] Piguet PF, Grau GE, Hauser C, Vassalli P. Tumor necrosis factor is a critical mediator in hapten induced irritant and contact hypersensitivity reactions. J Exp Med 1991;173:673–9. https://doi.org/10.1084/jem.173.3.673.

[128] Gabay C. Interleukin-6 and chronic inflammation. Arthritis Res Ther 2006;8:S3. https://doi.org/10.1186/ar1917.

[129] Kratofil RM, Kubes P, Deniset JF. Monocyte Conversion During Inflammation and Injury. Arterioscler Thromb Vasc Biol 2017;37:35–42. https://doi.org/10.1161/ATVBAHA.116.308198.

[130] Crane MJ, Daley JM, van Houtte O, Brancato SK, Henry WL, Albina JE. The Monocyte to Macrophage Transition in the Murine Sterile Wound. PLoS One 2014;9:e86660. https://doi.org/10.1371/journal.pone.0086660.

[131] Wynn TA, Vannella KM. Macrophages in Tissue Repair, Regeneration, and Fibrosis. Immunity 2016;44:450–62. https://doi.org/10.1016/j.immuni.2016.02.015.

[132] Webster NL, Crowe SM. Matrix metalloproteinases, their production by monocytes and macrophages and their potential role in HIV-related diseases. J Leukoc Biol 2006;80:1052–66. https://doi.org/10.1189/jlb.0306152.

[133] Zhao X, Chen J, Sun H, Zhang Y, Zou D. New insights into fibrosis from the ECM degradation perspective: the macrophage-MMP-ECM interaction. Cell Biosci 2022;12:117. https://doi.org/10.1186/s13578-022-00856-w.

[134] Braga TT, Agudelo JSH, Camara NOS. Macrophages During the Fibrotic Process: M2 as Friend and Foe. Front Immunol 2015;6. https://doi.org/10.3389/fimmu.2015.00602.

[135] Wang M, Qin X, Mudgett JS, Ferguson TA, Senior RM, Welgus HG. Matrix metalloproteinase deficiencies affect contact hypersensitivity: Stromelysin-1 deficiency prevents the response and gelatinase B deficiency prolongs the response. Proceedings of the National Academy of Sciences 1999;96:6885–9. https://doi.org/10.1073/pnas.96.12.6885.

[136] Giannandrea M, Parks WC. Diverse functions of matrix metalloproteinases during fibrosis. Dis Model Mech 2014;7:193–203. https://doi.org/10.1242/dmm.012062.

[137] Siller-López F, Sandoval A, Salgado S, Salazar A, Bueno M, Garcia J, et al. Treatment with human metalloproteinase-8 gene delivery ameliorates experimental rat liver cirrhosis. Gastroenterology 2004;126:1122–33. https://doi.org/10.1053/j.gastro.2003.12.045.

[138] Feng M, Ding J, Wang M, Zhang J, Zhu X, Guan W. Kupffer-derived matrix metalloproteinase-9 contributes to liver fibrosis resolution. Int J Biol Sci 2018;14:1033–40. https://doi.org/10.7150/ijbs.25589.

[139] Liu X-Y, Liu R-X, Hou F, Cui L-J, Li C-Y, Chi C, et al. Fibronectin expression is critical for liver fibrogenesis in vivo and in vitro. Mol Med Rep 2016;14:3669–75. https://doi.org/10.3892/mmr.2016.5673.

[140] Kish DD, Volokh N, Baldwin WM, Fairchild RL. Hapten Application to the Skin Induces an Inflammatory Program Directing Hapten-Primed Effector CD8 T Cell

Interaction with Hapten-Presenting Endothelial Cells. The Journal of Immunology 2011;186:2117–26. https://doi.org/10.4049/jimmunol.1002337.

[141] Kim N, Notik S, Gottlieb AB, Scheinman PL. Patch Test Results in Psoriasis Patients on Biologics. Dermatitis 2014;25:182–90. https://doi.org/10.1097/DER.0000000000000056.

[142] Myers W, Newman M, Katz B, Gottlieb AB. Ability to develop rhus allergic contact dermatitis in a patient with psoriasis receiving etanercept. J Am Acad Dermatol 2006;55:S127–8. https://doi.org/10.1016/j.jaad.2006.05.003.

[143] Rosmarin D, Bush M, Scheinman PL. Patch testing a patient with allergic contact hand dermatitis who is taking infliximab. J Am Acad Dermatol 2008;59:145–7. https://doi.org/10.1016/j.jaad.2008.02.016.

[144] Davignon J-L, Hayder M, Baron M, Boyer J-F, Constantin A, Apparailly F, et al. Targeting monocytes/macrophages in the treatment of rheumatoid arthritis. Rheumatology 2013;52:590–8. https://doi.org/10.1093/rheumatology/kes304.

[145] Zhou L, Braat H, Faber KN, Dijkstra G, Peppelenbosch MP. Monocytes and their pathophysiological role in Crohn's disease. Cellular and Molecular Life Sciences 2009;66:192–202. https://doi.org/10.1007/s00018-008-8308-7.

[146] Tracey D, Klareskog L, Sasso EH, Salfeld JG, Tak PP. Tumor necrosis factor antagonist mechanisms of action: A comprehensive review. Pharmacol Ther 2008;117:244–79. https://doi.org/10.1016/j.pharmthera.2007.10.001.

[147] Levin AD, Wildenberg ME, van den Brink GR. Mechanism of Action of Anti-TNF Therapy in Inflammatory Bowel Disease. J Crohns Colitis 2016;10:989–97. https://doi.org/10.1093/ecco-jcc/jjw053.

[148] Schaeffer DF, Walsh JC, Kirsch R, Waterman M, Silverberg MS, Riddell RH. Distinctive histopathologic phenotype in resection specimens from patients with Crohn's disease receiving anti–TNF-α therapy. Hum Pathol 2014;45:1928–35. https://doi.org/10.1016/j.humpath.2014.05.016.

[149] Torle J, Dabir PD, Korsgaard U, Christiansen J, Qvist N, El-Hussuna A. Levels of Intestinal Inflammation and Fibrosis in Resection Specimens after Preoperative Anti-Tumor Necrosis Factor Alpha Treatment in Patients with Crohn's Disease: A Comparative Pilot Study. Surg Res Pract 2020;2020:1–6. https://doi.org/10.1155/2020/6085678.

7 Declaration of Honor

I hereby declare that I prepared this thesis without impermissible help of third parties and that none other than the indicated tools have been used; all sources of information are clearly marked, including my own publications.

In particular I have not consciously:

- Fabricated data or rejected undesired results

- Misused statistical methods with the aim of drawing other conclusions than those warranted by the available data

- Plagiarized external data or publications

- Presented the results of other researchers in a distorted way I am aware that violations of copyright may lead to injunction and damage claims of the author and also to prosecution by the law enforcement authorities.

I hereby agree that the thesis may be reviewed for plagiarism by mean of electronic data processing.

This work has not yet been submitted as a doctoral thesis in the same or a similar form in Germany or in any other country. It has not yet been published as a whole.

Location, Date, Signatur